UNIVERSITY OF CAPE TOWN
IYUNIVESITHI YASEKAPA • UNIVERSITEIT VAN KAAPSTAD

CMSIRU

A study of the influence of aggregate grading on concrete penetrability

PREPARED BY:
Michael Loseby

SUPERVISOR:
Prof. Mark Alexander

CO-SUPERVISOR:
Assoc. Prof. Hans Beushausen

DATE:
26 October, 2014

Submitted in partial fulfilment of a Masters of Science in Civil Engineering

Plagiarism Declaration

1. I know that plagiarism is wrong. Plagiarism is using another's work and pretending that it is one's own.
2. I have used the Harvard Convention for citation and referencing. Each significant contribution to, and quotation in, this report from the work, or works of other people has been attributed and has been cited and referenced.
3. This report is my own work.
4. I have not allowed, and will not allow, anyone to copy my work with the intention of passing it off as his or her own work.
5. I acknowledge that copying someone else's assignment or essay, or part of it, is wrong, and declare that this is my own work.

Student Name	**Student Number**	**Signed**	**Date**
Michael Loseby	LSBMIC001	Signed by candidate	26/10/2014

Acknowledgements

I owe a depth of gratitude to Prof Mark Alexander and Assoc. Prof Hans Beushausen, who have given invaluable guidance as supervisors and served as inspirational mentors.

I am grateful for the guidance and assistance of the lab manager – Nooredien Hassen – and the lab technicians – Leonard Adams, Dunovan Ferris, Hector Mafungwa, Charles May and Alvino Witbooi, Furthermore, Charles Nicholas provided some of the necessary apparatus for the research. I am grateful for your fantastic craftsmanship as well as the hours of conversation.

I wish to acknowledge with gratitude the following for financial support of this work: The Cement and Concrete Institute (C&CI), The National Research Foundation (NRF), Sika (SA) Pty Ltd., The Concrete Manufacturer's Association, The Tertiary Education Support Programme (TESP) of ESKOM, and the Water Research Commission (WRC). Concrete materials were supplied by PPC and AfriSam.

Thanks to all friends at CoMSIRU for the moral support and for the willing input. In particular I would like to thank Philemon Arito, who was always happy to lend a helping hand and whose enthusiasm is contagious.

Finally I am eternally grateful to Dad and Viv. I am lucky to have you.

To Dad and Viv

Abstract

Concrete is generally perceived as being an inherently durable material. However, many concrete structures need substantial repairs and maintenance during their service life, with the resultant costs to the economy reaching 3 – 5 % of GNP in some countries. Durability is therefore key in concrete design and specification.

Aggregates constitute between 60 and 80 %, by volume, of typical concretes and have a profound influence on the physical properties of hardened concrete. The aggregate particle size distribution is usually selected so as to achieve a particle packing density that is equal to or near the maximum, which is seen as optimal for strength and durability. However, the influence of aggregate grading on durability apart from that which it has through its effect on particle packing density is not understood. Alternative mechanisms through which grading may effect durability include tortuosity and the porosity of the interfacial transition zone.

This research aimed to determine the extent of the influence that aggregate grading has on concrete durability independently of particle packing density and to determine whether fineness modulus (FM) is a suitable and sufficient parameter for the characterisation of aggregate particle size distribution with regard to the performance based specification of concrete where durability is the concern. The coefficient of uniformity (C_u) and the use of gap or continuous grading were two further factors considered.

Laboratory experiments – focused on concrete penetrability – were conducted on concrete samples where the grading of aggregates was varied but packing density was held constant. This was achieved by considering the aggregates to be binary combinations of fine and coarse constituents. The fine and the coarse fractions were blended in predetermined proportions so as to achieve a particular packing density. Both the packing density and the proportions to be blended were determined by way of a numerical packing model, namely the Modified Toufar Model (MTM).

The penetrability of the concretes was characterised by use of the South African durability index (DI) tests – including oxygen permeability index (OPI), water sorptivity index (WSI) and chloride conductivity index (CCI) tests. These tests measure potential durability, but taken together are a good representation of penetrability. Accelerated carbonation tests were also conducted as an indirect measure of permeability.

Correlations between C_u and OPI, in concretes with continuous grading, gave r = -0.472, where an increase in C_u of 3.5 units caused a decrease in OPI of 0.3 units. This was attributed primarily to the increase in D_{60} which, as a result of a greater level of localised bleeding which causes a greater water/binder ratio at the aggregate surface, causes a greater porosity in the ITZ. However there was little meaningful correlation between the same two parameters in concretes with a gap grading. There was little meaningful correlation between OPI and FM.

Correlations between FM and WSI gave r = -0.342 in concretes with gap grading where an increase in FM of 2.3 units caused a decrease in WSI of 2.03 $mm/hr^{0.5}$. This was explained by the relationship between FM and the volume of the total aggregate that is constituted of fine aggregates (y_1) whereby, in order to maintain constant packing density, as FM increased, so did y_1. As a result there was a greater proportion of particles of 75 μm and smaller, which refine the pore structure, particularly in the region of the ITZ. However there was little correlation between the same two parameters in concretes with a continuous grading. There was little meaningful correlation between WSI and C_u.

Correlations between FM and CCI, in concretes with continuous grading, gave r = 0.488 where, with an increase in FM of 2.3 units, an increase in CCI of 0.47 mS/cm was observed. This was attributed to the increase in the average particle size which, as a result of a greater level of localised bleeding which causes a greater water/binder ratio at the aggregate surface, causes a greater porosity in the ITZ. Furthermore, with a greater average aggregate particle size there is a lower level of tortuosity which allows for easier passage of a penetrating substance. However there was little meaningful correlation between the same two parameters in concretes with a gap grading. There was little meaningful correlation between CCI and C_u.

The thirty day accelerated carbonation results indicated a moderate relationship between penetrability and both FM and C_u in concretes with gap graded aggregate, such that it could not be concluded whether or not there was a meaningful effect. However, the concrete with continuously graded aggregate showed no correlation between carbonation depth and both FM and C_u. It was therefore concluded that the fine aggregate grading, in terms of both FM and C_u, had no meaningful effect on the penetrability as measured by carbon dioxide penetration.

Given the different effects of changes in FM and C_u on different parameters, a particular level of either of these two aggregate parameters cannot be prescribed for enhanced durability. The optimum FM required depends on whether the transport mechanism of concern is sorption or permeation and diffusion. However, given the limited effects that were observed from changes in FM and C_u it is recommended that for optimisation of concrete durability, a designer give greatest consideration to selection of water/binder ratio and binder type; aggregate grading can then be selected primarily to attain near maximum packing density.

Furthermore, given the overall low level of correlation between the measured penetrability properties and both FM and C_u, it is concluded that neither are suitable for the characterisation of aggregate grading with regard to concrete durability.

In all of the measured parameters, gap graded aggregates tended to yield better performance than continuously graded aggregates. However the observed improvements were less than what has been observed in other research for variations in water/binder ratio and binder type and content. Furthermore, overall the observed improvements were shown not to be statistically significant. It is therefore concluded that it is beneficial to use gap graded aggregates rather than continuously graded aggregates where gap graded aggregates are readily available. However, when optimising durability, water/binder ratio and binder type and content are of greater concern.

Table of Contents

List of Figures

List of Tables

Terminology

The terminology presented herein describes the particular definitions used in this research. Some of the terms may have subtle differences in their meaning when used elsewhere. For comprehensive descriptions, refer to Alexander and Mindess (2005).

Aggregates: Granular material such as sand, gravel, crushed stone, or iron blast-furnace slag, used with a cementing medium to form hydraulic cement concrete or mortar.

Fine aggregate: The portion of aggregate passing the 4.75 mm sieve and retained on the 75 μm sieve.

Coarse aggregate: The portion of aggregate retained on the 4.75 mm sieve.

Fineness modulus (FM): It is obtained by adding the total percentage of material, of the original mass of material, retained on each of the standard sieve sizes, excluding the 75 μm sieve, and dividing the total by 100.

Bulk volume of aggregate: The total volume occupied by aggregate, including the solid volume of particles and the void volume between the particles.

Coefficient of uniformity (C_u): The ratio of the aggregate particle diameter at which 60 % of of aggregate is smaller by mass and the diameter at which 10 % of the aggregate is smaller by mass. Thus, $C_u = D_{60} / D_{10}$.

Fines: The fraction of aggregate passing the 75 μm sieve.

Fresh concrete: Concrete with sufficient workability and plasticity that it can be placed and consolidated by the intended methods.

Grading: The distribution of particles of aggregate among various sizes expressed in terms of total percentages smaller than each of a series of sieve openings.

Packing density of aggregate: The ratio of solid volume of aggregates to bulk volume of aggregates.

Sieve analysis: Determination of the proportions of particles lying within certain size ranges in a granular material by separation on sieves of different size openings.

Slump: A measure of consistency of freshly mixed concrete obtained by placing the concrete in a truncated cone of standard dimensions, removing the cone and measuring the subsistence of the concrete.

Tortuosity: The complexity of the flow path of a permeating substance through the pore structure of concrete.

Water-cement ratio: The ratio of the mass of water, exclusive of that absorbed by the aggregates, to the mass of portland cement in concrete in concrete.

1. Introduction

"Despite extensive investigations carried out over many years, it has not been possible to determine from basic principles an optimum aggregate grading that will ensure suitability for any particular case. Suitable gradings are thus generally arrived at empirically by trial of the materials in a concrete mix" (Grieve, 2009b). The following research served to improve the understanding of the relationship between concrete durability and aggregate grading as understood from a first principle level.

1.1 Context

Concrete is generally perceived as being an inherently durable material. However, many concrete structures need substantial repairs and maintenance during their service life, with the resultant costs to the economy reaching 3 – 5 % of GNP in some countries (Alexander, Mackechnie & Ballim, 1999). Durability is therefore a characteristic that should receive significant attention in concrete design and specification, with a view to ensuring a reasonable service life. According to ISO 13823:2008(E) durability of a concrete structure is defined as "the capability of a structure or component of a structure to satisfy the design performance requirements over a specified period of time, with planned maintenance, under the influence of the environmental conditions in a given area."

The foremost cause of reinforced concrete deterioration is the corrosion of reinforcing steel. The reduction in alkalinity that results from the ingress of carbon dioxide, or the change in the ionic composition of the pore solution which results from the ingress of chlorides, or a combination of the two, results in the depassivation of the reinforcing steel which precedes corrosion. The susceptibility of concrete to these processes depends on its penetrability – that is the ease with which fluids and ions can pass through it – and thus penetrability is critical to durability. Transport mechanisms provide the means by which fluids and ions penetrate concrete. These include permeation, absorption, diffusion and migration.

Aggregates in concrete have been, and often continue to be, viewed as an inert filler, serving only to reduce the cost of concrete per unit volume. However aggregates make up between 60 and 80 %, by volume, of typical concretes and it has been established that aggregate properties can influence the physical properties of hardened concrete. Aggregates give concrete dimensional stability and control shrinkage and creep deformations. They improve

strength and stiffness of concrete and give it good wear resistance. Aggregates tend to be less permeable than cement paste and therefore improve the durability of concrete by diluting the cement paste. Aggregate of greatest packing densities tend to give concrete mixes of greatest workability. As such, mix proportioning guidelines generally strive to maximise aggregate packing density. However, the effect of aggregate grading on concrete penetrability has received little attention in the literature and is poorly understood.

The move towards performance based-design and specification requires thorough understanding of all factors that influence performance. It is possible that aggregate grading may influence concrete penetrability independently of the effects that it has through its influence on aggregate packing. Specifically, differences in the effects of coarse and fine aggregates, as well as the interaction between different particle sizes, may offset the benefit derived from maximising packing density. Furthermore, since aggregate grading directly affects the workability of fresh concrete, using aggregate grading to maximise packing density for durability may be impractical.

This research was aimed at achieving greater understanding of the relationship between aggregate grading and concrete penetrability in order to better allow for durability-focused specifications that cater for both practical construction needs and design life requirements of any given application whilst making best use of the available materials.

1.2 Problem statement

A performance-based approach involves designing a concrete mix to achieve optimal performance outcomes in terms of strength, durability, shrinkage and creep, and other important engineering parameters, specific to the particular application. Ultimately the advancement in the material science strives for understanding that allows for the purpose specific optimisation of material properties through the educated selection of ingredients, whilst limiting cost. Concrete compressive strength is simple to measure and the development of methods such as the South African durability index method is allowing for characterisation of durability performance. These two measures serve as indicators to two key aspects of concrete performance and thus enable measurable, desired performance outcomes to be defined. For the design of defined-performance concrete, predicting the material properties of concrete becomes more and more important (Fennis, 2012). Performance-based design of concrete should deliver the most economical and environmentally friendly solution for each application and thus it is a necessary approach (Fennis, 2011).

The performance-based approach requires a thorough understanding of all the inputs that affect the performance outcomes. Aggregate is one of these inputs. Aggregate packing density has a large influence on strength and durability, where near maximum packing density is seen as optimum (Wasserman et al., 2009; Alexander & Mindess, 2005). Packing density is largely influenced by aggregate particle size distribution (Johansen & Andersen, 1991), and as such South African, USA and British standards prescribe aggregate particle size distributions to achieve optimum packing density. However, beyond aggregate packing density, the influence that aggregate particle size distribution has on performance outcomes, including concrete durability, is poorly understood.

Besides packing density, there are two key aspects related to aggregate grading that influence concrete penetrability. First is that different particle sizes influence the concrete microstructure differently, and second that at constant packing density, decreasing the average particle size will lead to an increased tortuosity. It is difficult to directly measure either of these characteristics. However, by holding aggregate packing density constant, the collective influence of these characteristics on concrete penetrability, derived from the variation of aggregate grading, may be studied through measures of permeability and potential durability.

1.3 Research objectives

In order to improve the viability of the performance-based design approach the research aimed to obtain a better understanding of the influence of aggregate grading on concrete penetrability and potential durability. This presented two key objectives.

i. The first was to determine whether variations in aggregate particle size distribution have an influence on the penetrability and potential durability of concrete. Aggregate packing density is dependent on the aggregate particle size distribution and packing density has been the subject of much prior research. However, packing density is one of three characteristics which are linked directly to particle size distribution. Two other characteristics are tortuosity and the extent of porosity, particularly in the region of the interfacial transition zone. The primary aim of this research is to determine the extent of the influence of particle size distribution on concrete penetrability and potential durability when packing density is held constant and thus eliminated as a factor.
ii. The second aim was to evaluate the usefulness of two simple grading related parameters, namely fineness modulus and coefficient of uniformity, in characterising aggregate for durability focused concrete design. Fineness modulus (FM) is a measure

of the average particle size and is therefore dependent on the particle size distribution of an aggregate. Coefficient of uniformity C_u describes the ratio of the volume fractions of coarser and finer particles, and is essentially a measure of the slope of the grading curve.

1.4 Scope and limitations

1.4.1 Scope

In this study the concern was aggregate particle size distribution. Importantly, this research was not a study of the influence of particle packing density. The influence of packing density is covered in great detail in the literature and was therefore eliminated as a factor in this research by maintaining a constant aggregate packing density throughout all experimental samples. In the lab experiments, as far as possible, other inputs not critical to the research objectives were held constant, including water/binder ratio and binder content.

In order to remain in the realms of practical concrete specifications, the variations in aggregate grading were selected such that the fineness modulus and 4.75 mm and 75 µm size fractions were within particular limits. These limits were designated through the evaluation of relevant USA, European and South African standards.

The role and effects of grading of both coarse and fine aggregate were studied. However, particle sizes smaller than 75 µm exhibit behaviour and effects unique from larger aggregate sizes. The proportion of the fine aggregate constituted of aggregates finer than 75 µm was therefore held constant at 5 % by mass.

1.4.2 Limitations

The research had three limitations. The first was that the preparation of aggregates to be used in lab tests called for the use of packing models and packing density measurement techniques. Whilst both were selected in part because they were the most reliable methods available, there was a certain amount of uncertainty with each.

There are aspects related to aggregate grading which are co-dependent. For example, the volume fraction of coarse and fine aggregate is dependent on the fineness modulus. Thus it is difficult to isolate single properties to be studied and the analysis of the results had to take account of multiple variables.

The results for chloride conductivity index and water sorptivity index tests showed a high level of variability, in excess of that found in other studies (Nganga, 2011; Mackechnie et al., 2006). Evaluation of the procedures followed and inspection of the test specimens did not indicate any particular reasons for an unusual level of variability and samples consisted of 4 specimens as is common practice in the South African Durability Index Approach. Further tests would be helpful in verifying the findings of this research.

1.5 Plan of development

First a review of literature is presented, given in Chapter 2. This begins with a description of the concrete microstructure, followed by an overview of the factors that influence concrete durability, with a detailed look at transport properties. The literature review gives attention to concrete aggregate, with particular focus on the influence of different particle sizes and particle size distribution. Thereafter a critical review of the specifications of South African, USA and British standards, pertaining to the physical characteristics of concrete aggregates is presented. Finally existing particle packing models are reviewed.

The experimental methodology is presented in Chapter 3, which describes the selection of test parameters, and outlines the approach taken in preparing the aggregates for the laboratory tests. Use was made of the Modified Toufar Model, the theory behind which is presented in detail. The laboratory tests consisted of the South African Durability Index method which included measurement of the oxygen permeability index, the water sorptivity index and the chloride conductivity index as a means to characterise the potential concrete durability, as well as accelerated carbonation tests as a means to characterise concrete penetrability. The method by which each of these was carried out is described.

Analyses of data together with discussions of the findings are presented in Chapter 4. Statistical methods including correlation and regression analysis and hypothesis tests were employed to distinguish whether the variations in the test parameters had significant effects on the measured characteristics and if so which of the parameters was most accountable for the observed effects. A discussion uses the findings of the analysis to address the research questions.

Finally, in Chapter 5, conclusions are drawn from the results and recommendations for how aggregate grading may be considered in durability focused concrete specification, as well as where further research may be of benefit.

2. Literature review

2.1 Introduction

The role of aggregates in concrete goes beyond the traditional conception of it being an inert filler and is becoming increasingly important as designers move towards performance-based specification. The review of literature presented herein provides a platform to further investigate the role of particle size distribution in optimising concrete durability. The first section presents the concrete microstructure which is of critical importance to understanding concrete penetrability, which is covered in the second section. Next the physical properties of aggregate and their effects on concrete properties are outlined, followed by a critical review of the methods for specification of concrete aggregate. Finally, existing packing models are reviewed for the selection of the one most suitable for use in this research.

2.2 Concrete microstructure

Concrete is made up of three component phases, namely hydrated cement paste, aggregates and the interfacial transition zone (ITZ). The bulk of these phases constitute the concrete macrostructure. The microstructure is the structure of these phases which is not visible to the unaided human eye. This is typically any resolution smaller than 200 μm. The micro-structure is defined by the amount, type, size, shape and distribution of these phases. The properties and behaviour of the material are strongly linked to its microstructure. To understand why concrete exhibits particular properties it is therefore important to understand the phases that constitute its microstructure. The remainder of this sub-section therefore focuses on developing an understanding of the three phases.

2.2.1 Aggregates

It is the physical rather than the chemical or mineralogical characteristics of aggregates which typically affect concrete properties. The physical properties are discussed in detail in Section 2.4. Aggregates are usually stronger than the hydrated cement paste and therefore are typically not the determining factor with regard to concrete strength. However, as is discussed in detail in Section 2.2.3, the extent of the ITZ phase is strongly linked to aggregate size (Mehta & Monteiro, 2006).

2.2.2 Hydrated cement paste

Hydrated cement paste is the product of the reaction between anhydrous cement and water. The composition of anhydrous portland cement produced in South Africa is given in Table 2-1. Each compound is given in the standard formula as well as the form of the abbreviated notation commonly used in cement chemistry.

Table 2-1: Composition of cement produced in South Africa (Grieve, 2009)

Compound	Formula	Abbreviation	% by mass in cement
Tricalcium silicate	$3CaO.SiO_2$	C_3S	60 - 73
Dicalcium silicate	$2CaO.SiO_2$	C_2S	8 - 30
Tricalcium aluminate	$3CaO.Al_2O_3$	C_3A	5 - 12
Tetracalcium aluminoferrite	$4CaO.Al_2O_3.Fe_2O_3$	C_4AF	8 - 16
Magnesia	MgO	M	1.9 - 3.2
Gypsum	$CaSO_4$	-	4.4 - 6.7
Free Lime	CaO	-	0.2 - 2.5

Table 2-2: Name and content by volume of constituents of hydrated cement paste (Mehta & Monteiro, 2006)

Compound	Formula	Abbreviation	% by volume in hydrated cement
Calcium silicate hydrate	$3CaO.2SiO_2.3H_2O$	$C_3S_2H_3$	50 - 60
Portlandite	$Ca(OH)_2$	CH	20 - 25
Calcium sulfoaluminate hydrates including: Ettringite Monosulphate hydrate		 $C_6AS_3H_{32}$ C_4ASH_{18}	15 - 20
Anhydrous cement particles	-	-	*

* Content depends on the particle size distribution of anhydrous cement particles and the degree of hydration.

The components listed in Table 2-1 are consumed in the hydration reactions which result in a hydrated cement paste that has four primary solid constituents. The names and percentages of the total volume of the hydrated cement paste which they occupy are given in Table 2-2. With complete hydration, 1000 g of anhydrous portland cement will combine chemically with 280 g of water to form 615 g of calcium silicate hydrate ($C_3S_2H_3$) (represented by the acronym CSH) and 255 g of calcium hydroxide (CH) (Grieve, 2009). Volumetrically, through the process of hydration the water and anhydrous cement particles of the fresh cement paste are gradually replaced, in similar volumetric proportions, by hydration products,

such that there is very little change in volume between fresh and hardened cement paste. This characteristic is of great practical importance. The components that make up the hydrated cement paste are depicted schematically in Figure 2-1 and a scanning electron micrograph image of hydrated cement paste is shown in Figure 2-2.

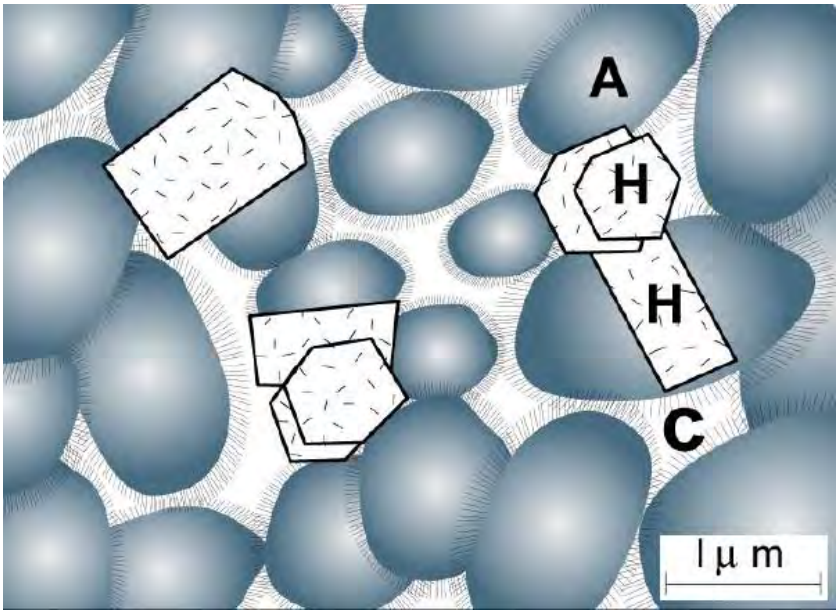

Figure 2-1: Schematic of a well hydrated portland cement paste depicting (A) aggregation of C-S-H particles; (H) hexagonal crystalline products such as calcium hydroxide and monosulphate hydrate and (C) capillary spaces (Mehta & Monteiro, 2006)

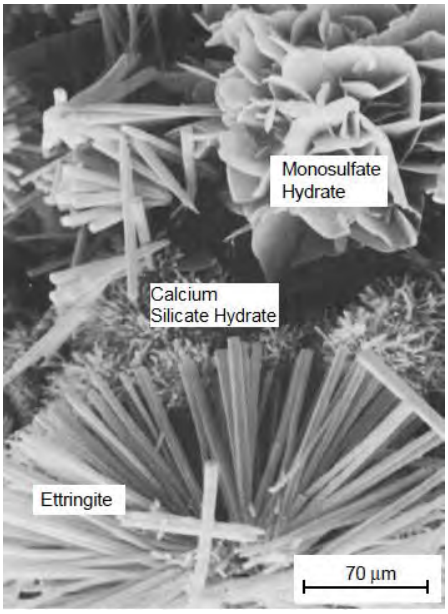

Figure 2-2: Scanning electron micrograph depicting elements of the of the concrete microstructure, including calcium silicate hydrate ($C_3S_2H_3$), monosulphate hydrate (C_4ASH_{18}) and ettringite ($C_6AS_3H_{32}$) (Mehta & Monteiro, 2006)

At a water/cement ratio of 0.4 there is just enough water for all cement to hydrate entirely (Czernin, 1980). This will lead to the densest possible cement paste, of which typically two thirds will be solid and one third pores (Grieve, 2009). These pores are depicted in Figure 2-1. Although pores account for a large proportion of the volume, the most dense hydrated cement pastes have a permeability significantly lower than that of most natural rocks. This is because of the smallness of the gel pores and the fact that at water/cement ratios less than 0.7 the capillaries become disconnected (Grieve, 2009). The section that follows discusses the different voids found in cement paste.

Voids in hydrated cement paste

The porosity of hydrated cement paste is determined by the initial water/cement ratio, the degree of hydration, the content of extenders and the extent of compaction (Hearn, 1994). There are three types of voids that may be found in hydrated cement paste, namely spaces that form between layers of CSH (gel pores), capillary voids and entrapped air voids. The relative scale of these different voids is represented in Figure 2-3.

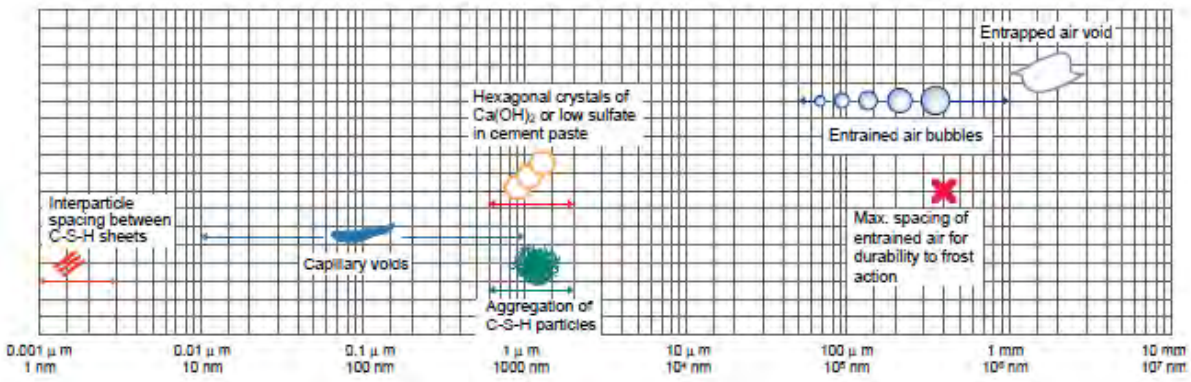

Figure 2-3: Illustration of the relative scale of various voids found in concrete (Mehta & Monteiro, 2006)

Gel pores

Gel pores are spaces that exist between layers within the CSH structure. Gel pores range in size from 5 and 25 Å (Feldman & Sereda, 1970). The loss of water from these spaces can result in creep and shrinkage deformations. However, gel pores are too small to influence penetrability or strength (Mehta, 1993).

At a water/cement ratio of 0.4 the products of hydration in the hardened cement paste exactly fill the space that was occupied by the water and anhydrous cement in the fresh cement paste (Czernin, 1980). Here, 34 % of the volume of the hydrated cement paste is occupied by gel pores, as illustrated in Figure 2-4 which shows the absolute volumetric proportions of the constituents of fresh and hydrated cement paste. It must be noted that the above statement and

Figure 2-4 are based on the assumption that all anhydrous cement particles are completely consumed in hydration, such that there are no remnants of anhydrous cement particles in the hydrated cement paste.

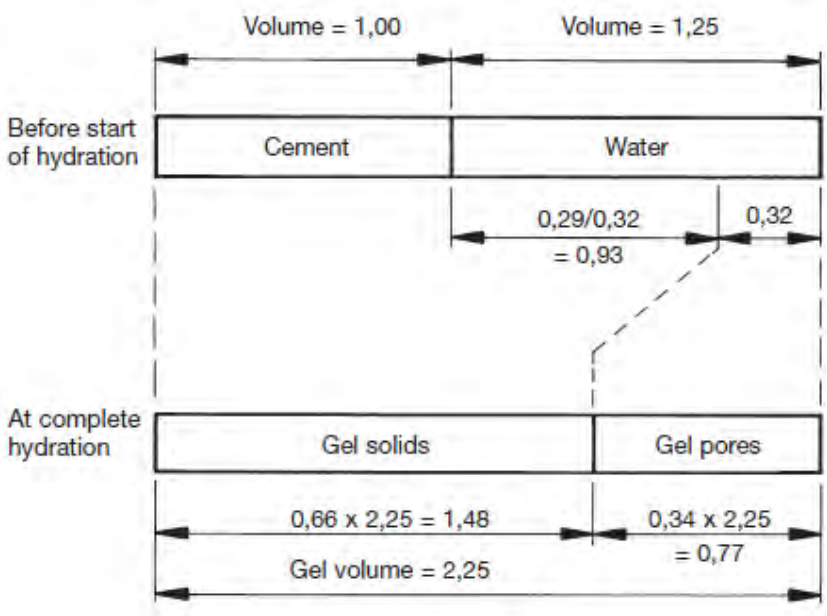

Figure 2-4: Absolute volumes of phases of cement paste for a w/c ratio of 0.4 (Grieve, 2009)

Capillary voids

The bulk density of hydrated cement paste is around two times that of anhydrous cement. Gradually, as the hydration reactions progress, the water and anhydrous cement that constitute the fresh cement paste are transformed into products of hydration. However, after hydration, the hydrated cement paste will typically still contain some anhydrous cement particles and water. The spaces occupied by water are capillary voids. The size of the capillary voids is determined by the distance between the anhydrous cement particles in the fresh cement paste - a function of water/cement ratio - and the degree of cement hydration (Mehta & Monteiro, 2006). Theoretically capillary voids begin to occur at water/cement ratios greater than 0.4. This is depicted in Figure 2-5.

Capillary voids have measurements ranging from 3 to 5 μm in cement pastes of high water/cement ratio to 10 to 50 nm in well hydrated cement pastes of low water/cement ratio. Macropores are capillary voids that are larger than 50 nm and micropores are those capillary pores that are smaller than 50 nm. It is macropores that have an influence on both penetrability and strength of hardened cement paste (Mehta & Monteiro, 2006).

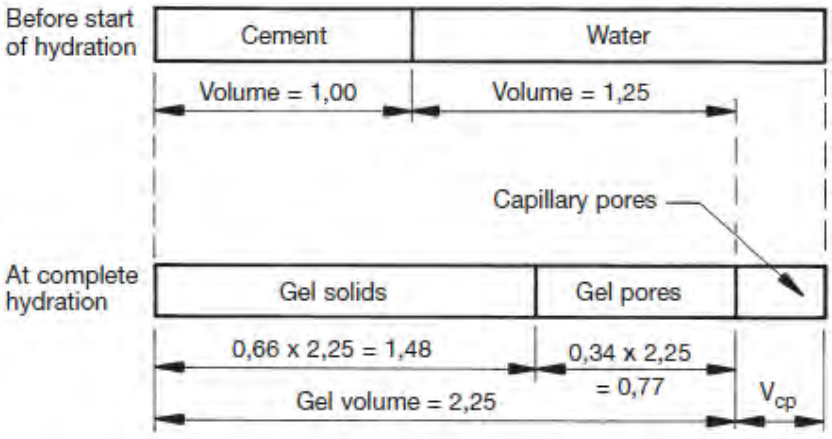

Figure 2-5: Absolute volumes of phases of cement paste for a w/c ratio greater than 0.4 (Grieve, 2009)

Air voids

Air voids present themselves through entrapment due to the inability of compaction techniques to remove all pockets of air during mixing and placement of fresh concrete, as well as, in applications where they are desired, through the action of air-entraining admixtures. Entrapped voids can be as large as 3 mm and entrained voids between 50 and 200 µm (Mehta & Monteiro, 2006).

2.2.3 Interfacial transition zone

Winslow and Liu (1990) found that, compared to pure cement paste, the cement paste in both mortar and concrete samples had different pore structures. The paste in the mortar and concrete both had a greater total porosity. Furthermore, this additional porosity was largely constituted of pores of a greater diameter than the largest pores observed in the plain paste, which has obvious implications for the penetrability. The pastes in mortar and concrete were found to have similar pore structures. (They believed that this was due to the fact that a large portion of the total aggregate surface area in concrete is accounted for by the fine aggregate. Thus the mortar – with only fine aggregate – had similar aggregate surface area which gave it a similar pore structure.) Halamickova et al. (1995) found that this increased porosity was reflected by transport coefficients for permeability and ion diffusivity.

Through studies using scattered electron microscopy (SEM), a distinct region of greater porosity and different concentrations of the solid constituent compounds to that of the bulk cement paste was observed to surround the aggregate particles. This interfacial transition zone typically had a thickness of 40 to 50 µm (Bentz, et al., 1992; Scrivener & Gartner, 1987; Bentur & Cohen, 1987). Ping et al. (1991) used electrical conductivity methods to characterise the ITZ and around fine aggregate particles of different sizes. It was found that the paste around at the aggregate interface was less dense than the bulk paste. The thickness

of the region of lower density increased with increased aggregate particle size. Similar results were observed by Elsharief et al. (2003). Their study of the ITZ by way of backscattered electron imagery showed that a layer of increased porosity and lower concentrations of anhydrous cement particles surrounds aggregate particles and the thickness of this layer increased with the increase in particle size from 150-300 μm to 2.36-4.75 mm.

Winslow et al. (1994) conducted experiments in which the volume fraction of sand in mortars was varied and the samples tested under mercury intrusion porosimetry (MIP). It was found that at a particular sand volume fraction, a jump in the volume intrusion of the MIP was observed. This was attributed to the percolation of the interfacial transition zones surrounding individual particles, which created a continuous path for permeation through the samples. Using the results of Winslow and Liu (1990) it was deduced that a similar phenomenon would be observed in concrete.

Diamond and Huang (2001) dispute that the composition and permeability of the ITZ is not as different from the bulk paste as is suggested by the abovementioned authors. They concede that there is a wall effect but that the spaces it creates are filled in by CH deposits as well as deposits of CSH resulting from through solution. The deposition of CH and CSH also reduces the compositional differences claimed to exist between the paste of the ITZ and the bulk paste.

Observation of a section through a concrete sample with the unaided eye suggests that concrete is a two phase material consisting of hydrated cement paste and aggregates. However, the region of the cement paste directly adjacent to the surface of aggregate particles exhibits significantly different properties to those of the bulk cement paste. This region – called the interfacial transition zone (ITZ) - is recognised as the third, unique phase which, together with the hydrated cement paste and aggregate phases, constitutes hardened concrete.

The ITZ typically spans between 20 and 50 microns between the aggregate surface and the bulk paste. At these thicknesses the ITZ constitutes between 30 and 60 of the non-aggregate phase.

The solid constituents of the ITZ are the same as those of the bulk hydrated cement paste but are present in significantly different volume fractions. There are low concentrations of CSH and higher concentrations of ettringite. CH crystals are present. There is a very low concentration of anhydrous cement particles. The ITZ is more porous than the bulk cement paste. The structure and composition of the three phases are depicted in Figure 2-6.

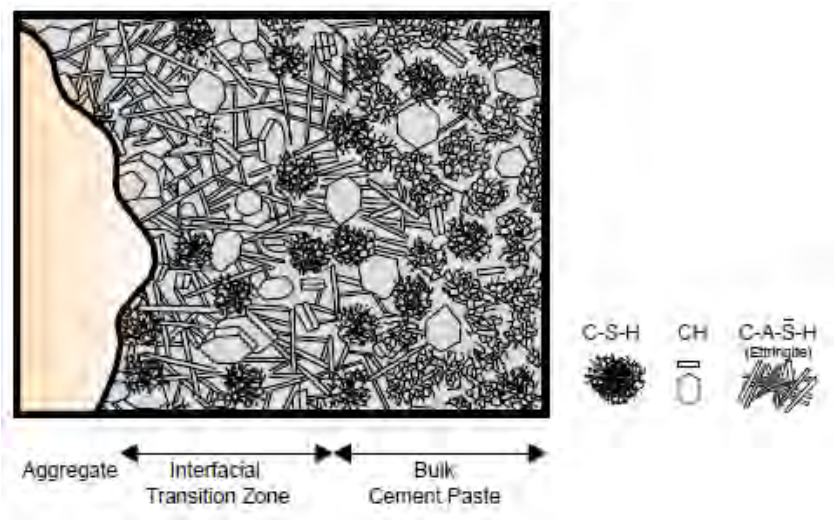

Figure 2-6: Schematic of the ITZ near the surface of an aggregate particle (Mehta & Monteiro, 2006)

There are three mechanisms which give rise to the ITZ. Firstly the fine cement particles pack inefficiently against the surface of the larger aggregate particles. This mechanism, known as the wall effect, results in a lower concentration of cement particles near the aggregate surface compared to the bulk paste further away (Alexander & Mindess, 2005). This mechanism is effective within a few tens of microns of the aggregate surface (Scrivener, 2000), and is considered to be the most significant contributor to the ITZ formation. The wall effect is depicted in Figure 2-7.

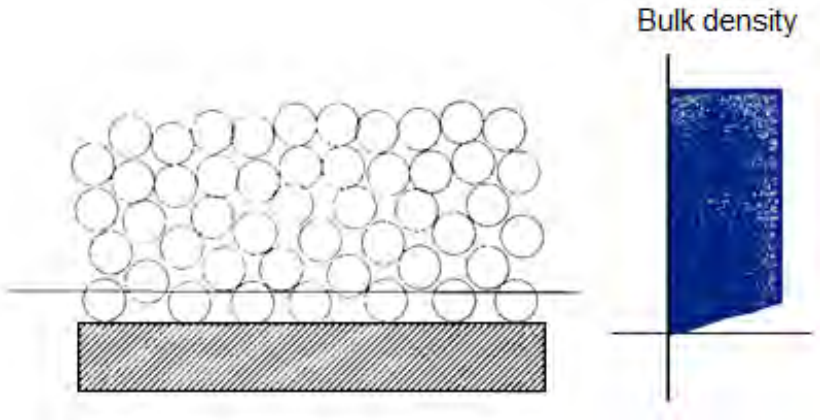

Figure 2-7: Wall effect experienced at the interface between large and small particles (Johansen & Andersen, 1991)

The second mechanism, as illustrated in Figure 2-8, is localised bleeding which causes a layer of water to form around the larger aggregate particles. This increases the water/cement ratio at the aggregate interface and causes heterogeneities which result in varying calcium hydroxide concentrations between different aggregate surfaces (Alexander & Mindess, 2005; Scrivener, 2000). The extent of accumulation of bleed water depends on the aggregate

particle size. The larger the aggregate particle the greater the amount of bleed water it will attract (Mehta & Monteiro, 2006).

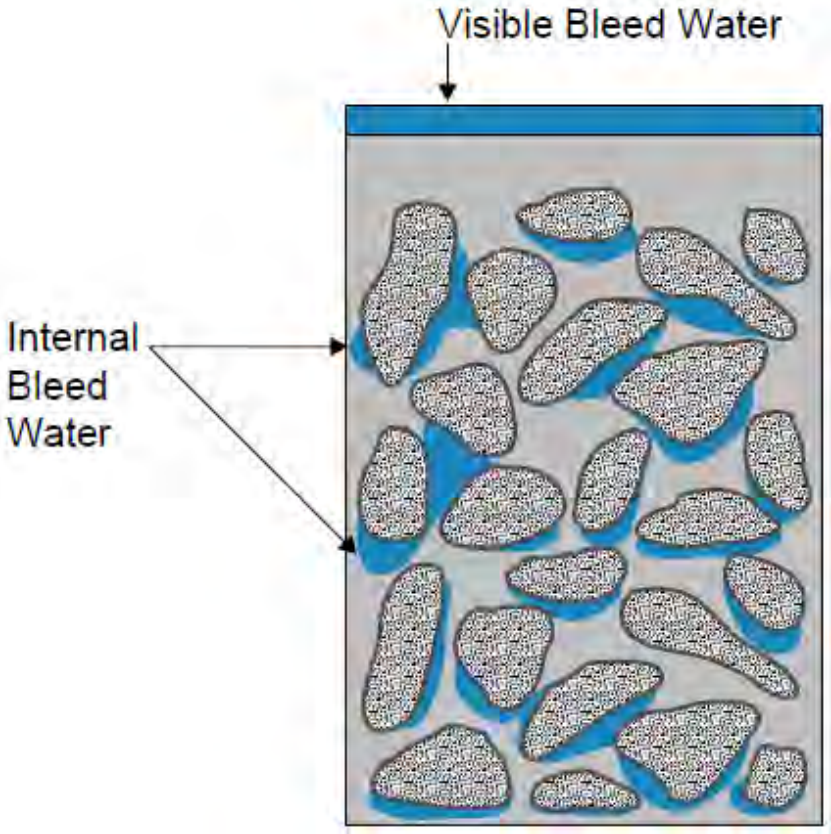

Figure 2-8: Illustration of the bleed water that accumulates around larger aggregate particles (Mehta & Monteiro, 2006)

Finally, the reaction at the aggregate surface which forms a chemical bond between the aggregate and the cement paste has been found to contribute to the different characteristics observed in the ITZ. Other than in the case of reactive aggregates this mechanism only has effect within 1 μm of the aggregate surface and is therefore generally of little concern (Scrivener, 2000).

When aggregate particles are sufficiently spaced, the ITZs around individual particles are separated by bulk paste which forms discontinuities between these more penetrable regions. However, as the aggregate concentration increases, the ITZs become increasingly connected. At a great enough aggregate concentration the interconnection between ITZs is great enough that there is a continuous path of this more penetrable phase that runs through the concrete. This phenomenon - known as percolation – is depicted schematically in Figure 2-9. At the threshold aggregate concentration at which percolation begins to occur, there is a noticeable rise in permeability. However, what would be an even greater instantaneous jump is

moderated by inconsistencies in the bulk paste, as well as bridging effects that occur with increasing aggregate concentrations. Further increase in aggregate concentration beyond this critical point causes further, but more gradual, increase in penetrability. (Alexander & Mindess, 2005).

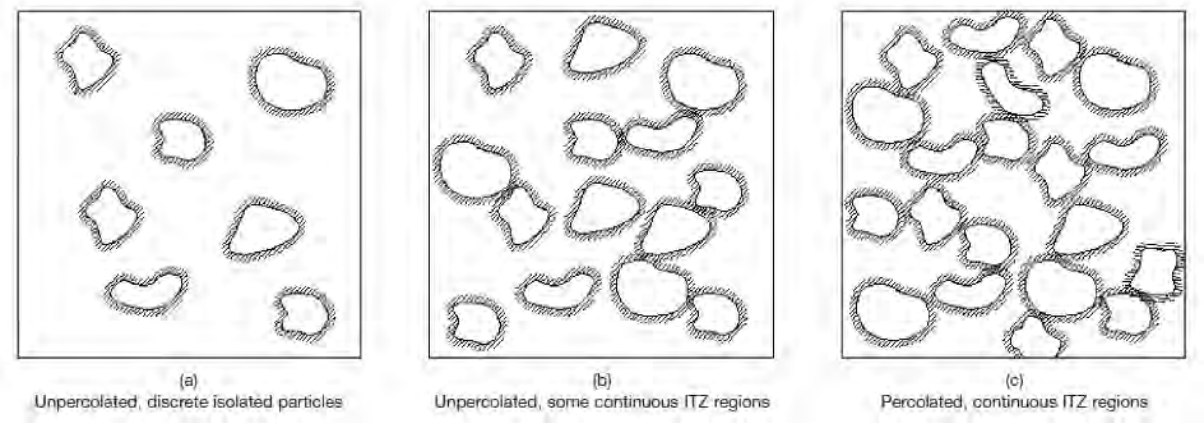

Figure 2-9: The overlapping of the interfacial transition zone with increasing aggregate concentration, eventually leading to percolation (Alexander & Mindess, 2005)

2.3 Concrete durability

Durability is the ability of a concrete structure to withstand the conditions of the environment in which it exists without any loss of serviceability or need for unplanned maintenance within the duration of its design life (ASTM, 1988). Deterioration of a concrete structure may be brought about either by physical or chemical mechanisms, as listed in Table 2-3. Of these, corrosion of steel reinforcement is one of the foremost causes of premature deterioration of structures. Along with the other chemical deterioration mechanisms, it is caused by the ingress of water and aggressive ions into the concrete. These deleterious agents move through the concrete via the concrete pore structure by way of transport mechanisms. The degree to which a concrete permits transport through it is known as the penetrability which depends on the size, distribution, continuity and connectivity of the pore structure (Alexander & Mindess, 2005). The pore structure of concrete was discussed in detail in Section 2.2. Depending on the nature of the environment, corrosion can either be carbonation-induce or chloride induced. The remainder of this section will firstly describe the different transport mechanisms and will then look at carbonation and chloride-induced corrosion in detail.

Table 2-3: Physical and chemical mechanisms of concrete deterioration (Ballim, et al., 2009)

Physical	Chemical
-Abrasion -Cavitation -Erosion -Freeze-thaw -Salt chrystallisation -Cracking due to loading or thermal/hygral effects	-Ionic exchange, removal or addition through reactions between products of hydration -Corrosion of steel reinforcement

2.3.1 Transport mechanisms

Ion and fluid movement occurs by way of the concrete's pore structure and therefore the extent of transport is determined by the concrete's penetrability. Penetration occurs through mechanisms of permeation, sorption, diffusion and migration. Deterioration processes of chemical attack, leaching, chloride ingress and carbonation act through these mechanisms (Ballim, et al., 2009).

Permeation

Permeation is the movement of fluids through a saturated material under an externally applied pressure (Alexander & Mindess, 2005). The extent of the permeability of concrete depends on the moisture condition of the concrete and the characteristics of the permeating fluid (Ballim, et al., 2009; Alexander, et al., 1999) as well as the characteristics of the concrete microstructure which include the narrowness and tortuosity of pores and cracks and the friction at the pore and crack walls (Nilsson, 2003).

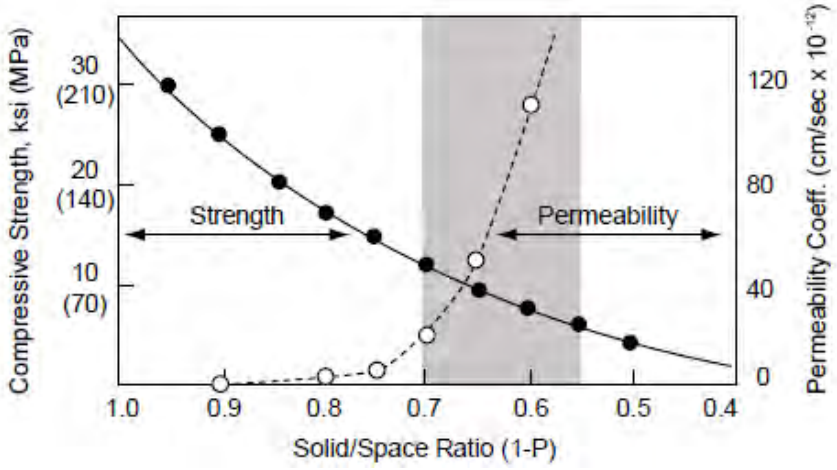

Figure 2-10: Relationship between the solid volume fraction of concrete and strength and permeability (Mehta & Monteiro, 2006)

The relationship between the coefficient of permeability to the solid volume fraction, which is inversely proportionate to the porosity, is illustrated in Figure 2-10. According to (Richardson, 2004) the greatest influences on concrete permeability is the water cement ratio and the degree of hydration, as long as materials are well proportioned and the concrete is well compacted.

Sorption

Absorption is the process whereby capillary forces draw a fluid into a porous, unsaturated material. Absorption takes place almost exclusively in capillary pores (Powers & Brownyard, 1947). The strength of the capillary force depends on the pore geometry and the degree of saturation of the material. Larger capillaries and their degree of connectedness is a major influencing factor of sorptivity. The extent of capillary porosity is largely determined by the water/cement ratio and the degree of hydration (Mehta & Monteiro, 2006). As a result, the sorptivity of covercrete is sensitive to curing and finishing, since this determines the local degree of hydration (Alexander & Mindess, 2005). Further factors which effect capillary porosity, and therefore sorptivity, of concrete include compaction, aggregate orientation and distribution and mix composition (Ballim, et al., 2009).

Diffusion

Diffusion is the process whereby a concentration gradient causes the movement of a fluid or ions through a porous material. Diffusion occurs in partially and fully saturated concrete. The rate of diffusion depends on temperature, the moisture content of the concrete, the properties of the diffusant and the diffusibility of the concrete (Alexander, et al., 1999; Ballim, et al., 2009).

There is a relationship between the permeation and diffusion properties of concrete. A theoretical approach to this relationship has been presented by (Nilsson & Luping, 1995) developed around the Hagen-Poiseuille law, based on the assumption that flow in the pore system is laminar. The relationship is given in Equation (2-1).

$$K = Constant \times D^b \quad \textbf{(2-1)}$$

K represents the permeability coefficient and D the diffusion coefficient. The power b depends on the substance being transported and empirical values have been found as shown in Table 2-4. The constant depends on the pore geometry and the diffusion coefficient of the permeating fluid.

Table 2-4: Empirical values b values (Nilsson & Luping, 1995)

Substance in permeation	Substance in diffusion	b
Water	Water vapour	1.80
Gas	Gas	1.00
Water	Ions	1.50

It is noted that the flow of gasses is influenced by the pore moisture content and the permeating/diffusing species can interact with the pore surface. These factors are not accounted for in Equation (2-1).

Migration

The process where an electric field causes the movement of ions in a solution is known as migration (Ballim, et al., 2009).

2.3.2 Carbonation

Reinforcement corrosion occurs through one or both of two mechanisms only. These mechanisms are depassivation of the steel through reduced pH of the surrounding concrete by carbonation and the penetration of chloride ions (beton, 1982). Carbonation is a physicochemical process which involves the penetration of concrete by externally derived carbon ions and the reaction between these ions and concrete hydration products. Carbon ions are available in increasing abundance in atmospheric carbon dioxide. Thus, if conditions of temperature and moisture content are correct, a concrete structure will be susceptible to carbonation, underlining the importance of improving concrete resistance to carbonation. This section will first discuss the physicochemical processes involved in carbonation and then look at the conditions that influence carbonation.

Chemical reactions

Carbonation involves a number of chemical reactions. However, Equation (2-2 represents the reaction which is detrimental to concrete durability. The consumption of portlandite causes with a drop in pH from around 12.5 to around 8.5, resulting in the depassivation of the passivating gamma-ferric layer which surrounds steel in an alkaline environment and protects it from corrosion (Ballim, et al., 2009).

$$CO_2 + Ca(OH)_2 \rightarrow CaCO_3 + H_2O \quad \textbf{(2-2)}$$

The carbonation reactions form part of a broader physicochemical process which constitutes carbonation. The physicochemical process includes the following steps (Papadakis, et al., 1991b):

1. Carbonatable materials are produced through the hydration reactions;
2. Atmospheric CO_2 diffuses into the gaseous pores of concrete;
3. $Ca(OH)_2$ dissolves in the pore water and diffuses through the pore structure of the concrete in an aqueous phase;
4. CO_2 dissolves in the pore water and reacts with the dissolved $Ca(OH)_2$;
5. CO_2 reacts with other solid products of hydration in the hardened cement paste;
6. The pore volume is reduced as it is taken up by products of hydration and carbonation;
7. Water vapour condenses on the walls of the concrete pores to a point where equilibrium is reached at the ambient temperature and relative humidity conditions.

From the above steps it is evident that transport properties - diffusion most significantly - play a significant role in the carbonation process. Furthermore, the flow of moisture through the concrete is due to capillary suction and the chemical reactions involved in carbonation take place in the pore solution (Papadakis, et al., 1991a). The pore structure of the concrete is of importance to carbonation. Transport properties are discussed earlier in this section and the concrete pore structure is discussed in Section 2.2.

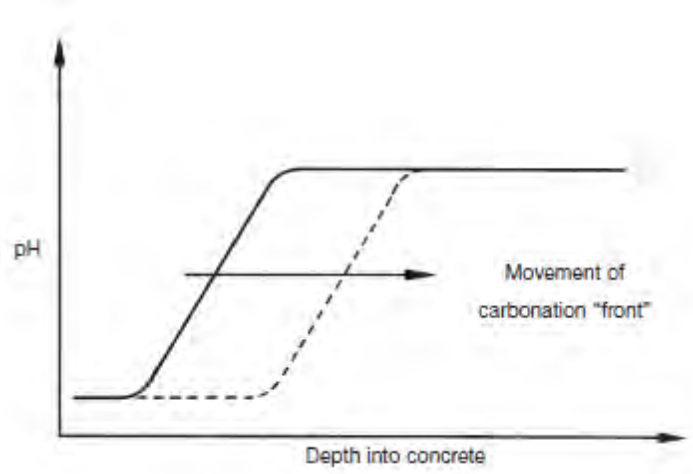

Figure 2-11: Progression of carbonation from concrete surface as a front (Ballim et al. 2009)

The progression of carbonation through concrete is idealised as a front. This idea is illustrated in Figure 2-11. The commonly used test of carbonation depth involves the use of phenolphthalein solution as an indicator. At pH below 9 the solution is a clear liquid but above 9 it takes on a deep purple colour. Thus when applied to a section cut through a carbonated specimen, it presents a line where it changes colour where the pH goes above 9. This corresponds with the concept of a carbonation front. However, the indicator test does not

show the full depth of carbonation. There are areas at greater depth that will have undergone carbonation to a lesser extent and where pH has been reduced but not yet gone below 9. In the study of concrete durability the indicator test suffices as depassivation, and thus corrosion, only occurs at pH < 9 (Thiery, et al., 2007).

Environmental factors affecting carbonation

Moisture content

The moisture content of concrete, which is dependent on the environmental relative humidity, is critical to carbonation. A low RH will reduce the pore moisture which reduces the amount of CO_2 and hydration products that can dissolve. On the other hand, if the RH is too high and the pores contain too much moisture, CO_2 will be unable to penetrate the concrete. The optimal environmental RH range for carbonation is 50 to 70 % (Wierig, 1984).

Temperature

The temperature affects both the reaction rate and the degree of dissolution and saturation of different species in water. At lower temperatures a larger amount of portlandite and carbon dioxide can dissolve in water, meaning that there are more moles that can react. However, at lower temperatures there is a lower reaction rate (van Balen, 2005).

Carbon dioxide concentration

Carbon dioxide penetrates concrete by way of diffusion which is the movement along a concentration gradient. Thus the concentration of carbon dioxide influences the carbonation rate (Salvoldi, 2010).

Carbonation prediction models

It is not necessary here to give a thorough review of carbonation models. However, it is useful to note that, as first observed by Nishi (1962), the carbonation depth is a function of the square root of time as shown below in Equation (2-3) .

$$x = A\sqrt{t} \tag{2-3}$$

Where x is the carbonation depth (mm), t is time (generally in years) and A is the carbonation coefficient (mm/annum$^{1/2}$). The relationship in Equation (2-3) has been validated using Fick's first law of diffusion and mass balance equations (Meyer, et al., 1967).

2.4 Aggregates in concrete

Aggregates have in the past been, and often continue to be, considered as inert fillers, serving only to increase the bulk of concrete and reduce the cost. However, aggregates constitute up to 80 per cent of the bulk volume of concrete and consequently they have a significant influence on concrete properties and performance. Aggregates give concrete volumetric stability and provide similar thermal expansion properties to steel, allowing for steel reinforced concrete to function effectively as a composite. Cement paste alone would not allow for this property. Furthermore, aggregates significantly reduce moisture related deformations in concrete. Concrete typically exhibits shrinkage of 10 to 15 per cent of that of pure cement paste. They restrain creep and thereby reduce long-term concrete deformation. They generally improve the strength and stiffness of concrete and provide necessary rigidity. They provide wear resistance as well as traction for concrete in applications subjected to traffic. As aggregates tend to be the most durable material in concrete, they typically improve concrete durability (Alexander & Mindess, 2005).

2.4.1 Properties of aggregates - overview

There are several aggregate properties – physical, mechanical and chemical – which have influences on the fresh and hardened concrete properties. A summary of the important aggregate properties is given in Table 2-5. A similar table is presented in far greater detail by Alexander and Mindess (2005). It is not necessary to give a detailed explanation of all of the properties in Table 2-5 here. However, further discussion of some of the properties is helpful.

Table 2-5: Important aggregate properties and their significance in concrete (NSA, 1980)

Aggregate property	Significance
Size and grading	Workability of fresh concrete, economy, strength
Hardness, toughness and wear resistance	Resistance to abrasion
Soundness	Durability, resistance to weathering
Porosity, permeability and absorption	Resistance to freeze-thaw, durability, mix proportioning calculations
Particle shape and surface texture	Workability of fresh concrete, strength, architectural appearance when exposed
Volume stability	Drying shrinkage
Thermal properties	Durability
Specific gravity and bulk unit weight	Mix proportioning calculations and concrete density
Chemical stability	Resistance to chemical attack, strength, durability

Size and grading

It is noted in Table 2-5 that aggregate size and grading has an effect on economy. The reason for this is two-fold.

The first reason is that grading directly influences density at which the aggregate particles pack together (Johansen & Andersen, 1991). This will be referred to as aggregate packing density from here on. The greater the aggregate packing density the less void space between aggregate particles there is that physically needs to be filled by cement paste. Since the cement is the most expensive component, aggregates with greater packing densities yield more economical concretes.

The second reason is linked to the effect that size and grading has on workability. For an aggregate of a grading that gives poor workability, the concrete will require more water to achieve a given workability than a concrete with aggregate with a grading that gives better workability. To achieve similar strength the water/binder ratio would need to be maintained, thus the former would require more cement and thus be less economical. Workability has been found to be linked to packing density but also to the yield stress in shearing – the governing factor of the two depending on the shear rate (Johansen & Andersen, 1991; de Larrard, 1999). The yield stress is the dominant factor at low shear rates (Tattershall & Banfill, 1983).

Aggregate grading and packing density is a central topic in this research and as such are reviewed in greater detail in Sections 2.4.2 and 2.4.5 respectively.

Particle shape and surface texture

Particle shape is a factor that determines aggregate packing density. As highlighted earlier in Section 2.2.1, aggregates are usually the strongest phase in concrete. Thus, by dilution of the weaker paste phase, increased aggregate packing density increases strength. This is therefore the first mechanism through which aggregate shape influences strength. The second is that aggregate shape determines the level of tortuosity for crack propagation. This is the complexity of the path through the connected regions of cement paste that a propagating crack must follow.

Surface texture influences the bond strength between the paste and aggregates and thereby influences the strength of the concrete.

Changes in grading are common in coarse aggregates because of the tendency for segregation during stock-piling, transportation and other handling situations (Galloway Jr., 1994).

2.4.2 Grading

The aggregate grading describes the quantitative distribution of all of its various particle sizes. It is characterised as the proportion of particles which pass through, or are retained on, sieves with square openings of particular apertures (Grieve, 2009). Concrete aggregates are a composite of different size fractions, namely coarse aggregates and fine aggregates. These size factions have different effects and thus have unique sets of requirements and considerations for their specification. Fine and coarse aggregates are discussed separately in Sections 2.4.3 and 2.4.4 respectively, but first aspects of grading that apply to both fine and coarse aggregates are looked at in more detail.

The procedure for determining aggregate grading is the sieve analysis. This involves passing the aggregates through a stack of sieves of standard aperture with decreasing aperture sizes from top to bottom, usually with the application of shaking or vibration. The precise procedure to be followed is specified in standards such as the ASTM C136, BS EN 933-1 or SANS 201. Standard sieve sizes of different countries can be different. The sieve sizes for ASTM, BS and SANS as well as ISO standards are presented in Tables 2-6 and 2-7. The results of a sieve analysis are typically presented on a graph in the form of a grading curve with the log of the sieve aperture on the x-axis and the percentage of the total mass of aggregates which passes a particular sieve aperture on the y-axis.

Table 2-6: Fine aggregate sieve sizes below 1 mm from various standards

ASTM C33	ISO 565 Principle R20/3	SANS 3001 AG1
600 µm		600 µm
	500 µm	
		425
	355	
300		300
	250	
	180	
150		150
	125	
	90	
75		75
	63	

Table 2-7: Coarse aggregate sieve sizes from various standards

ASTM C33	BS EN 22620: 2013	ISO 565 Principle R20/3	SANS 3001 AG1
75.00 mm			75.0 mm
63.00	63.0 mm	63.0 mm	63.0
	56.0		
50.00			50.0
	45.0†	45.0	
	40.0‡		
37.50			37.5
	31.5	31.5	
25.00			25.0
	22.4†	22.4	
	20.0‡		20.0
19.00			
	16.0	16.0	
	14.0‡		14.0
12.50	12.5‡		
	11.2†	11.2	
	10.0‡		10.0
9.50			
	8.0	8.0	
			7.1
	6.3‡		
	5.6†		
			5.0
4.75			
	4.0	4.0	
2.36			
			2.0
		1.4	
1.18			
	1.0	1.0	1.0

† BS EN 12620: 2013 basic set plus set 1
‡ BS EN 12620: 2013 basic set plus set 2

A concrete aggregate grading can fall within one of three nominal classifications. These are described below (White, 1991):

Uniform: Aggregate consists of predominantly one particle size;
Continuous: Aggregate contains particles across a wide range of sizes. Also called well graded

Gap: Aggregate is deficient in one or more of the intermediate particle sizes (Shacklock, 1959).

These nominal aggregate gradings are represented schematically in Figure 2-12 and Figure 2-13 gives representative grading curves for each.

In practice either gap or continuously graded aggregates are used. Which of the two is employed depends on the local practice which in turn usually depends on what is locally available (Alexander & Mindess, 2005).

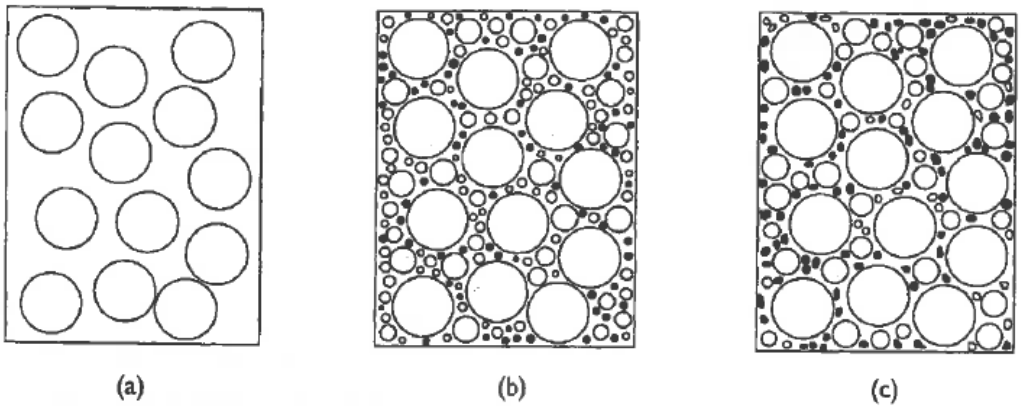

Figure 2-12: Schematic of (a) uniform grading, (b) continuous grading and (c) gap grading of concrete aggregates (after Alexander and Mindess, 2005)

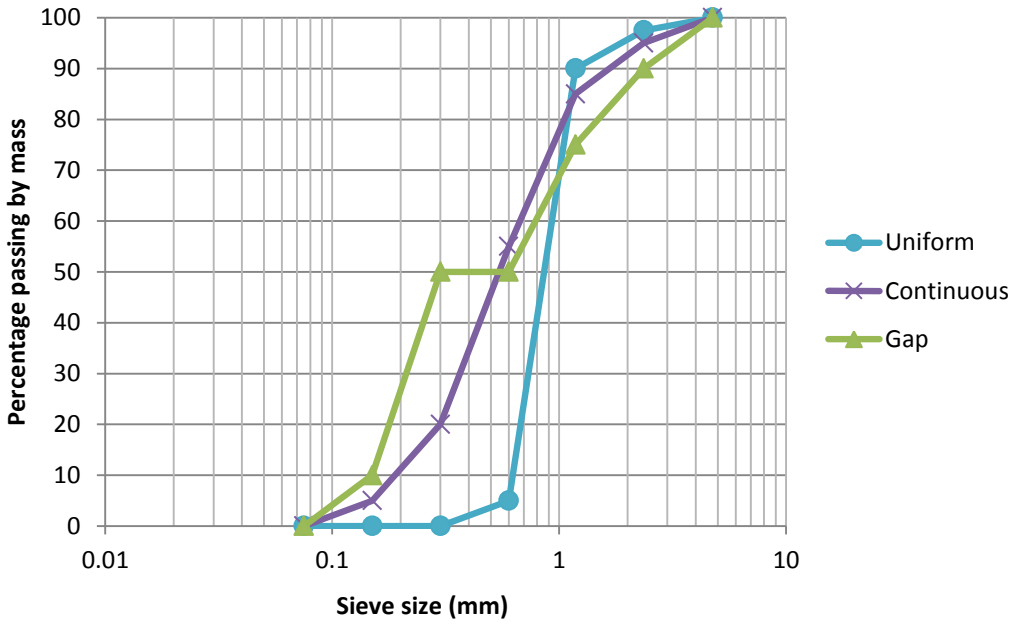

Figure 2-13: Representative grading curves that typify uniform, continuous and gap graded aggregates

Aggregate grading and concrete properties

The workability and cohesiveness of a fresh concrete are strongly dependent on aggregate grading. Thus, provided other constituents are correctly proportioned, appropriate selection of aggregate grading will give a concrete that is easily compacted and, given suitable curing, is ultimately a dense concrete of good strength and durability (Alexander & Mindess, 2005).

Gap graded aggregates have been found to create microstructural defects in the concrete as a result of internal bleeding and segregation (Johansen & Andersen, 1991). Galloway (1994) suggests that continuously graded aggregates with representative amounts of particles on each standard sieve size are most ideal and that a deficiency of particles of any size can lead to poor workability and possibly poor durability.

Continuously graded aggregates with particles of all sizes may experience particle interference and a high degree of friction which may compromise workability. This is more prevalent in aggregates with poor shape such as crushed aggregates. Sometimes it is beneficial to use gap graded aggregates formed through combining a continuously graded fine aggregate with a nominally single sized coarse aggregate. Here the gap, which lies between the fine and coarse aggregate constituents serves to reduce friction and particle interference (Alexander & Mindess, 2005).

Much of the focus in the specification of aggregates is centred on aggregate grading. This is discussed in detail in Section 2.4.6. However, Grieve (2009) notes that "despite extensive investigations carried out over many years, it has not been possible to determine from basic principles an optimum aggregate grading that will determine suitability for any particular case. Suitable gradings are thus generally arrived at empirically by trial of concrete materials in a concrete mix".

However first it is necessary to look at the property of aggregate size.

Concrete aggregates are a composite of different size fractions, namely coarse aggregates and fine aggregates. These size factions have different effects and thus have unique sets of requirements and considerations for their specification. They are discussed in separate sections below.

2.4.3 Fine aggregates

Fine aggregate - also referred to as sand - is constituted of particle sizes smaller than 4.75 mm. The portion of fine aggregates that pass through a fine sieve size, usually 80, 75 or 63 μm, is referred to as fines or dust.

Fine aggregate grading has a significant influence on the rheological properties of concrete. If the fine aggregate is too coarse it will result in a harsh mix prone to bleeding and segregation. If it is too fine there will be a large surface area which will increase water demand and there may also be segregation (Galloway Jr., 1994; Alexander & Mindess, 2005). There are particular size fractions in fine aggregates, of which a deficiency or surplus has significant adverse effects, particularly in fresh concrete.

300 µm: The coarseness of fine aggregates is determined by the percentage retained on the 300 µm sieve. In South Africa it is preferable to have 20-40 per cent of fine aggregates pass the 300 µm sieve, although ASTM C33 allows for as little as 10 per cent. Too little of the minus-300 µm fraction can lead to harshness, a lack of cohesion and therefore segregation. Too much will lead to a sticky mix with excessive water requirement (Alexander & Mindess, 2005).

150 µm: This fraction has similar effects to the 300 µm fraction. Alexander and Mindess (2005) suggest a lower limit of 3 per cent passing the 150 µm to avoid problems segregation and bleeding. A larger amount of the minus 150 µm fraction can improve workability as they come between coarser particles and facilitate them sliding and rolling over one another (Alexander & Mindess, 2005).

Alexander and Mindess note that fine aggregates below 100 µm start to have less of an effect on the ITZ as the size of the particles approaches the thickness of the ITZ and even begins to improve ITZ properties by way of the fine filler effect.

Sub-75 µm: Fines make a mix cohesive and therefore play a role in preventing segregation. The minus-75 µm fraction is the most important factor in controlling bleeding. However, too much of this fraction can lead to excessive water requirement (Alexander & Mindess, 2005).

BS EN 12620-2013 makes reference to *filler aggregate* which is defined as an aggregate where most of the material is finer than 63 µm. This is a reference to the "filler" effect, whereby sub-75 µm (or in this case sub-63 µm) particles refine the pore structure, both of the bulk pasts and in the ITZ. The filler effect results from two mechanisms. Firstly, the ultra-fine particles act as reaction nucleation sites for the precipitation sites (Powers & Brownyard, 1947). Secondly, the finer particles tend to segment the internal flow channels of water, and thereby reduce bleeding. This reduces the size of the water layer that collects at the underside of larger aggregate particles, mitigating the localised increase in water/cement ratio and thereby reducing the porosity of the ITZ (Mehta & Aitcin, 1990). This refinement of the concrete pore structure improves strength and reduces permeability.

Fineness Modulus

This is a dimensionless parameter that describes the average particle size (Grieve, 2009) and thus gives an indication of the fineness or coarseness of the aggregate (Cole & Viljoen, 2001). It is obtained by adding the total percentage of material, of the original mass of material, retained on each of the standard sieve sizes, excluding the 75 μm sieve, and dividing the total by 100.

The limiting fineness modulus range for fine aggregates for use in concrete manufacture is 1.2 to 3.5, as specified in SANS 1083:2006. A limiting fineness modulus is not specified for coarse aggregates, since coarse aggregates are usually specified and produced in nominal sizes.

Coefficient of uniformity

In soil mechanics the coefficient of uniformity, C_u, given by Equation 2-4, is used to describe the soil grading by giving an indication of the slope of the grading curve (Craig, 2004).

$$C_u = \frac{D_{60}}{D_{10}} \quad \textbf{(2-4)}$$

Where D_i is the particle size such that i % of all the particles are smaller. The name is misleading as the greater the value of Cu, the more continuously or "well" graded is the soil or aggregate sample. Beach sands have a Cu between 2 and 3 while continuously graded aggregates have a Cu of up to 15.

The coefficient of uniformity, as described above, was used by Nanthagopalan and Santhanam (2010) in their experiments to relate particle size distribution to packing density. It was found that there exists a strong correlation between the coefficient of uniformity and the aggregate packing density. This is discussed further in Section 2.4.5.

SANS 1083:2013 specifies that coarse aggregates delivered by a supplier for a project will be of a consistent grading and maintain a certain predetermined and specified adjusted coefficient of uniformity. This is represented as follows:

$$U_a = \frac{D_{60}}{D_{30}}$$

2.4.4 Coarse aggregates

Coarse aggregates contain particle sizes in the range from 4.750 mm up to the maximum specified aggregate particle size, which is project specific.

One of the most important factors to be considered in the selection of coarse aggregates is the maximum particle size. In South Africa the maximum size of aggregate is the standard sieve immediately smaller than the smallest standard sieve through which all particles pass. The same definition is used in Canada. However, no particular definition is universally accepted. In the United States, the maximum aggregate size is the smallest standard sieve size through which all aggregates pass. It is therefore important to ensure that the local practices are well understood.

The larger the maximum stone size, the less aggregate surface area there is and therefore less paste is required to entirely cover all aggregates. With reduced paste there is less shrinkage and creep and the concrete is more economical as less cement is used (Alexander & Mindess, 2005). However it is worth noting that smaller stone sizes produce concrete which is easier to handle and place and which is less prone to segregation (Grieve, 2009).

Mehta and Monteiro (2006) note that larger particles attract more bleed water, as depicted in Figure 2-8. The wall effect is also more severe at the interface of larger particles. Thus the porosity of the ITZ of larger aggregate particles tends to be greater. This is reaffirmed through the results of a study, as shown in Figure 2-14, which were published before the idea of the ITZ had been conceptualised. Galloway (1994) therefore suggests that as the concrete design strength is increased, smaller maximum aggregate sizes must be used for most efficient use of cement.

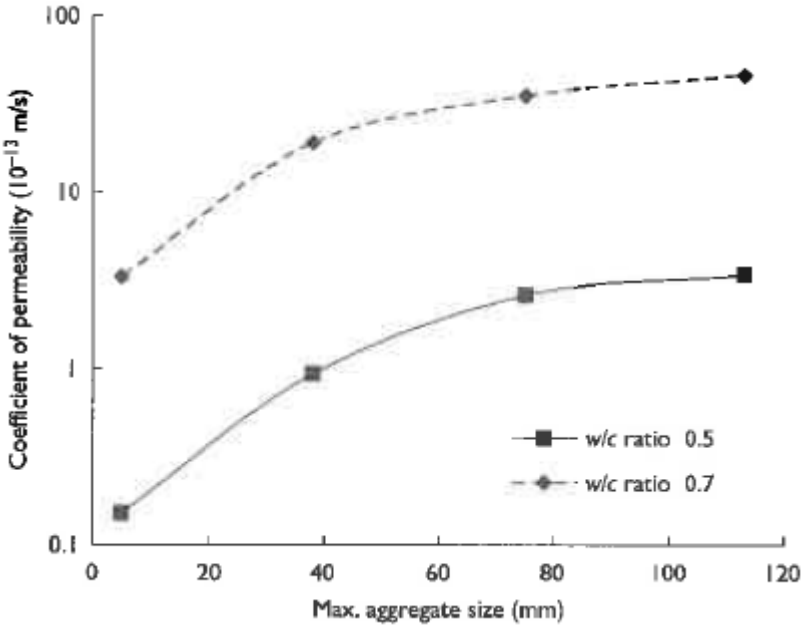

Figure 2-14: Graph showing the effects of maximum aggregate size on the coefficient of permeability of concrete (adapted from USBR, 1975)

2.4.5 Aggregate packing

Aggregates are particulate materials and the way in which the constituent particles are arranged is referred to as packing. The packing of a polydisperse mixture of particles is influenced by the following three parameters (Johansen & Andersen, 1991):

- The size of the particles in the mixture, as described by the grading curves;
- The shape of the particles;
- The method by which the particles are packed.

Particles pack against one another but – as a result of geometrical incompatibility – do not fill all the available space. Voids will be present throughout the particulate mix. The bulk density of an aggregate is the mass of that aggregate that can fill a unit volume given the void content that that aggregate will have. Packing density φ – also referred to as packing degree – is the volume fraction occupied by solids as shown in Equation (2-5, where ρ_{agg} is the aggregate particle density, ρ_{bulk} is the bulk density of the aggregate, v_s is the total volume of solids and v_t is the total volume occupied by the aggregate particles and the voids between them. Porosity is the volume fraction occupied by voids and specific volume is the inverse of packing density (Alexander & Mindess, 2005).

$$\varphi = \frac{\rho_{agg}}{\rho_{bulk}} = \frac{v_s}{v_t} \quad \textbf{(2-5)}$$

Research in the ceramics and nuclear energy industries has looked for ways of achieving the most efficient packing of particles (Johansen & Andersen, 1991; Stovall, et al., 1986). However, the greatest aggregate packing density does not necessarily produce concrete with optimum properties (Powers, 1968). Furthermore the particle shape of concrete aggregates is highly variable and irregular. Together these considerations make particle packing in concrete technology a unique and difficult problem, a fact that is reaffirmed by the amount of approaches that have been taken to accurately model aggregate packing. The various approaches are discussed in detail in Section 2.5.

The particles of different sizes in concrete aggregates interact through two mechanisms, both of which influence the aggregate packing density. The first mechanism is the wall effect where inefficiency in the packing of smaller particles at the interface of larger particles, causes a localised increase in the void content (McGeary, 1961). This effect is depicted in Figure 2-7. The second is the loosening effect which occurs when a smaller particle is slightly

bigger than the void that would exist between larger particles in a mix. The smaller particle pushes the larger particles apart (de Larrard, 1999). This effect is depicted in Figure 2-15.

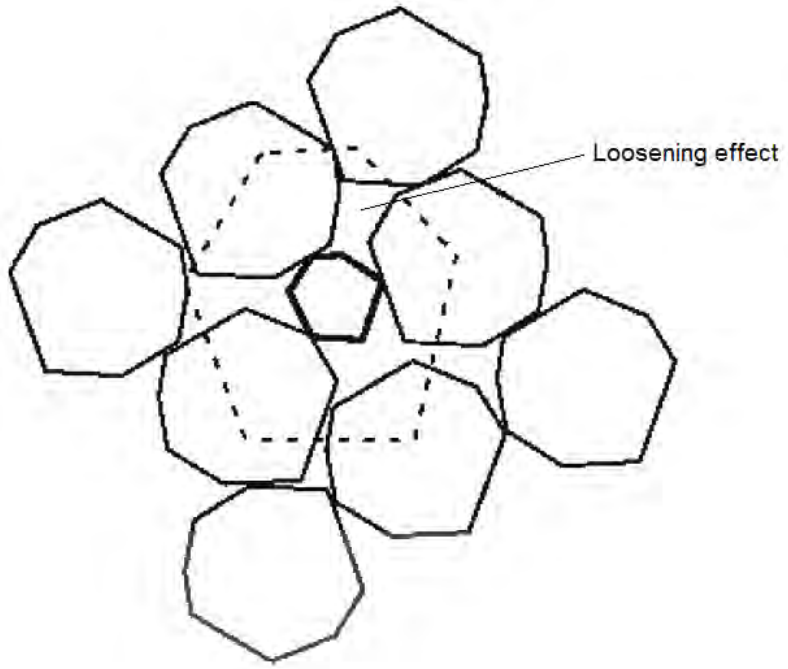

Figure 2-15: The loosening effect (de Larrard, 1999)

Packing and rheology

The effect of aggregate packing on the rheology of fresh concrete has been found to depend on the shear rate. At a low shear rate lower aggregate packing density gave the better workability, whilst at high shear rates the plastic viscosity, which was a function of the volume fraction of coarse aggregate, was more of a determinant (Andersen, 1990). This suggests that the ideal grading is dependent on the application, where high packing density is less important than the maximum aggregate size and coarse aggregate content, as required in pumped mixes, but in most other applications packing density may be the most important factor.

Packing and hardened properties

With increasing aggregate packing density there is a dilution effect whereby the more porous cement paste is substituted by less porous aggregate. Furthermore when aggregate particles are sufficiently spaced the ITZs around individual particles are separated by bulk paste which forms discontinuities between these more penetrable regions. However, as the aggregate concentration increases, the ITZs become increasingly connected. At a great enough aggregate concentration the interconnection between ITZs is great enough that there is a continuous path of this more penetrable phase that runs through the concrete. This

phenomenon is known as percolation and is depicted schematically in Figure 2-9 in Section 2.1.3 (Alexander & Mindess, 2005).

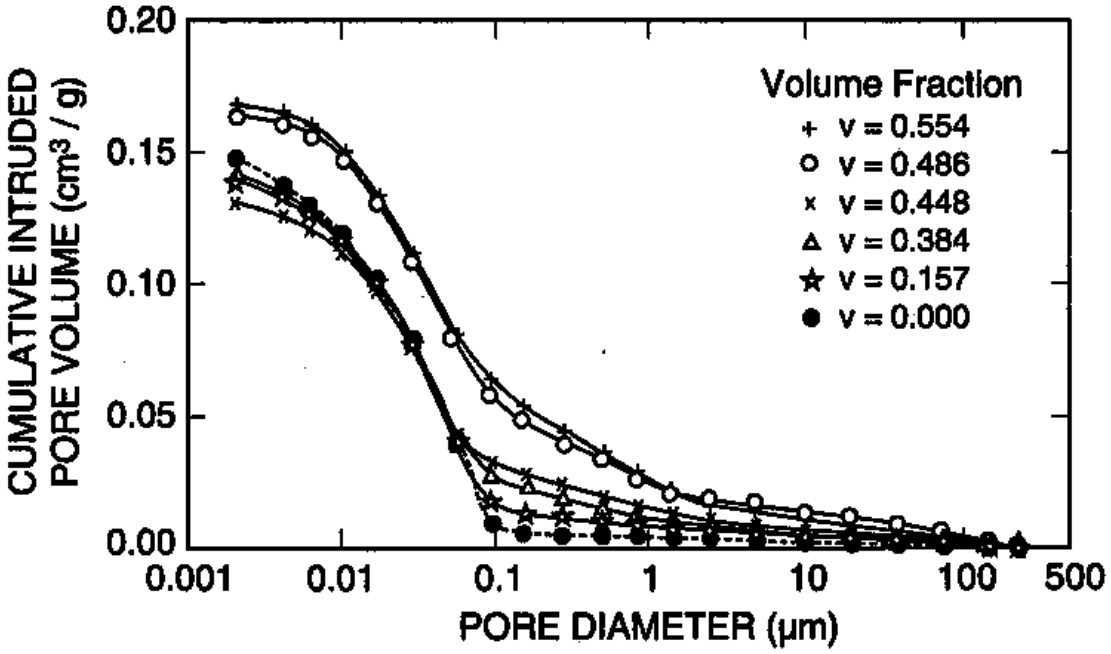

Figure 2-16: Mercury intrusion results of samples with different aggregate contents, expressed as the cumulative intruded pore volume, from largest pore diameters to smallest (Winslow et al., 1994)

The two abovementioned phenomena were observed clearly in the research of Winslow et al. (1994) as shown in Figure 2-16. In concretes with aggregate volume fractions of v = 0.448 and smaller, the total intruded pore volume decreased with increased aggregate content. This was a result of the dilution effect. There was a large increase in the intruded pore volume between concretes with v = 0.448 and v = 0.486. It was at aggregate volume fractions between these two values that percolation began to occur, thus causing a large jump in concrete penetrability. At increase aggregate volume fractions, above the percolation threshold, very little change in penetrability was observed. This increased penetrability adversely affects the concretes durability.

Given that concrete aggregate is usually stronger than cement paste, an increase in the volume fraction of concrete constituted of aggregate, in combination with the inclusion of pore-refining filler materials and/or cement extenders, leads to increased strength (Reschke, 2000). Above the percolation threshold there is evidence that increased in aggregate content leads to minor improvements in strength (Dhir et al., 2005).

Since it is the cement paste which undergoes creep and shrinkage, the aggregate inclusion has the effect of restraining these deformations in concrete. Thus increased aggregate packing density results in reduced creep and shrinkage (Neville, 1995).

Powers (1964) noted that, whilst it is not necessarily the aggregate with the greatest packing density that yields the best concrete, near maximum packing density is desirable. As discussed in the preceding section, in most applications (those not requiring pumped concrete), aggregate gradings that lead to greater packing density generally yield improved workability and thus allow for use of lower water/binder ratios, thereby allowing for improved strength and durability. Furthermore, ensuring higher aggregate packing density, and thus less cement paste volume fraction, is beneficial, given the need to reduce CO_2 emissions. Thus increased aggregate packing density often gives concrete with greater all-round performance. However, packing density should not be viewed as a measure of the optimum aggregate.

Aggregate grading and packing

Early ideas around aggregate packing were based around the belief that the maximum packing density for a given aggregate would produce the best concrete. Thus the optimal grading was seen as that which gave the greatest packing density. This was the basis around which Fuller and Thompson (Fuller & Thompson, 1907) developed the first widely used ideal grading curve for concrete aggregates. This grading curve, known as the Fuller curve, represents the starting point for the development of theory of ideal aggregate grading and was also used in packing theories which is discussed further in Section 2.5.

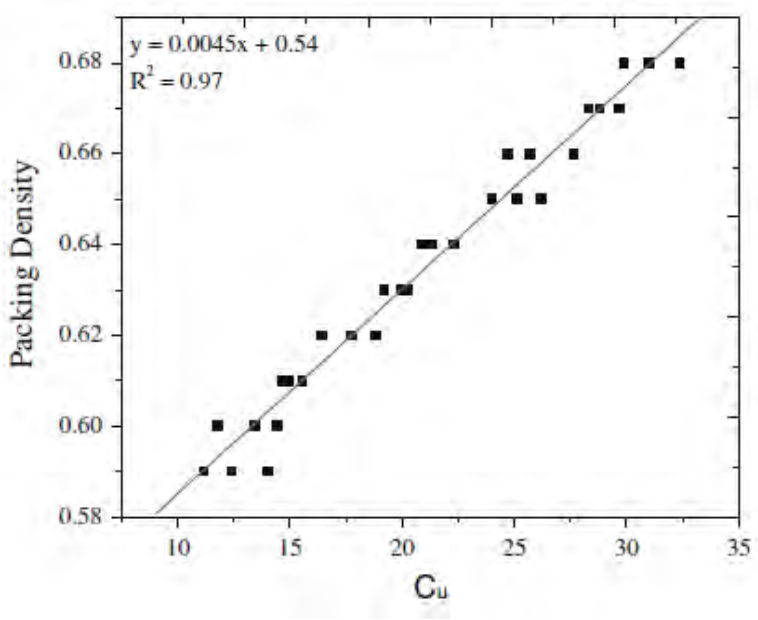

Figure 2-17: Relationship between aggregate packing and coefficient of uniformity (Nanthagopalan & Santhanam, 2012)

Powers (1968) suggested that a high aggregate packing density, but not necessarily the highest, is usually optimal. Power's work formed the basis for the widely used contemporary guidelines for mixture proportioning published in ACI 211.1-81, as is discussed in Section

2.4.7. Grading related parameters that have been observed to reflect aggregate packing density include the volume fraction of finer or coarser material in a binary mix (Johansen & Andersen, 1991) as well as the coefficient of uniformity (Nanthagopalan & Santhanam, 2012). The relationship between the latter and packing density is shown in Figure 2-17.

It must be noted that for aggregates used in concrete production, packing density is not the measure of optimum grading. The optimum grading depends on the water requirement and workability needs of the application as well as prevention of segregation and ease of finishing. Furthermore, the effects of grading on transport properties are poorly understood and it is possible that the greatest packing density may not always translate into optimised transport properties.

Measurement of aggregate packing density

A method for the measurement of aggregate packing density is presented in ASTM C 29. This method entails pouring the test aggregate by hand into a collection bucket of a particular volume, with the fall of the aggregate serving to impart some compaction energy. Once the bucket is full the aggregate is struck off and the mass of compacted aggregate in the bucket determined by subtracting the empty mass of the bucket from the combined mass of aggregate and bucket. SANS 5045 prescribes the same procedure for the measurement of aggregate packing density.

Figure 2-18: The apparatus used by Nanthagopalan and Santhanam (2010) to determine aggregate packing density

Nanthagopalan and Santhanam (2010) identified two key limitations to this method. These were that both the method of pouring aggregates and the height from which the aggregates were poured were both subjective and thus prone to error. This prompted the development of a modified technique which aimed to solve both of these problems.

The developed apparatus, as shown in Figure 2-18, consists of a steel bucket with a tightly fitting trap door attached to the bottom. The bucket has a top diameter of 340 mm and a bottom diameter of 140 mm and a height of 310 mm. This bucket sits upon a stand, suspended above a catchment bucket, such that the distance between the bottom of the top bucket and the top of the bottom catchment bucket is 200 mm. The catchment container is a cylindrical bucket with a capacity of 10 l and a diameter of 270 mm, so chosen such that the cylinder diameter is greater than 10 times the diameter of the largest aggregate. This particular apparatus was developed for an experiment where a maximum nominal aggregate size of 20 mm was used. This allows for the packing inefficiencies due to the wall effect to be avoided (Goltermann, Johansen & Palbol, 1997).

2.4.6 Aggregate specifications

This section has been included to outline the way in which aggregates are specified in South Africa as well as in Europe and the United States. It highlights significant provisions of various codes as well as relevant mix proportioning guidelines that have found wide usage. This section makes it evident that aggregate selection is very much governed by what materials are locally and economically available. As mentioned previously, whilst the perception of the role of aggregates in concrete is changing, the fact remains that it is added to concrete to increase the bulk with minimal effect cost. Economy will therefore always be a factor of foremost relevance in the selection of aggregates. Cost depends on the distance of transport between the source and the point of use and the costs of extraction and preparation. In order to keep preparation costs to a minimum and to minimize wastage, natural aggregates are typically used as they are when extracted from the source and crushed aggregates are used as they are when they come out of the crusher. Thus there is an element of control over this key ingredient that is relinquished in the name of economy, which increases the complexity of performance based specification. This sets innovation in concrete technology apart from other material sciences where input parameters are controlled with great precision to achieve a specific level of performance.

South Africa

Concrete aggregate specification in South Africa is in accordance with SANS 1083: 2013 – Aggregates for Concrete.

Coarse aggregates

SANS 1083: 2013 specifies ranges for the percentage of material to pass standard sieve apertures for nominally sized coarse aggregates. These ranges are presented in Table 2-8.

The range between the maximum and minimum particle sizes for each of the coarse aggregates presented therein is relatively narrow compared to those specified in America. This is as a result of the extensive use of crushed coarse aggregates in South Africa which is more economical to produce to a uniform grading. Furthermore, workability is improved through the omission of particles in the size range between 6 and 13 mm - this reduces the particle interference that occurs with crushed aggregates as a result of the angular particle shape (Alexander & Mindess, 2005).

Fine aggregates

For fine aggregates SANS 1083: 2013 specifies limiting ranges for the percentages passing the 5000, 4750 and 150 µm sieves. These are given in Table 2-9. There are no particular limits placed on the size fractions retained on any of the sieves within the range of fine aggregate sizes and it is said that these are to be specified at tender.

As shown in Table 2-9, SANS 1083: 2013 specifies the maximum content of fines separately for crushed aggregates and aggregates derived from the natural disintegration. A higher content is permitted for crushed aggregates as they are more prone to harshness because of a more angular particle shape. The SANS standard makes allowance for a greater fines content, provided the methylene blue absorption value is less than 0.7 or, if this limit is exceeded, that the clay content is less than 2 percent by mass. If these requirements are met, the maximum fines content is increased to 10 % and 20 % respectively.

SANS 1083: 2013 further specifies limit a limiting range for the fineness modulus, as shown in Table 2-9. The fineness modulus is limited between 1.2 and 3.5.

Table 2-8: SANS 1083:2013 requirements for coarse aggregates

Property	Requirement							
	Nominal size of aggregate							
Grading, mass percentage of material that passes sieves of nominal aperture size, mm	**75**	**53**	**37.5**	**26.5**	**19**	**13.2**	**9.5**	**6.7**
75.00	100	100						
53.00	0 - 50	85 - 100	100					
50.00	0 - 43	70 - 85	90 - 100					
37.50	0 - 25	0 - 50	85 - 100	100				
28.00	0 - 7	0 - 28	15 - 55	90 - 100				
26.50	0 - 5	0 - 25	0 - 50	85 - 100	100			
20.00		0 - 7	0 - 28	15 - 55	90 - 100			
19.00		0 - 5	0 - 25	0 - 50	85 - 100	100		
14.00			0 - 7	0 - 28	15 - 55	90 - 100		
13.20			0 - 5	0 - 25	0 - 50	85 - 100	100	
10.00				0 - 7	0 - 28	15 - 55	90 - 100	
9.50				0 - 5	0 - 25	0 - 55	85 - 100	100
7.10					0 - 9	0 - 30	25 - 58	92 - 100
6.70					0 - 5	0 - 25	0 - 55	85 - 100
5.00						0 - 7	0 - 28	15 - 55
4.75						0 - 5	0 - 25	0 - 55
2.36							0 - 5	0 - 25
2.00							0 - 4	0 - 28
1.18								0 - 5
1.00								0 - 4
Dust content, material that passes a 75 µm sieve, mass percentage, max.	2							

Table 2-9: SANS 1083:2013 requirements for fine aggregates

Property	Fine aggregate derived from the natural disintegration of rock and any mixture (blend) of this class and fine aggregate derived from the mechanical crushing or milling of rock	Fine aggregate derived from the mechanical crushing or milling of rock
Grading, mass percentage that passes sieves that have square apertures of nominal size: 5 000 µm 4 750 µm 150 µm	 92 - 100 90 - 100 5 - 25	
Dust content, material that passing a 75 µm sieve, mass percentage, max.	5	10
Fineness modulus	1.2 - 3.5	

Europe

The European Committee for Standardisation centrally publishes standards which apply to all of its member nations. Each nation has a version that is adapted, where necessary, to local conditions and needs. However, fundamentally the codes are the same throughout. The European standard for concrete aggregates is EN 12620: 2013. This section will review the British Standards' version which is BS EN 12620: 2013 – *Aggregates for Concrete*.

The specifications are based around the idea of an ideal grading curve.

The standard defines aggregate sizes in terms of the ratio d/D, where d is a lower and D an upper sieve size.

The European standard makes provisions for coarse and fine aggregates as well as an all-in aggregates and natural graded 0/8 mm aggregates. The definitions of these are provided in the sub-sections that follow. Aggregates for concrete are permitted to be a single aggregate, an all-in aggregate or a combination of two or more single aggregates.

"Size designations and grading categories are essentially categories of convenience and different sizes and grading categories may be used by agreement between supplier and purchaser."

Coarse aggregates

In the standard coarse aggregates are normatively defined as having a maximum particle size $D > 4$ mm and a minimum particle size $d \geq 0$. However, there are cases for example aggregates with designation 1/3 where $d = 1$ and $D = 3$, that do not conform to the definition of fine-, coarse- or all-in-aggregates. These are treated as coarse aggregates. A coarse aggregate must conform to one of the gradings specified under category G_cX/Y for coarse aggregates in Table 2-10.

The standard further defines a graded coarse aggregate. This type of aggregate can either have $D/d \geq 2$ mm and $D > 11.2$ mm or $D/d > 4$ and $D \leq 11.2$. Table 2-11 gives specifications percentage of material passing mid-range sieve sizes by mass for graded coarse aggregates.

Fine aggregates

BS EN 12620: 2013 defines fine aggregates similarly to both SANS 1083:2013 and ASTM C33. That is: aggregate is classified as fine when $D \leq 4$ mm and $d = 0$. Grading of fine aggregates is specified according to the limits presented in Table 2-10 for category G_FX/Y.

Natural graded 0/8 mm aggregates

Natural graded 0/8 mm aggregates are natural aggregates of glacial and/fluvial origin with D ≤ 8 mm. The specified grading limits for natural graded 0/8 mm aggregates are presented in Table 2-10 under the category $G_{NG}X$.

Table 2-10: BS EN 12620: 2013 grading requirements for concrete aggregates

Aggregate	Size	Percentage passing by mass					Category
	mm	2D	1.4D	D	d	d/2	G
Coarse	D>4 d≥1	100	100	90 to 99	0 to 10	0 to 2	G_c90/15
		100	98 to 100	90 to 99	0 to 15	0 to 5	G_c90/10
		100	98 to 100	85 to 99	0 to 20	0 to 5	G_c85/20
		100	98 to 100	80 to 99	0 to 20	0 to 5	G_c80/15
	D≤4 d≥1	100	95 to 100	85 to 99	0 to 15	-	G_G85/15
		100	98 to 100	85 to 99	0 to 20	0 to 5	G_G85/20
Natural graded aggregates	D=8 d=0	100	98 to 100	90 to 99	-	-	G_{NG}90
Fine	D≤4 d=0	100	95 to 100	85 to 99	-	-	G_F85
All-in	D>4 d=0	100	98 to 100	90 to 99	-	-	G_A90
		100	98 to 100	85 to 99	-	-	G_A85

Table 2-11: BS EN 12620: 2013 limits for percentage passing mid-range sieve sizes by mass for graded coarse aggregates

D/d	Mid-size sieve (mm)	Overall limits at mid-size sieves (percentage passing by mass)	Category G
< 4	D/1.4	25 to 80	$G_{25/15}$
		20 to 70	$G_{20/15}$
≥ 4	D/2	20 to 70	$G_{25/17.5}$
No requirement			G_{NR}

All-in aggregates

An all-in aggregates are defined as aggregates with a combination of fine and coarse aggregates with D > 4 and d = 0. Grading of all-in aggregates is specified according to the limits presented in Table 2-10 for category G_AX. Further provision is made for cases where it is necessary to restrict the proportions of aggregates at intermediate sizes. These limits are presented in Table 2-12.

Table 2-12: BS EN 12620: 2013 intermediate sieve size grading limits for all in aggregates

Size (mm)	Overall limits at the intermediate sieves (Percentage passing by mass)			
	D/2	4 mm	2 mm	1 mm
D ≤ 10	50 to 90	-	-	20 to 60
10 < D < 32	50 to 90	-	20 to 60	-
D ≥ 32	50 to 90	20 to 60	-	-

Fines content

No particular limits are set for fines content. However, if the fines content of fine or all-in aggregates exceeds 3 percent then it is required that the fines quality be tested either by way of the sand equivalent or the methylene blue value. The standard provides categories by which to classify the fines based on the results of either of the fines quality tests. These categories are not relevant to the study and are thus not provided here.

United States

The standard used in the United States is ASTM C33.

Coarse aggregates

The only physical characteristic of coarse aggregates controlled by way of specification in ASTM C33 is the grading. 15 different gradings, classified by size numbers, are provided, with ranges of percentages of material to pass particular sieve sizes specified. These are shown in Table 2-13.

Fine aggregates

ASTM C33 specifies a grading envelope with allowable ranges for percentage material passing each standard sieve size between from 9.5 mm down to 150 μm are provided, as given in Table 2-13. Fine aggregates are not permitted to have more than 45 per cent passing one sieve size but retained on the next consecutive sieve size of those shown in Table 2-13. The fineness modulus cannot be less than 2.3 or greater than 3.1.

The code allows for deviations from the above prescriptions provided that it can be demonstrated that concrete of the class specified can be made with the aggregate in question to have relevant properties at least equal to a concrete with the same ingredients but with a reference fine aggregate with a proven performance record.

Table 2-13: ASTM C33 grading limits for nominal coarse aggregates

Size Number	Nominal Size (Sieves with Square Openings)	Amounts Finer than Each Laboratory Sieve (Square-Openings), Mass Percent													
		100 mm (4 in.)	90 mm (3½ in.)	75 mm (3 in.)	63 mm (2½ in.)	50 mm (2 in.)	37.5 mm (1½ in.)	25.0 mm (1 in.)	19.0 mm (¾ in.)	12.5 mm (½ in.)	9.5 mm (⅜ in.)	4.75 mm (No. 4)	2.36 mm (No. 8)	1.18 mm (No. 16)	300 µm (No.50)
1	90 to 37.5 mm (3½ to 1½ in.)	100	90 to 100	...	25 to 60	...	0 to 15	...	0 to 5	...	...	...	...	...	...
2	63 to 37.5 mm (2½ to 1½ in.)	...	...	100	90 to 100	35 to 70	0 to 15	...	0 to 5	...	...	...	...	...	...
3	50 to 25.0 mm (2 to 1 in.)	...	...	...	100	90 to 100	35 to 70	0 to 15	...	0 to 5	...	...	...	...	...
357	50 to 4.75 mm (2 in. to No. 4)	...	...	...	100	95 to 100	...	35 to 70	...	10 to 30	...	0 to 5	...	...	...
4	37.5 to 19.0 mm (1½ to ¾ in.)	...	...	...	...	100	90 to 100	20 to 55	0 to 15	...	0 to 5	...	...	...	...
467	37.5 to 4.75 mm (1½ in. to No. 4)	...	...	...	...	100	95 to 100	...	35 to 70	...	10 to 30	0 to 5	...	...	...
5	25.0 to 12.5 mm (1 to ½ in.)	...	...	...	...	...	100	90 to 100	20 to 55	0 to 10	0 to 5	...	...	...	...
56	25.0 to 9.5 mm (1 to ⅜ in.)	...	...	...	...	...	100	90 to 100	40 to 85	10 to 40	0 to 15	0 to 5	...	...	...
57	25.0 to 4.75 mm (1 in. to No. 4)	...	...	...	...	...	100	95 to 100	...	25 to 60	...	0 to 10	0 to 5	...	...
6	19.0 to 9.5 mm (¾ to ⅜ in.)	...	...	...	...	...	...	100	90 to 100	20 to 55	0 to 15	0 to 5	...	...	...
67	19.0 to 4.75 mm (¾ in. to No. 4)	...	...	...	...	...	...	100	90 to 100	...	20 to 55	0 to 10	0 to 5	...	...
7	12.5 to 4.75 mm (½ in. to No. 4)	...	...	...	...	...	...	...	100	90 to 100	40 to 70	0 to 15	0 to 5	...	...
8	9.5 to 2.36 mm (⅜ in. to No. 8)	...	...	...	...	...	...	...	...	100	85 to 100	10 to 30	0 to 10	0 to 5	...
89	9.5 to 1.18 mm (⅜ in. to No. 16)	...	...	...	...	...	...	...	...	100	90 to 100	20 to 55	5 to 30	0 to 10	0 to 5
9[A]	4.75 to 1.18 mm (No. 4 to No. 16)	...	...	...	...	...	...	...	...	...	100	85 to 100	10 to 40	0 to 10	0 to 5

[A] Size number 9 aggregate is defined in Terminology C125 as a fine aggregate. It is included as a coarse aggregate when it is combined with a size number 8 material to create a size number 89, which is a coarse aggregate as defined by Terminology C125.

A maximum of 3 percent of the total fine aggregate is permitted to be finer than 75 μm for applications subject to abrasion. For all other applications a maximum of 5 percent is permitted. If no specification is made, the 3 percent limit shall apply.

The code notes that there is a possibility, with proportions of the 150 and 300 μm that are on the lower end of the prescribed ranges, difficulties may be experienced with workability, pumping and excessive bleeding. To overcome these difficulties the use of entrained air, additional cement or suitable mineral admixture is prescribed.

2.4.7 Mixture proportioning

ACI Standard 211.1-91

The American Concrete Institute Committee 211 published the widely used "*Standard practice for selecting proportions for normal, heavy-weight and mass concrete*".

The document presents a 9-step procedure for obtaining the proportions of the concrete constituents to be used. The procedure is specified on the basis that the particular ingredients have been selected and that particular properties are known. For the selected aggregates the necessary information includes sieve analysis results of fine and coarse aggregates, the unit weight of coarse aggregates and the bulk specific gravities and absorption of the aggregates.

Of the 9 steps specified, 3 steps are dedicated to obtaining aggregate proportions and properties. The first is Step 2, which calls for the selection of the maximum coarse aggregate particle size. It is suggested the largest economically available nominal aggregate size which conforms to the limitations resulting from member and form dimensions, as described in section, be selected. The stated basis for this guideline is that larger nominal coarse aggregate sizes provide for greater aggregate packing densities and thus require less cement paste.

The next step pertaining to aggregate selection is Step 6: The selection of coarse aggregate content. This selection is guided by Table 2-14, which specifies the volume of coarse aggregate, per a unit concrete volume, to be used based on the selected maximum coarse aggregate particle size and the fineness modulus of the fine (Sizes of aggregates have been converted from ASTM and to SANS standard sizes and thus there are occasions where the displayed aggregate size varies from that which appears in the ACI document by a few millimetres). Importantly it is noted that the variations in workability to be expected from differences in particle shape and grading are accounted for in the dry-rodded packing density.

The volume of fine aggregate is determined in Step 6, by difference, as the amount to make up the bulk of the concrete, after all other ingredients' proportions have been determined.

Table 2-14: ACI Standard 211.1-91 guidelines for selection of aggregates

Nominal maximum size of aggregate (mm)	Volume of oven-dry-rodded coarse aggregate per unit volume of concrete for different fineness moduli of fine aggregate			
	2.4	2.6	2.8	3.0
9.5	0.50	0.48	0.46	0.44
13.2	0.59	0.57	0.55	0.53
19.0	0.66	0.64	0.62	0.60
26.5	0.71	0.69	0.67	0.65
37.5	0.75	0.73	0.71	0.69
53.0	0.78	0.76	0.74	0.72
75.0	0.82	0.80	0.78	0.76

C&CI Method

The Cement and Concrete Institute of South Africa present their own method for mix design which is based around ACI Standard 211.1-91. It prescribes 24 steps as opposed to 9 steps in the ACI Standard, but this is largely due it unpacking many of the actions which are either required to be completed prior to commencing the USA procedure or are implicit in other steps. The aggregate related steps in the C&CI method which differ from the ACI method are discussed below.

Steps 8 and 9 provide for the selection of fine and coarse aggregates. The selection, it is suggested, must be made to meet the aggregate specification requirements, with consideration of economy. Nothing further is said of the somewhat vague *aggregate specification requirements*, but this most likely speaks of the limits on aggregate size resulting from member and form dimensions and whether high strength concrete is to be made, which would dictate a smaller maximum aggregate size.

Step 16 prescribes a unique method for calculating the stone content, which is done by way of Equation 2-6.

$$M_a = CBD(K - 0.1FM) \quad \textbf{(2-6)}$$

Where:
- M_a = Mass of coarse aggregate in one cubic meter of concrete (kg)
- CBD = Dry compacted bulk density of coarse aggregate (kg/m^3)
- K = Factor obtained from Table 2-15
- FM = Fineness modulus of fine aggregate

The C&CI method for calculating stone content takes into account the required workability as well as the factors of maximum coarse aggregate particle size and the fineness modulus of the fine aggregate as accounted for in the ACI method. Finally the fine aggregate content is selected by way of working out the difference required to complete the required volume of concrete.

Table 2-15: K-values for use in Equation (2-6 for the determination of packing density by the C&CI method

Approximate slump range, mm	Placing requirement	K				
		Maximum size of stone, mm				
		9,5	13,2	19,0	26,5	37,5
75 - 150	Hand compaction	0,75	0,84	0,94	1,00	1,05
25 - 100	Moderate vibration	0,80	0,90	1,00	1,06	1,10
0 - 25	Heavy vibration	1,00	1,05	1,08	1,10	1,15
60 - 125	Pumped	-	0,83	0,86	0,87	-
25 - 50	Concrete roads*	-	-	-	-	1,2
* Calculated on CBD of 37,5-mm stone when using a blend of 37,5- and 19-mm stone						

From this it is evident that the ITZ is the main mechanism through which aggregate influences concrete penetrability.

Table 2-16: C&CI recommended sand grading (after Grieve, 2009)

Sieve size (mm)	Cumulative percentage passing sieve	
4.75	90 - 100	
2.36	75 - 100	
0.18	60 - 90	
0.6	40 - 60	
0.3	20 - 40	
0.15	10.0 - 20	
0.075	Natural Sand	Crusher Sand
	5 - 10.0	5 - 20.0

There are limits placed on the dust content of aggregates for concrete production. These limits can be found in Table 3. The smaller the average aggregate particle size the greater the total aggregate surface area. Thus the greater is the water requirement to wet all aggregate particles and allow them to slide over one another. In other words, the smaller the aggregate, the greater amount of water is required to give the same workability. However, increased

water demand leads to greater shrinkage, poorer strength and greater permeability. Hence limits have been put in place to limit dust content (Alexander & Mindess, 2005).

Of further concern is the ratio between coarse and fine aggregates. There are several suggested methods for selecting quantities of coarse and fine aggregates. The amounts of coarse and fine aggregate to be used in a mix are interdependent but usually depend further on separate factors. Table 3 presents a guide for selecting the amount of coarse aggregates to be used. Alternatively, Addis and Goodman (2009) recommend calculation of coarse aggregate content using an equation that factors fines modulus, maximum nominal stone size and the compacted bulk density of the coarse aggregate used. The amount of fine aggregate required can depend on the application, the richness of the mix and the amount of coarse aggregate but is commonly calculated as the amount of material required to make up the volume of a mix.

Table 2-17: Guidelines for selection of coarse aggregate volume per unit volume of concrete (after Kosmatka et al., 1995) (adapted from ACI, 1991)

Nominal max. size of aggregate (mm)	Volume of dry-rodded coarse aggregate per unit volume of concrete for different fineness moduli of fine aggregate			
	2.4	2.6	2.8	3
10	0.5	0.48	0.46	0.44
20	0.66	0.64	0.62	0.6
40	0.75	0.73	0.71	0.69
80	0.82	0.8	0.78	0.76

The specifications in the South African National Standards for each are presented in Tables 2 and 3 respectively. Each of the properties that appear in these tables is discussed briefly below.

Often, aggregates are graded to recommended or specified grading envelopes which aim to optimise concrete properties based on empirical findings. Such an envelope is given in Table 2, after Grieve (2009).

2.5 Particle packing models

Particle packing models provide a tool with which to either estimate packing density for a given combination of particle sizes or determine the required volume fractions of different particle sizes to achieve, a particular packing density. Many packing models have been developed by various authors, as shown in Figure 2-19 which distinguishes between discrete and continuous models. Discrete models describe a particle size distribution consisting of

particles of specific different size classes, resulting in a gap between consecutive particle sizes. Continuous models are based on a particle size distribution containing particles of all possible sizes within the given range.

Comparisons between experimental results and model predictions show that most models reasonably predict actual packing densities, but differ in their accuracies depending on the geometries of the systems tested (Johansen & Andersen, 1991). Whilst there are several factors which affect the accuracy of each model, (Jones, et al., 2002)Jones et al. (2002) found that the size ratio can serve as a good indicator of model suitability. This section provides an overview of the existing models,

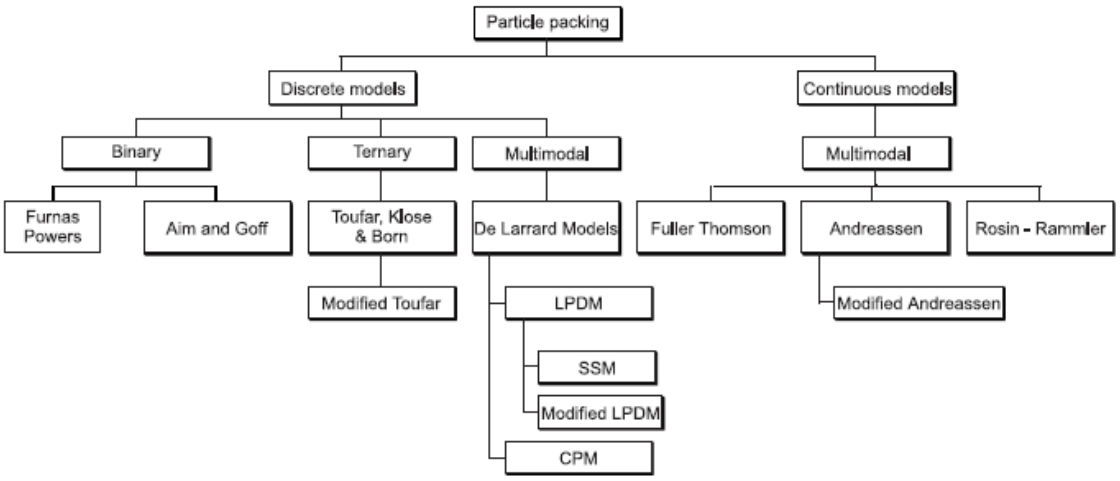

Figure 2-19: Classification of the various existing particle packing models (Senthil Kumar and Santhanam, 2003)

2.5.1 Overview of packing models

This section presents a basic overview of existing packing models and briefly talks about the defining principles behind each. This will allow for the comparison of the accuracy of the different models from various studies, which is presented in Section 2.5.2. It is not necessary to delve into the detailed theory behind each model here. Fennis (2011) presents a thorough review of the theories behind many of the models discussed.

Discrete Models

In 1929, Furnas published a model describing the ideal packing of spherical particles to achieve maximum packing density. The Furnas model was developed for combinations of different sized particles where one size class, d_1, is small enough to fit between the interstices of the next biggest size class, d_2. This occurs at diameter ratios d_1/d_2 less than 0.22. Furnas considered two cases: One with a large volume fraction of small particles and one with a large volume fraction of large particles. However, if $d_1 << d_2$, then the packing density will

also depend on the diameter ratio, d_1/d_2 (Johansen & Andersen, 1991). This is due to both the loosening effect and the wall effect as described in Section 2.4.

Aim and Goff (1967) presented a modification of the Furnas model which accounts for increased porosity observed in the first layer of spherical grains in contact with a plane and smooth wall. When the fraction of fine particles tends towards the lower limit, the model becomes identical to the Furnas model (Johansen & Andersen, 1991).

(Toufar, et al., 1976; Toufar, et al., 1977)Toufar, Klose and Born proposed a model which calculates the packing density of multimodal mixtures as a weighted average of the total number of binary mixes with diameter ratios $0.22 < d_1/d_2 < 1.0$. Golterman et al. (1997) proposed a minor modification to the Toufar model, which, for binary mixes of coarse and fine aggregates, produced results which were closer to experimental data for smaller volume fractions of fine aggregates. At greater fine aggregate volume fractions the results of the original and the modified Toufar models converged.

The Linear Packing Density Model (LPDM), developed by (Stovall, et al., 1986)Stovall et al. (1986), which accounted for both interaction effects, namely the wall effect and the loosening effect. However, for small diameter ratios, where interaction effects diminish, the LPDM becomes identical to the Furnas model. Modifications of the LPDM include the Modified LPDM which introduced the concept of eigen packing (Kumar V & Santhanam, 2003) and the Solid Suspension Model (SSM) which differentiated between the actual packing density and the virtual packing density which is the maximum packing density achievable, with every particle maintaining its original shape and particles being placed one at a time (de Larrard & Sedran, 1994).

de Larrard (1999) developed the Compressible Packing Model (CPM), based on the same principles as the LPDM, to include the influence of compaction energy. This was achieved by through the introduction of a compaction index, with different values for different compaction methods. Like the SSM, the CPM distinguishes between virtual and actual packing density. However the CPM has unique expressions for determining interaction coefficients that account for the wall effect and loosening effect.

Fennis (2011) extended the CPM to include the effects of interparticle forces that occur between sub-150 μm particles. This model is known as the Compaction-Interaction Model.

Continuous models

As mentioned in Section 2.4, Fuller and Thompson (Fuller & Thompson, 1907) developed the Fuller curve which described the ideal grading to achieve maximum packing density. This

is given in Equation (2-7) where CPFT is the cumulative volume percentage finer than, d is the particle size and D is the maximum particle size.

$$CPFT = 100\left(\frac{d}{D}\right)^{0.5} \quad \textbf{(2-7)}$$

The Fuller curve formed the basis for the Andreassen and Modified-Andreassen models. The Andreassen model was identical to the Fuller curve but with the inclusion of a the distribution coefficient to replace the coefficient of 0.5. This allowed for the accommodation of variations in the volume fraction of finer or coarser material according to the needs of the application. The value of q typically varies between 0.2 and 0.3, with lower values representing aggregates with more fine material. The modified Andreassen model takes account of the fact that the size of the smallest particle in a real mix has a value within a finite range.

Rosin-Rammler Distribution

Rosin and Rammler (1933) developed an equation which describes the distribution of powdered coal. It has since been found that concrete aggregates have a similar distribution (Johansen & Andersen, 1991). Equation (2-8 represents the Rosin-Rammler distribution.

$$R(D) = exp^{-\left(\frac{D}{D'}\right)^n} \quad \textbf{(2-8)}$$

Where
- D - Particle diameter;
- R(D) - Residue fraction – the fraction of particles larger than D;
- D' - Characteristic diameter;
- n - constant which characterises the distribution, ranging from 1.04 – 4.0 but usually between 1 and 2

The characteristic diameter D' in the Rosin-Rammler distribution is equivalent to what would be the mean diameter if the particle sizes were normally distributed (Austen, 1939). D' is the particle size for which R(D') = 0.368. This is proven in Equation (2-9) where D = D'.

$$R(D') = exp^{-\left(\frac{D'}{D'}\right)^n} \quad \textbf{(2-9)}$$

$$= exp^{-1}$$

$$= 0.368$$

Continuous models prescribe an ideal grading curve. Whilst they have been developed at least in part to achieve optimum packing density, they do not give an evaluation of the

expected packing density from the prescribed grading. They therefore do not fulfil the needs of this research and will not be considered further.

2.5.2 Model estimates vs. measured packing density

In 1981, Petersen found that, of all models developed to that date, the Toufar model gave the best description of experimental data for binary mixes with diameter ratios greater than 0.22, whilst the Aim and Goff model was better for smaller diameter ratios.

There have been mixed findings on the validity of the CPM. de Larrard (1999) and Nanthagopalan and Santhanam (2003) found that estimations of packing density made using the CPM corresponded well with experimental measurements. Jones et al. (2001) compared the LPM, CPM the Toufar model and the Dewar model for the estimation of the packing density of binary mixes. They concluded that all provide a relatively good estimate of the volume fractions of the constituents at which the maximum packing density occurs. The Toufar model and their modified version of the CPM showed the best fit with experimental results at all volume fractions, whilst the original CPM tended to underestimate and the Dewar model tended to overestimate packing density. These results for one mix are illustrated in Figure 2-20.

Andersen and Johansen (1993) and Roy et al. (1993) used the Toufar model to derive their recommendations for aggregate proportioning for maximum packing density of concrete aggregates.

Fennis (2012) showed that as the amount of grain size classes in an aggregate mix increases, as it does for example between a binary and a ternary mix, the Toufar and modified Toufar models underestimate the packing density in an increasing extent.

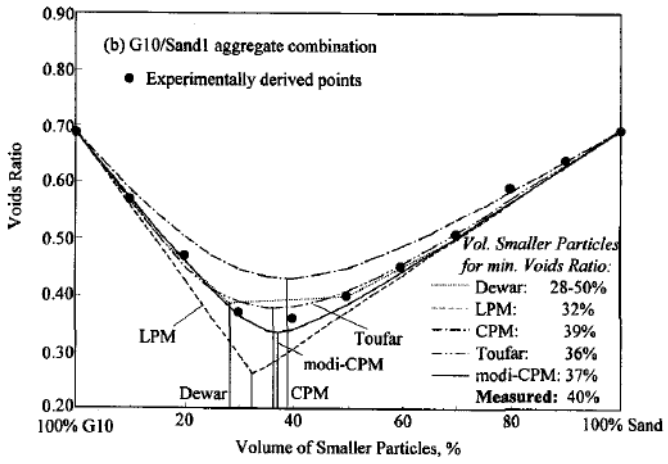

Figure 2-20: Comparison of different packing models' estimations against measured packing density (Jones, et al., 2002)

2.5.3 Concluding remarks

For simple binary mixes the Toufar and modified Toufar models are generally the most accurate in estimating the packing density. These two models can be applied to multimodal mixes but the accuracy is diminished. For multimodal mixes the CPM may be the most effective model.

2.6 Modified Toufar Model

As a model of aggregate particle packing, the Modified Toufar Model (MTM), discussed in Section 2.4.1, had the following advantages:

- Sound scientific basis;
- Relatively simple;
- Corresponds well with experimental data (Jones et al., 2002; Golterman et al. 1997).

The MTM was found to be the most accurate model in predicting the actual packing density in multiple studies. Furthermore, it suited the needs of this research. As such packing density calculations were done using the MTM.

As the name suggests, the MTM is a modified version of the original Toufar Model. Both make use of the diameter ratio. To explain the diameter ratio it is useful to think of an aggregate created by blending three different groups of particles. Each group will have a different average diameter - which is also known as a characteristic diameter. The diameter ratio is the ratio between the characteristic diameter of one group of particles and that of the group of particles with the next largest characteristic diameter. Both the Toufar and the modified Toufar models are based on the fundamental concept that when the diameter ratio is greater than 0.22, the smaller particles will be larger than the interstices between the larger particles.

As a result of the distribution of particle sizes the characteristic diameter is not equal to or near D_{50} – that is the diameter which 50 % of the particles are smaller than (by mass). As mentioned in Section 2.5.1, the Rosin Rammler distribution has been found to be representative of the particle size distribution of concrete aggregates (Johansen & Andersen, 1991). As such it is a suitable estimator of the characteristic diameter for aggregates for which the grading is known. According to the Rosin Rammler model the characteristic diameter is that which 63.3 % of particles are smaller than (or 36.8 % larger than, as shown in Equation (2-9).

Another concept of importance is the bulk volume. This is the total volume that an aggregate occupies with the solid volume of the particles along with the void volume. The MTM provides for the calculation of aggregate packing density φ as given in Equation 2-10 (Goltermann et al., 1997).

$$\varphi = \frac{1}{\frac{y_1}{\varphi_1}+\frac{y_2}{\varphi_2}-y_2\left(\frac{1}{\varphi_2}-1\right)k_d k_s} \quad \textbf{(2-10)}$$

Where:

y_1/φ_1	-	bulk volume of fine particles where y_1 is the fine aggregat volume fraction and φ_1 is the packing density of the fine aggregate;
y_2/φ_2	-	bulk volume of coarse particles where y_2 is the coarse aggregat volume fraction and φ_2 is the packing density of the coarse aggregate;
$y_2(\frac{1}{\varphi_2}-1)$	-	void volume between coarse particles;
k_d	-	factor that accounts for the effects of diameter ratio;
k_s	-	a statistical factor

y_i is specified, and φ_i is a property of the aggregate which depends on particle size distribution and particle shape. For k_d the original Toufar model gave k_d by Equation 2-11 (Toufar et al., 1976, 1977):

$$k_d = \frac{(d_2 - d_1)}{(d_1 + d_2)} \quad \textbf{(2-11)}$$

Where d_1 and d_2 are the characteristic diameters of the fine and coarse aggregates respectively, which is the size of each aggregate particle in a monosized aggregate. The original Toufar model assumed that each fine particle in the binary combination is placed between four of the coarse particles to give Equations 2-12 and 2-13.

$$k_s = 1 - \frac{(1 + 4x)}{(1 + x)^4} \quad \textbf{(2-12)}$$

Where

$$x = \frac{y_1 \varphi_2}{y_2 \varphi_1 (1 - \varphi_2)} \quad \textbf{(2-13)}$$

However, Golterman et al. (1997) found that for combinations of fine and coarse aggregates, where the proportion of fine aggregates approached zero, the Toufar model predicted that the

packing density was not affected by changes in the proportion of fine aggregate content. To correct for this, the modification given by Equation 2-14 was proposed.

$$k_s = 0.3881\left(\frac{x}{0.4753}\right) \quad \text{for } x < 0.4753$$
$$k_s = 1 - \frac{(1+4x)}{(1+x)^4} \quad \text{for } x \geq 0.4753 \qquad \textbf{(2-14)}$$

The Toufar model was developed for aggregates formed through combinations of monosized aggregates. Andersen and Johansen (1993), Roy et al. (1993) and Golterman et al. (1997) found that it could be applied in cases where the constituent aggregates were not mono-sized by using the Rossin-Rammler distribution, as discussed in Section 2.5.1, to find a characteristic diameter and applying this as the mean diameter for each aggregate fraction. It has been found that this equation is effective in describing the size distribution of concrete aggregate particles (Johansen and Andersen, 1993).

The residue fraction R(D) is described as 1 - F(D) where F(D) = P(d<D), that is the cumulative probability that diameter d is less than D. F(D) is found experimentally by sieve analysis and the Rosin-Rammler distribution can then be used to find the characteristic diameter D' and constant n (Anderson & Johansen, 1993).

2.7 Discussion

2.7.1 Aggregate grading and packing density

As highlighted by Grieve (2009b) the aggregate grading that is ideal for concrete is not known, despite great research efforts on the topic. It is understood that near maximum packing density is usually optimum for strength and durability (Powers, 1961; Alexander and Mindess, 2005) and that there is a strong link between grading and packing density (Johansen & Andersen, 1991; de Larrard, 2001) as well as workability (Andersen, 1990). As such, mix proportioning guidelines both in America and South Africa attempt to achieve the greatest packing density for a given combination of coarse and fine aggregates. However, there are other factors that are influenced by the aggregate particle size distribution which have been found to affect concrete properties, including durability. These include the extent of the porosity in the interfacial transition zone and tortuosity, which determines the complexity of the flow path of a permeating fluid through the concrete (Mehta and Monteiro, 2006). Neither the extent of the effects of aggregate grading on these factors, nor the implications these have on concrete properties, are understood. This research aimed at providing greater insight into

the latter, with a particular focus on durability. To achieve this, a set of laboratory experiments were carried out on concrete specimens with different aggregate grading but the same aggregate packing density. The experimental method is discussed further in Chapter 3.

2.7.2 Methods of characterising aggregate grading

A grading curve describes the distribution of particle sizes. The curve is typically of a complex shape that may possibly at best be represented by a step-wise function. However, this would be complex and cumbersome, and therefore not suited for use in aggregate specification. For performance based specification purposes it is necessary to ask: What properties of the raw ingredients are performance outcomes sensitive to and how can these best be characterised. A good characterising parameter accurately describes the changes that influence the performance outcomes whilst being simple.

So here the question is: Is there any one characteristic of the grading curve which particularly influences concrete penetrability? As discussed in Section 2.7.3, two of the important pieces of information contained within a grading curve are the average particle size and the grading type, being uniform or continuous. The former may be characterised by the FM whilst the latter may be characterised by C_u.

As shown in Section 2.4, the FM finds use in design codes and standards around the world. However, in these cases limits are set on FM because of its relation to workability. C_u has found no use in the concrete industry to date. However, in understanding the influence of aggregates on concrete penetrability, since they capture two significant properties of an aggregate grading curve, these parameters are useful in studying the influence of aggregate particle size distribution on concrete penetrability.

2.7.3 Fineness modulus vs. coefficient of uniformity

In Section 2.4 the concepts of fineness modulus (FM) and coefficient of uniformity (C_u) were introduced and defined. FM is recognised as a descriptor of the average particle size. An increase in FM corresponds with a shift in the centroid of the grading curve to the right. A generalised example of the implication for the grading curve with increasing FM is illustrated in Figure 2-21.

FM is however not particularly sensitive to the gradient of the grading curve. A steeper gradient corresponds with a more uniformly graded aggregate whilst a gentler gradient corresponds with a more continuously graded aggregate. C_u is sensitive to the average gradient of the grading curve. This is illustrated in Figure 2-22.

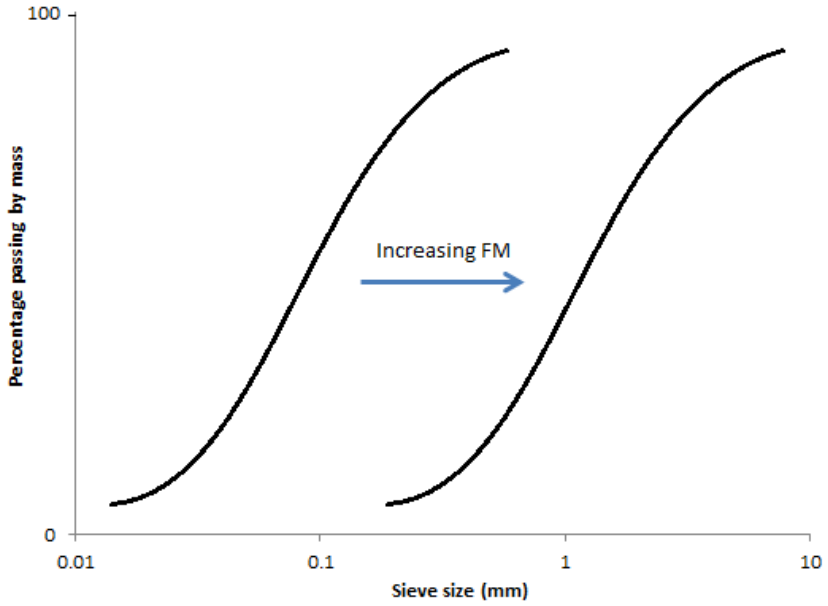

Figure 2-21: Change in FM with minimal change in Cu

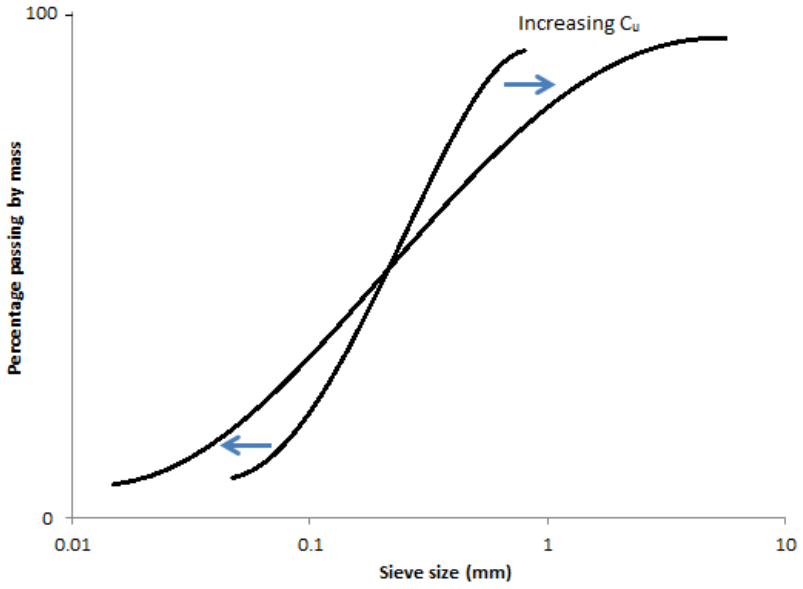

Figure 2-22: Change in aggregate grading where the FM remains constant whilst the C_u increases

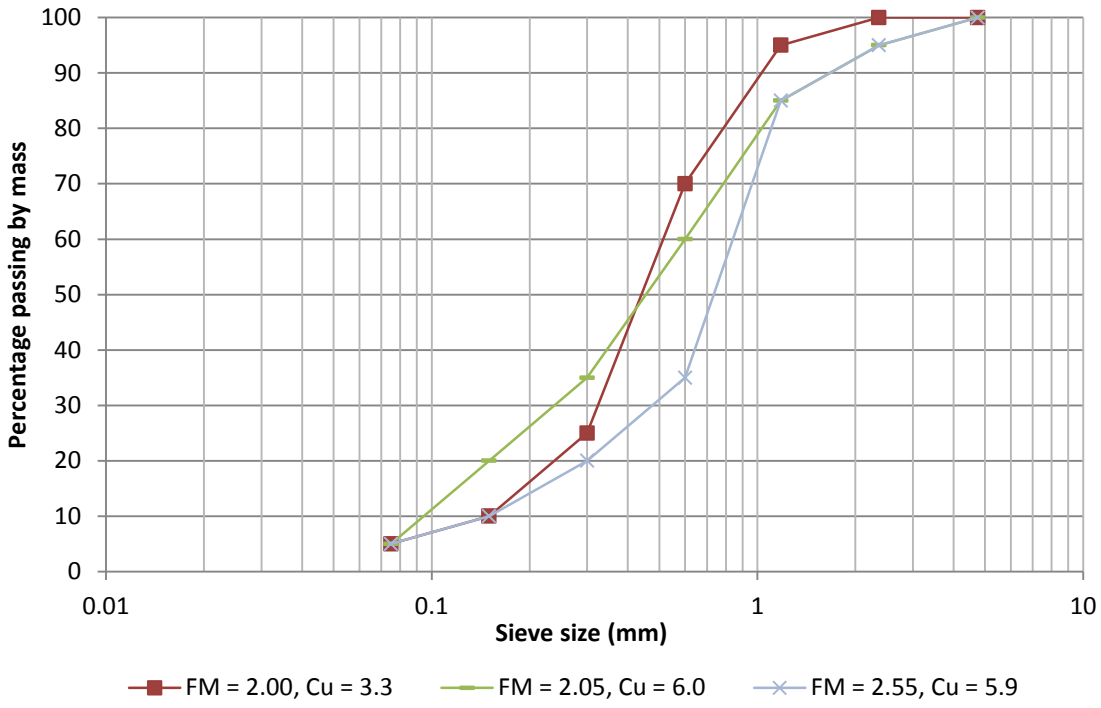

Figure 2-23: Comparison of 3 different fine aggregate grading curves illustration

There are cases where both the average particle size and the slope of the grading curve may change simultaneously, thereby resulting in a simultaneous change in FM and C_u. Furthermore it must be noted that FM and C_u are only partially independent of one another. This is a result of the log-distribution of particle size. When there is a horizontal shift in the grading curve, such as in Figure 2-21, the rates at which D_{60} and D_{10} change differ. Thus there will be a change in C_u without a change in gradient. However, a change in average gradient would have a far greater influence on C_u. This is illustrated in Figure 2-23 by way of three fine aggregate curves that may represent real aggregates used in concrete.

3. Methodology

3.1 Introduction

The move towards performance based design and specification requires thorough understanding of all factors that influence performance. Current understanding is that both strength and durability share a similar relationship with aggregate packing density – all other factors being equal, the higher the packing density the higher the strength and the better the durability. As such specifications of both South African and USA standards are centred upon optimising the packing density. However as the literature review highlighted, there are other grading related aspects, such as tortuosity and porosity of the ITZ, which influence the penetrability of concrete but which are neglected in the design process.

Furthermore, in performance based design there is a need for parameters that, as simply as possible, describe properties of the constituent materials that are linked to performance outcomes in the concrete. A good example of this is the strength classification system of cement. The current parameter for fine aggregate is fineness modulus and for coarse aggregate there is normally the specification of maximum particle size and a nominal description of the total aggregate (constituted of fine and coarse aggregate) as gap or continuously graded, which ultimately reflects the particle size distribution of the coarse aggregate.

A set of laboratory-based experiments was conducted whereby grading of aggregate was varied but packing density was held constant. This was achieved by considering the aggregate to be a binary combination of fine and coarse constituents. The fine and the coarse fractions were blended in predetermined proportions so as to achieve a particular packing density. Both the packing density and the proportions to be blended were determined by way of a numerical packing model.

3.1.1 Research method

A comprehensive review of the literature defined the objectives and questions central to this research. A set of laboratory experiments offered the most appropriate method through which to address these objectives. This chapter details the experimental methodology used.

3.2 Experimental design

In order to meet the research objectives, the lab experiments had the following general requirements, which are expanded on where necessary later:

- The experiments had to remain in the realm of practicality. Thus a target slump for all mixes was set between 50 mm and 100 mm. Fineness modulus, fines content and stone size were selected with consideration of relevant ASTM, BS and SANS standards. This is presented in Section 3.3
- As far as possible, the experiments had to eliminate any other aggregate related variables which may have influenced results. These include maximum particle size, particle shape and texture. These are discussed further in Section 3.3
- Aggregate packing density had to be eliminated as a factor. Thus between different test samples the aggregate packing density had to be held constant. This was achieved through the use of the Modified Toufar Packing Model, the details of which are given in Section 3.4.
- A technique or parameter, other than qualitative description, was required for the characterisation of both the coarse and fine aggregate. This parameter had to be sensitive to changes in the particle size distribution (PSD). For this two parameters were used, namely fineness modulus (FM) and coefficient of uniformity (C_u). This is discussed further below.

In Section 2.4 it was found that fineness modulus is used in standards that govern the use of aggregate in concrete, including ASTM C33 and SANS 1083:2013, and methods of mixture proportioning used in the United States and South Africa. Furthermore, it was shown that FM is sensitive to variations in aggregate grading which resulted in changes in the average particle size. Thus fineness modulus was selected as the primary test parameter for the fine aggregates. As a secondary test parameter the coefficient of uniformity (C_u) was selected because it is sensitive to changes in aggregate grading where the proportion of coarser material is increased or decreased relative to the finer material, while the average particle size might not change.

In studying variations in coarse aggregate, of primary interest was the difference between gap and continuously graded aggregate. Here the fineness modulus was useful in quantitatively describing the aggregate. The coarse aggregate used in gap grading was deficient in particles less than 13 mm in size whereas the coarse aggregate that gave a continuous grading had as much as 55 percent of the material passing the 13 mm sieve. Thus the average particle size of the latter was smaller and this was reflected by the coarse aggregate FM, which was therefore suitable for the quantitative characterisation of the coarse aggregate. To distinguish from the

FM of the fine aggregate, the coarse aggregate fineness modulus is denoted CFM in this research.

It must be noted that in the case of the coarse aggregate the FM served to quantitatively distinguish between aggregates yielding gap and continuous gradings. In the case of coarse aggregates it was therefore not the effects of FM but rather the effects of the grading profile, being either gap or continuous, which was of interest. The effects of varying FM were primarily studied through the fine aggregate. Since CFM was sufficient in capturing the change between different coarse aggregates from one yielding a continuous grading to one yielding a gap grading, it was not necessary to further characterise a C_u for the coarse aggregates.

Using FM and C_u for fine aggregate and CFM for coarse aggregates as the test variables, a factorial style experiment was setup, whereby each level of fine aggregate from F1 to F9 was tested against each level of coarse aggregate, C1 and C2, as shown in Table 3-1. This provided insight into the effects of variations of the fine aggregate and the coarse aggregate independently.

Water/binder ratio and water content were both fixed so as to avoid variations through their respective influences. This meant that workability had to be controlled through the use of a chemical admixture. Therefore, as a result of controlling workability, the amount of admixture used in each mix was different, making it an uncontrolled factor. This was not expected to have any significant influence on the results.

3.3 Aggregates

3.3.1 Source

All aggregates used were crushed materials derived from greywacke parent rock. Any effects that may have derived from different particle shapes were thereby avoided.

3.3.2 Fine aggregate

Fine aggregate characteristics

The limiting ranges for FM specified in ASTM C33 (2.3 – 3.1) and SANS 1083:2013 (1.2 – 3.5) guided the selection of limits of the fine aggregate fineness modulus values tested. The selected range was 1.5 to 3.0. At the intermediate FM values it was possible to obtain the same FM value with different particle size distributions. C_u was used as a secondary

descriptor to characterise the particle size distribution to account for these changes at fixed FM.

Table 3-1: Characteristics of test aggregates

Concrete	y_1	Grading	Coarse aggregate		Fine aggregate		
			Code	CFM	Code	FM	C_u
C1F1	0.34	Continuous	C1	8.37	F1	1.50	4.3
C1F2	0.37				F2	2.00	3.3
C1F3	0.34				F3	2.00	4.4
C1F4	0.35				F4	2.05	6.0
C1F5	0.37				F5	2.25	3.8
C1F6	0.37				F6	2.30	6.8
C1F7	0.36				F7	2.50	5.6
C1F8	0.38				F8	2.55	5.9
C1F9	0.42				F9	3.00	5.2
C2F1	0.40	Gap	C2	9.03	F1	1.50	4.3
C2F2	0.45				F2	2.00	3.3
C2F3	0.40				F3	2.00	4.4
C2F4	0.40				F4	2.05	6.0
C2F5	0.44				F5	2.25	3.8
C2F6	0.44				F6	2.30	6.8
C2F7	0.42				F7	2.50	5.6
C2F8	0.46				F8	2.55	5.9
C2F9	0.60				F9	3.00	5.2

Table 3-1 presents the FM and C_u data of the tested fine aggregates. The sub-75 μm fraction was fixed at 5 % of the mass of fine aggregate. This selection was guided by the limits specified in ASTM C33 and SANS 1083:2013 as presented in Section 2.4. A fixed fines content – the fraction of fine aggregate that passed the 75 μm sieve – was used throughout to ensure that all mixes were sufficiently cohesive and were not susceptible to excessive bleeding. The grading curves of selected fine aggregates are shown in Figure 3-1 and Figure 3-2. For the sake of clarity some have not been presented here. Appendix A gives data for all fine aggregates. Figure 3-1 shows the grading curves of aggregates with the most similar C_u at different values of FM. Fine aggregates F2 and F4 had similar FM values but a difference in C_u of 2.7, with C_u of F4 almost twice that of F2. This means that, whilst there was little change in the average particle size as indicated by the constant FM, there was an increase in the average size of the particles in the coarser fraction and a decrease in the average size in the finer fraction. This is characterised by the rotation of the grading curve from the position of F2 to the position of F4 in Figure 3-2.

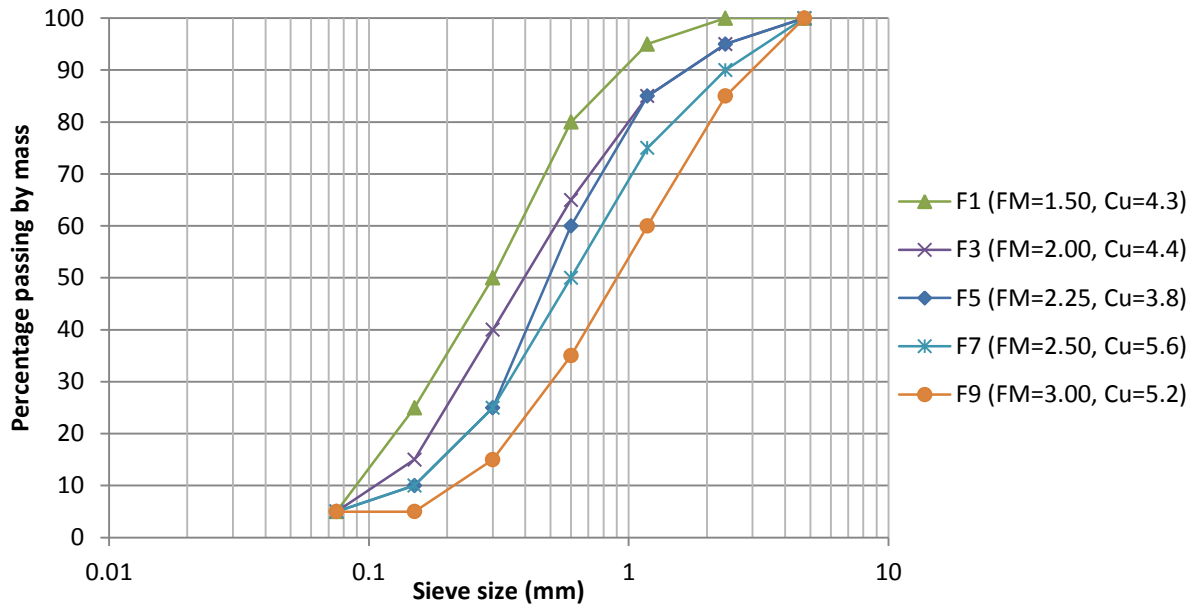

Figure 3-1: Grading curves of fine aggregates with similar C_u at different FM

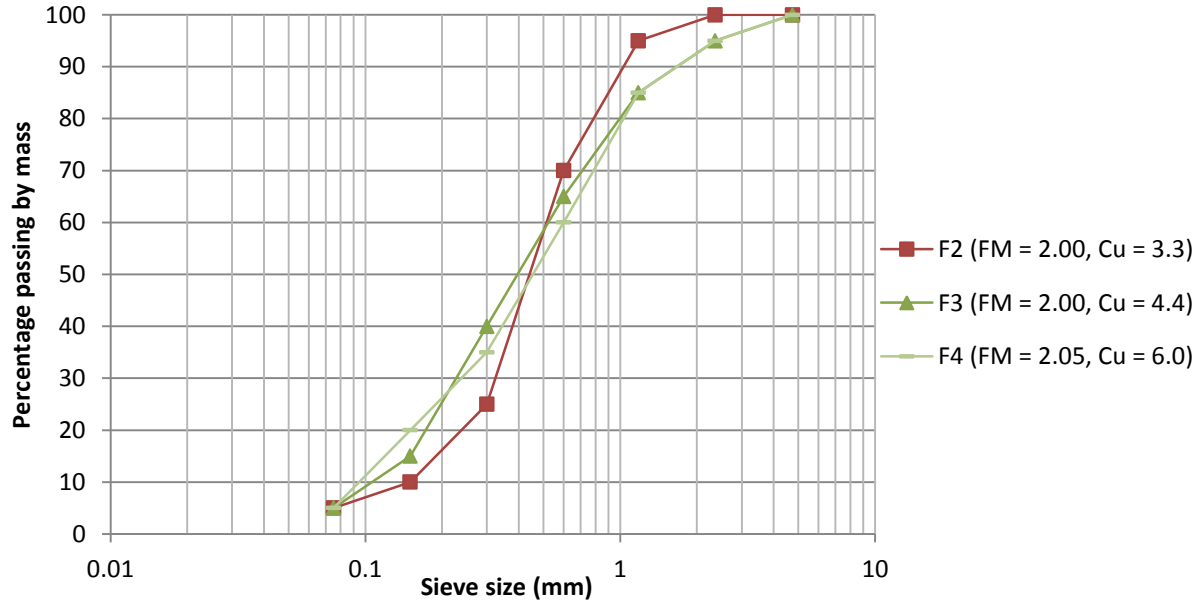

Figure 3-2: Grading curves of fine aggregates with different Cu at similar FM

Fine aggregate sample preparation

Greywacke crusher sand, supplied by AfriSam formed the source of all fine aggregate used in the experiments. After drying in an oven at 100 °C for 24 hours the sand was sieved into standard size fractions as given by SANS 1083:2006. These are presented in Table 3-2. (Whilst the literature review presents the standard sieve sizes from SANS 1083:2013, this research was commenced prior to the publication of the 2013 edition). Sieving was conducted using a sieving machine, as depicted in Figure 3-3, upon which sieves of standard apertures

were placed in decreasing size from top to bottom, similar to the setup used for a sieve analysis. Each sieving run entailed placing 2kg of crusher sand in the top sieve and vibrating for 30 minutes, after which material retained on each sieve was brushed over for 2 minutes with a bristle brush. This was sufficient to ensure that, for an additional 1 minute of sieving, no more than 0.1 % of the original 2 kg mass would pass through any of the sieves. The sorted aggregates were stored and this procedure was repeated until there were sufficient amounts of each size fraction.

Table 3-2: Sieve sizes used in the sorting of fine aggregates

SANS 1083:2006 Standard Sieves
4.75 mm
2.36
1.18
600 µm
300
150
75
<75

The fine aggregates for the tests were created by blending the sorted fractions in the predetermined ratios. The total amount of each of the fine aggregate blends required depended on the ratio of coarse aggregate to that particular fine aggregate necessary to obtain the fixed, predetermined packing density. The procedure of determining these ratios is discussed in Section 3.4.4. Aggregate was blended to the required amount to avoid variations that may have been introduced through batching.

Figure 3-3: Sieving apparatus used

3.3.3 Coarse aggregate

Two coarse aggregates were tested. One of the coarse aggregates was a nominal 19 mm as per SANS 1083:2013 which was uniformly graded and therefore deficient in particle sizes from 4.75 mm to 13 mm. The other had a particle size distribution corresponding with aggregate size number 57 in ASTM C33 (ASTM C33/57), which had a continuous grading between 4.75 and 19 mm. The grading curves of each are shown in Figure 3-4.

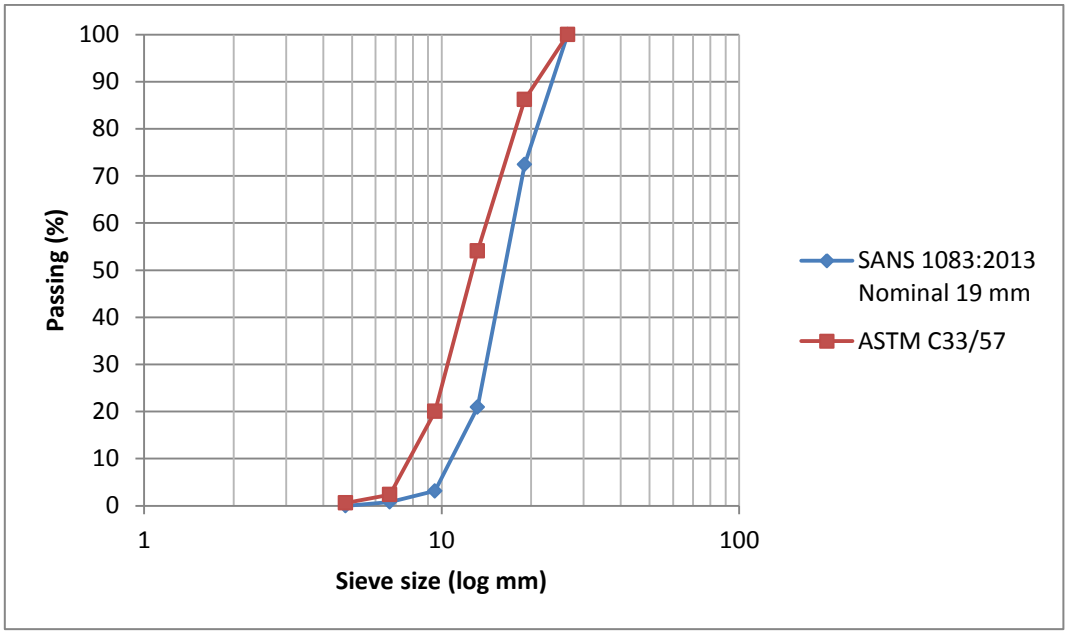

Figure 3-4: Coarse aggregate grading curves

In combination with a fine aggregate, the nominal 19 mm coarse aggregate renders a gap grading whilst the ASTM C33/57 gave a more continuous grading. The nominal 19 mm aggregate is widely used in South Africa as it does not require any intermediate coarse aggregate sizes. Thus is was desirable to study the nominal 19 mm aggregate and the ASTM 57 aggregate was a suitable continuously graded aggregate to compare it with as it has the same maximum stone size. The two coarse aggregates, the FMs (denoted CFM to distinguish from FM of fine aggregate) of which are given in Table 3-3, were sufficient for the needs of this research.

The SANS 1083:2013 nominal 19 mm, crushed greywacke was supplied by AfriSam. Coarse aggregate grading conforming to ASTM C33/57 was created by combining the nominal 19 mm with the nominal 13 mm crushed greywacke aggregates as supplied by AfriSam, in the proportions 1:1.

Table 3-3: Tested coarse aggregate characteristics

COARSE AGGREGATE		
Code	**Type**	**CFM**
C1	ASTM C33 Aggregate 57	8.37
C2	SANS 1083:2013 19 mm	9.03

3.4 Control of packing density

The packing density of the aggregate was held constant throughout the experiments. The aggregate was a binary combination of coarse and fine aggregate. Each of the fine and the coarse aggregates had different packing densities. However, the two were proportioned so as to achieve a particular overall packing density. This section presents the method through which the desired packing density, φ, for all mixes was determined and the method used to determine the volume fractions of fine (y_1) and coarse (y_2) aggregate required to achieve this packing density. The flowchart shown in Figure 3-5 summarises the procedure followed.

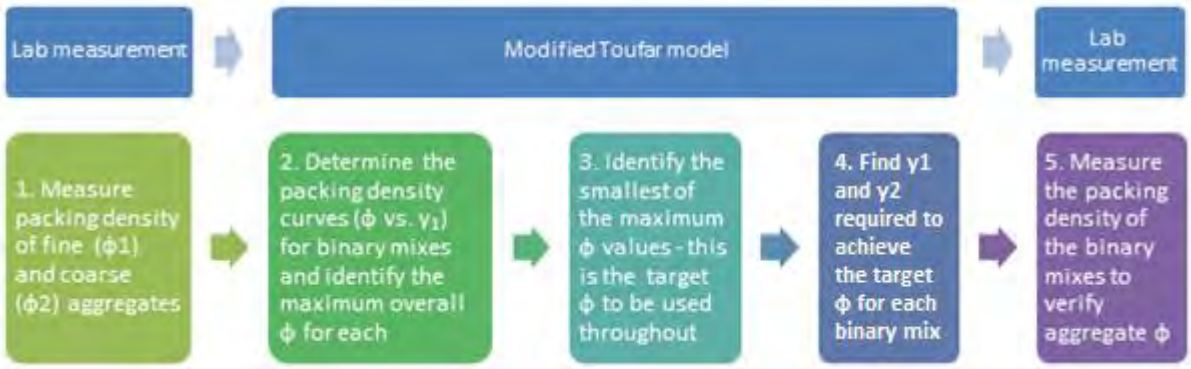

Figure 3-5: Procedure for creating the experimental aggregate

3.4.1 Modified Toufar Model

The literature review presented in Chapter 2 found that the Modified Toufar Model (MTM) had the following advantages:

- Sound scientific basis;
- Relatively simple;
- Corresponds well with experimental data (Jones et al., 2002; Golterman et al. 1997).

The MTM was found to be the most accurate model in predicting the actual packing density in multiple studies (Jones et al., 2002; Golterman et al. 1997). Furthermore, it suited the

needs of this research. As such, packing density calculations were done using the MTM. The mathematical representation of the MTM is presented in Section 2.6. The Rosin-Rammler distribution was used to determine the characteristic diameter which is necessary for the MTM. The Rosin-Rammler distribution is presented in Section 2.5.1. Table 3-4 summarizes the important input parameters required by the MTM and the way in which these parameters were obtained in this research.

The procedure followed was to model the packing density across the range of fine aggregate proportions from 10 to 90 % in 10 % increments. The modelled relationship between packing density and fine aggregate proportion for the 18 different test aggregate combinations is presented in Appendix B.

Table 3-4: Input parameters for the Modified Toufar packing model and the methods for obtaining them

Input parameter	Symbol	Method for determining parameter
Packing density of constituent aggregates	ϕ_1 & ϕ_2	Measured in laboratory
Characteristic diameter of constituent aggregates	d_1 & d_2	Rosin-Rammler distribution
Constituent volume fractions	y_1 & y_2	ϕ calculated at values y1 of between 0.1 and 0.9 in increments of 0.1.

3.4.2 Measurement of packing density

As discussed earlier in Section 3.4, estimation of the aggregate packing density φ by the MTM requires the input of the packing densities of the fine and coarse aggregates, φ_1 and φ_2 respectively, that constitute the overall aggregate. These values were determined in the lab by way of a modified version of the method prescribed in SANS 5045 for the determination of aggregate packing density. The method was devised and used by Nanthagopalan and Santhanam (2010) who noted that the method prescribed in ASTM C 29 was susceptible to inconsistencies resulting from both the manual pouring of aggregates which when done by hand would not take place from the same height each time, and the compaction of the sample which was done by hand, thereby introducing inconsistencies. To overcome these problems a device consisting of two buckets with a stand to hold the one bucket above the other was developed. The aggregate being tested is released from the top bucket and falls into the bottom bucket with the fall providing the compaction energy. Thus the compaction energy is the same for every run of the test.

The apparatus was constructed to the same form as that used by Nanthagopalan and Santhanam (2010) but with different dimensions. The apparatus consisted of an upper bucket, a lower catchment bucket and a stand to hold the upper bucket above the lower bucket, as

shown in Figure 3-6a. The floor of the upper bucket was modified to swing open by way of a hinge and was fitted with a quick-release latch. The lower bucket had a cylindrical shape with walls of steel, 3 mm thick, to ensure that it did not deform as aggregate fell into it. The lower bucket was made to a diameter of 375 mm, which, being significantly greater than 10 times the maximum particle size of 19 mm, ensured that there were minimal wall effects between the aggregate and the bucket wall. Furthermore, the large diameter ensured that all aggregate from the top bucket fell into the bottom bucket. The lower bucket had a height of 300 mm. The stand held the upper bucket such that its base was 600 mm above the ground and the base of the lower bucket.

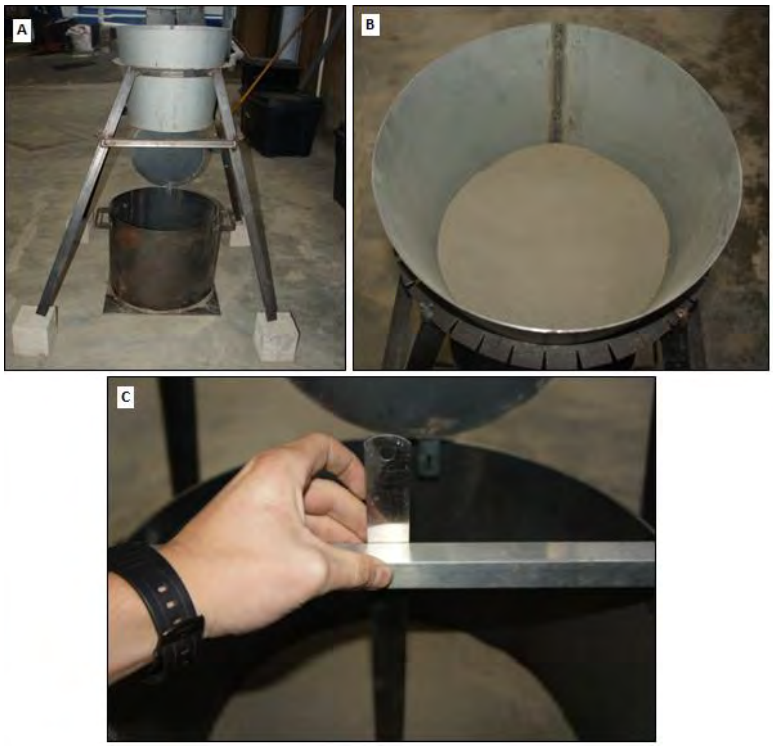

Figure 3-6: Measurement of aggregate packing density including A) View of the entire apparatus; B) The top bucket filled with sand to be tested; C) Measurement of the depth of sand in the bottom bucket after it has been levelled off.

The procedure followed in measuring the packing density using the abovementioned apparatus was carried out according to the following steps:

i. 9 kg of the aggregate being tested was measured out;
ii. The bottom of the upper bucket was secured in the closed position and the aggregate was poured in. The surface of the aggregate was levelled on the horizontal plane with a straight edge;
iii. The quick-release latch was released and the aggregate allowed to fall through the distance of 600 mm and into the bottom bucket;
iv. The surface of the aggregate was levelled gently with a straight edge, so as not to impart any further compactive energy;

v. The distance from the surface of the aggregate to the top of the bucket was measured, as depicted in Figure 3-6 C. Given the aggregate mass and the diameter of the bucket, the bulk density of the agrregate could then be calculated.

The data from the measurement of packing density is summarised in Table 3-5 with comprehensive data presented in Appendix C. It is noted that the packing density of the more coarse and uniformly graded aggregate C2 had a greater packing density than the finer, continuously graded C1. This suggests that there was a loosening effect, as discussed by de Larrard (1999), caused by the finer particles in aggregate C2, which reduced the packing efficiency.

Table 3-5: Summary of data from the lab measurement of aggregate packing densities

Aggregate	Distance from aggregate surface to top of bucket (mm)	Compacted bulk density (kg/m^3)	Packing density
F1	267	1579	0.60
F2	265	1513	0.57
F3	268	1620	0.61
F4	268	1617	0.61
F5	266	1550	0.58
F6	266	1555	0.59
F7	268	1610	0.61
F8	266	1541	0.58
F9	266	1541	0.58
C1	251	1213	0.46
C2	255	1288	0.49

3.4.3 Calculation of characteristic diameter

The characteristic diameter is a representation of the average diameter of a collection of particles. As mentioned in Chapter 2, as a result of the distribution of particle sizes in concrete aggregates, the characteristic diameter is not equal to or near D_{50} – that is the diameter for which 50 % of the particles are smaller (by mass). The Rosin Rammler distribution has been found to be representative of the particle size distribution of concrete aggregates (Johansen & Andersen, 1991). As such it is useful in providing the characteristic diameter of a concrete aggregate for which the grading is known. The procedure followed in using the Rosin-Rammler distribution to calculate the characteristic diameter is presented below.

As a starting point it is useful to present the equation of the Rosin-Rammler distribution, as given in Equation 3-1..

$$R(D) = exp^{-\left(\frac{D}{D'}\right)^n} \quad \textbf{(3-1)}$$

Where D - Particle diameter;
R(D) - Residue fraction – the fraction of particles larger than D;
D' - Characteristic diameter;
n - constant which characterises the distribution, ranging from 1.04 – 4.0 but usually between 1 and 2

Thus

$$\ln\frac{1}{R} = \left(\frac{D}{D'}\right)^n \quad \textbf{(3-2)}$$

$$\ln(\ln\frac{1}{R}) = n\ln D - n\ln D' \quad \textbf{(3-3)}$$

Plotting Equation (3-3) with natural log scales in the x- and y-axis gives a linear relationship of the form y=mx+c with y=(ln(ln(1/R)), with the intercept given by Equation 3-4.

$$Intercept = -n\ln D' \quad \textbf{(3-4)}$$

This equation can be manipulated to make the characteristic diameter the subject od the formula, as given in Equation 3-5.

$$D' = exp^{-\left(\frac{intercept}{n}\right)} \quad \textbf{(3-5)}$$

.

An example of this procedure is presented below using aggregate C1. The relationship between ln(D) and ln(ln(1/R)) is determined through the particle size distribution as presented in Table 3-6 (where F is the percentage of the aggregate that is smaller than the indicated particle size) and plotted in Figure 3-7. Using the plot, the intercept (as represented in Equation 3-4) and the slope (n) were determined. These values are given in Table 3-7. By use of Equation 3-5 the characteristic diameter (D') was determined.

The important data from the calculation of the characteristic diameters for each of the aggregates is summarised in Table 3-8 and presented in detail in Appendix B.

Table 3-6: Determination of ln(D) and ln(ln(1/R)) from aggregate particle size distribution

Particle size - D (mm)	Ln D	Aggregate C1 (ASTM C33/57)				
		F (%)	R=1-F	1/R	ln(1/R)	ln(ln(1/R))
37.50	3.62	100.00	0.00	-	-	-
26.50	3.28	100.00	0.00	-	-	-
19.00	2.94	86.21	0.14	7.25	1.98	0.68
13.20	2.58	54.06	0.46	2.18	0.78	-0.25
9.50	2.25	20.04	0.80	1.25	0.22	-1.50
6.70	1.90	2.38	0.98	1.02	0.02	-3.73
4.75	1.56	0.60	0.99	1.01	0.01	-5.11

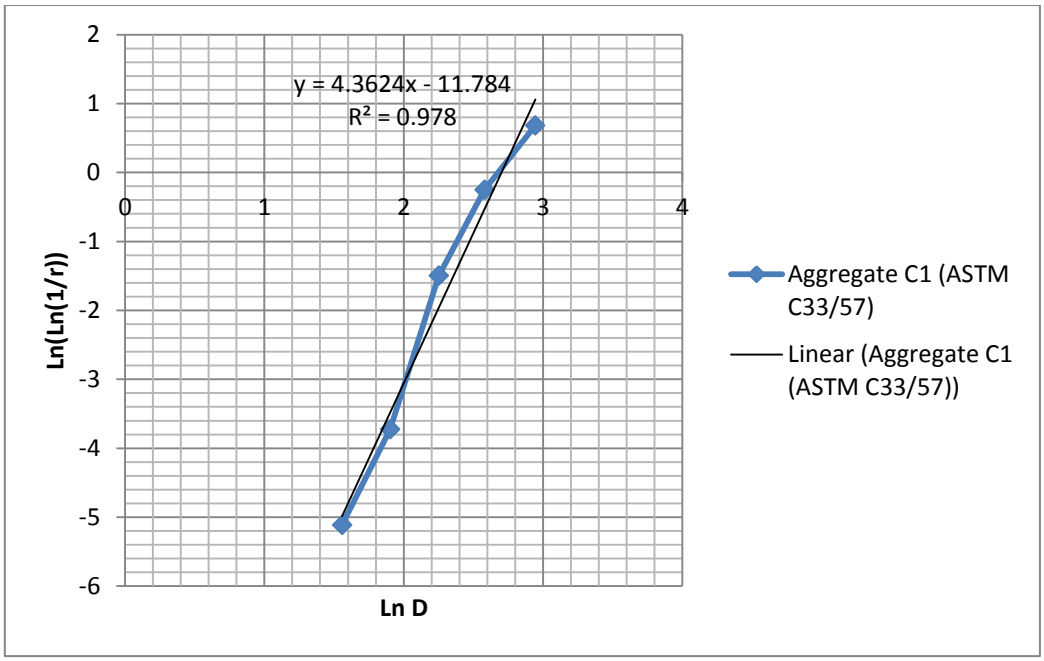

Figure 3-7: Relationship between ln(D) and ln(ln(1/r)) for aggregate C1

Table 3-7: Data for the determination of characteristic diameter derived from the relationship between ln(D) and ln(ln(1/R) for aggregate C1

DISTRIBUTION PARAMETER	PACKING DENSITY	INTERCEPT	CHARACTERISTIC DIAMETER
n	ϕ	C	D' (mm)
4.362	0.486	-11.784	14.90

Table 3-8: Summary of data from the calculation of the characteristic diameter using the Rosin-Rammler distribution

Aggregate	n	Intercept	D' (mm)
F1	1.43	1.12	0.46
F2	1.53	0.81	0.59
F3	1.18	0.40	0.71
F4	1.14	0.37	0.72
F5	1.25	0.28	0.80
F6	1.18	0.25	0.81
F7	1.15	0.04	0.96
F8	1.23	0.09	0.93
F9	1.15	-0.35	1.36
C1	4.36	-11.78	14.90
C2	5.00	-14.46	18.07

3.4.4 Determination of y_1

y_1 is the volume fraction of the total aggregate constituted by the fine aggregate. Once the characteristic diameter and the packing densities (given in Tables 3.5 and 3.6 respectively) of the coarse and fine aggregates had been measured, the packing density for a given combination of coarse and fine aggregate could be determined for different volume fractions of each, using the MTM. Thus for each of the combinations of coarse and fine aggregate the packing density, φ, was determined at increasing fine aggregate volume fractions, y_1, from 0.1 to 0.9 in increments of 0.1. This is illustrated in Figure 3-8. For the sake of example, the plot of φ vs. y_1 for only aggregate C1F1 is given here. Detailed model data for each of the aggregates is presented in Appendix D.

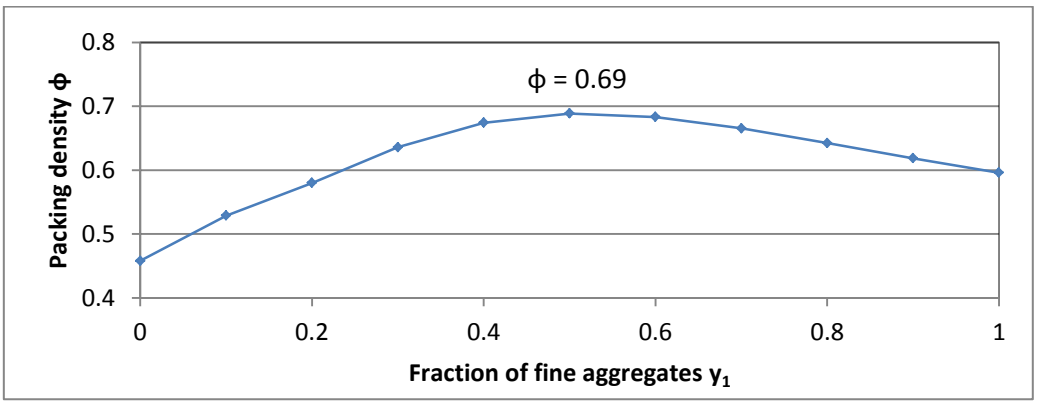

Figure 3-8: Modelled packing density for aggregate C1F1 at different values of y1. 0.69 is the maximum achievable packing density for this aggregate blend which occurs at y_1=0.5.

The MTM indicated that the maximum achievable packing density with aggregate C1F1 was 0.69 at $y_1 = 0.5$. This is reflected in the first row of Table 3-9. Columns 2 and 5 of Table 3-9 give the maximum achievable packing density for all aggregates as found by the MTM. Of these values the lowest value was selected as the packing density to be used for all aggregates in the experiments. This was $\varphi = 0.65$ which was found for aggregate C2F9 and is highlighted in Table 3-9. For clarity this is reaffirmed in Table 3-9 where Columns 3 and 6 present the packing density used for each aggregate in the experiments, where all values given are the same as the highlighted value of 0.65 for C2F9.

Table 3-9: Modelled maximum packing density and the packing density used in experiments for each experimental aggregate.

Sample	Highest achievable ϕ	y1 to achieve ϕ = 0.65	Sample	Highest achievable ϕ	y1 to achieve ϕ = 0.65
C1F1	0.69	0.34	C2F1	0.68	0.40
C1F2	0.67	0.37	C2F2	0.66	0.45
C1F3	0.69	0.34	C2F3	0.68	0.40
C1F4	0.69	0.35	C2F4	0.68	0.40
C1F5	0.67	0.37	C2F5	0.66	0.44
C1F6	0.67	0.37	C2F6	0.66	0.44
C1F7	0.68	0.36	C2F7	0.68	0.42
C1F8	0.67	0.38	C2F8	0.66	0.46
C1F9	0.66	0.42	C2F9	0.65	0.60

Given the target packing density of 0.65, the volume fraction of fine and coarse aggregate for each mix was determined by extrapolation between values of y_1 for which φ was calculated. For example, with reference to Figure 3-8, for aggregate C1F1 $\varphi = 0.64$ at $y_1 = 0.3$ and $\varphi = 0.67$ at $y_1 = 0.4$. Thus $\varphi = 0.65$ occurred at a y_1 value between 0.3 and 0.4. By extrapolation the required y_1 was found was found to be 0.34. The y_1 values for all mixes are presented in Table 3-9.

3.5 Mix design

3.5.1 Materials

Aggregate

To avoid effects derived from variations in aggregate particle shape, all aggregate was of the same source. Crushed greywacke aggregates were used because of its availability in all of the sizes of interest.

Cement

The cement used throughout all experiments was PPC Surebuild conforming to strength class 42.5 N of SANS 50197. The product specification was CEM II-B/M (L-S), indicating an extender content of between 20 & 35 %, constituted of a mixture of ground limestone and Corex slag.

Admixture

The workability of the concrete mixes was controlled through the addition of a superplasticiser. The product used was Chryso Optima 175. This is a powerful, high range water reducing admixture selected for use in these experiments due to the expected harshness of the mixes resulting from the aggregate used. It is based on polycarboxylate and modified phosphonate. Prior to adding the admixture, the other ingredients, including the water, were mixed for a minute. Thereafter, with the mixer still running, the admixture was slowly added until the mix was observed to have the desired consistency and the slump fell within the range of 50 to 100 mm. The final admixture dosages and slumps are presented in Table 3-10.

3.5.2 Mix proportioning

The volume fractions of fine (y_1) and coarse (y_2) aggregates for each mix were selected so as to obtain $\varphi = 0.65$. The procedure followed in obtaining the aggregate volume fractions has been described in Section 3.3.

The water/binder ratio, was fixed at 0.55 throughout. The w/b ratio was held constant as it was not part of the focus of the research and changes in w/b ratio have significant effects on both strength and durability.

Through trial mixes it was determined that a water content of 200 l/m^3 gave mixes that were cohesive and typically had a slump of between 40 and 50 mm prior to the addition of admixture. A low workability was expected given the shape of the aggregate. With consideration of cost in practice, a water content greater than 200 l/m^3 was undesirable. In general it was found that with the addition of a superplasticiser the mixes attained a desired workability with slumps within the range of 50 to 100 mm, whilst maintaining good cohesiveness. The mix designs used in the experiments are given in Table 3-10, where y_1 is the volume fraction of the overall aggregate constituted by the fine aggregate.

Table 3-10: Summary of concrete mix designs

Mix	Water	W/B	CEM II B 42.5	y_1	Sand	13 mm Stone	19 mm Stone	Super-plasticiser		Slump
	kg	-	kg		kg	kg	kg	l/m^3	% of cement mass	mm
C1F1	200	0.55	364	0.34	598	585	585	2.77	0.8	75
C1F2	200	0.55	364	0.37	646	561	561	2.00	0.6	85
C1F3	200	0.55	364	0.34	608	580	580	2.31	0.7	70
C1F4	200	0.55	364	0.35	610	579	579	2.15	0.6	95
C1F5	200	0.55	364	0.37	649	559	559	1.54	0.4	90
C1F6	200	0.55	364	0.37	648	560	560	1.31	0.4	80
C1F7	200	0.55	364	0.36	637	566	566	0.92	0.3	65
C1F8	200	0.55	364	0.38	670	549	549	0.77	0.2	85
C1F9	200	0.55	364	0.42	769	520	520	1.15	0.3	90
C2F1	200	0.55	364	0.40	699	-	1069	4.15	1.2	70
C2F2	200	0.55	364	0.45	790	-	979	2.69	0.8	90
C2F3	200	0.55	364	0.40	702	-	1066	1.77	0.5	95
C2F4	200	0.55	364	0.40	704	-	1064	2.69	0.8	90
C2F5	200	0.55	364	0.44	777	-	991	2.08	0.6	80
C2F6	200	0.55	364	0.44	773	-	995	2.08	0.6	80
C2F7	200	0.55	364	0.42	741	-	1027	1.46	0.4	70
C2F8	200	0.55	364	0.46	813	-	955	2.38	0.7	80
C2F9	200	0.55	364	0.60	1061	-	707	2.00	0.6	70

3.6 Specimen preparation

Laboratory test specimens were prepared in accordance with the specifications of SANS 5860 and SANS 5861 (1, 2 & 3). Each mix was made in a volume of 13 litres, from which twelve no. 100 mm cubes were cast, of which 3 were tested for compressive strength, 4 were used for durability index tests, and 2 were used in the carbonation tests. The remaining 3 cubes were spare. The further specimen preparations that were specific to the durability index tests are described in Sections 3.6.1 to 3.6.3.

3.6.1 Compressive strength test specimens

The 100 mm cubes were cured for 28 days in a water bath at 23 °C prior to testing for compressive strength.

3.6.2 Durability index test specimens

The samples for all durability index tests were 30 mm thick slices of 70 mm diameter cores cut from the sample 100 mm cubes. A core was cut perpendicular to a face of a cube, through to the opposing face, and the slices were taken 5 mm from each end of the core. For the durability index tests, four no. 100 mm cubes from each mix were cast and cured in a water bath at 23 °C for 28 days. Thereafter the cubes were cored and cut and the test samples were placed in an oven at 50 °C for 7 days.

3.6.3 Carbonation test specimens

100 mm cubes were cured for 28 days in a water bath at 23 °C and then left to dry for 10 weeks in a standardised lab climate with a temperature of 23 °C and 65 % relative humidity to ensure that the moisture content in the concrete was conducive to carbonation. Thereafter the 100 mm cubes were prepared by sealing four faces with epoxy, leaving two opposing cast faces exposed thus allowing for unidirectional carbonation.

3.7 Compressive strength

Compressive strength tests were conducted at an age of 28 days in accordance with SANS 5863. These tests were done to ensure that sample preparation, including batching, mixing and curing, had been done correctly and consistently throughout.

3.8 Durability index tests

Deleterious agents penetrate concrete by way of transport mechanisms. A first step in characterising the durability of concrete is therefore to evaluate each of the transport properties of the concrete. The South African Durability Index approach provides an effective and comprehensive method to do this. Thus each of the tests incorporated therein, namely the chloride conductivity index, oxygen permeability and water sorptivity index tests, were employed in this research. This section describes the methods through which these tests were carried out.

3.8.1 Water sorptivity index

Absorption is the process whereby a fluid is drawn into an unsaturated porous medium under the action of capillary forces. The rate at which absorption takes place is known as sorptivity.

The South African Durability Index prescribes the water sorptivity index test to measure the sorptivity in the cover region.

After oven drying, the samples were place in a desiccator to cool for 3 hours. The circumferential surface of each of the samples was then sealed with tape to ensure unidirectional absorption. The dry mass of the taped samples was measured. The samples were placed on paper towel immersed in a few millimetres of saturated sodium hydroxide solution. The mass was measures at 3, 5, 7, 9, 12, 16, 20 and 25 minutes. The samples were then placed in chamber under a vacuum pressure of 80 kPa for 3 hours. Thereafter the chamber was flooded with saturated calcium hydroxide solution and kept under a vacuum pressure of 80 kPa for one hour before the pressure was zeroed and the samples left for 18 hours. The saturated mass was then measured.

The test data when plotted, yields a linear relationship between the mass of water absorbed and the square root of time. This allows for the sorptivity to be calculated by Equation 3-6.

$$S = \frac{\Delta M_t}{t^{1/2}} \cdot \frac{d}{M_{sat} - M_0} \quad \textbf{(3-6)}$$

where ΔM_t - change in mass with respect to the dry mass (g)
M_{sat} - saturated mass of concrete (g)
M_0 - dry mass of concrete (g)
d - sample thickness (mm)
t - period of absorption (hr)

3.8.2 Chloride conductivity index

Diffusion is one of the key transport mechanisms. It is the movement of ions through a medium from a region of high concentration to a region of low concentration. Diffusion in concrete takes place over a long period of time. In order to reduce this time and cater a more practical and useful test, the chloride conductivity index test uses an applied potential difference to accelerate the flow of ions across a test sample. This test gives a measure of the conductivity which gives an indication of the diffusion properties of the concrete through Equation 3-7.

$$Q = \frac{D}{D_0} = \frac{\sigma}{\sigma_0} \quad \textbf{(3-7)}$$

where	Q	-	diffusibility
	D	-	diffusivity of ions through the material
	D_0	-	diffusivity of ions in the pore solution
	σ	-	conductivity of the material
	σ_0	-	conductivity of the pore solution

Samples were prepared by vacuum saturation in a 5M NaCl solution for 24 hours prior to conducting the tests. The apparatus used to conduct the tests is illustrated in Figure 3-9. A 10 V potential difference was applied across the sample and the resulting current flow through the sample was measured and used to determine the chloride conductivity. This is given in Equation 3-8.

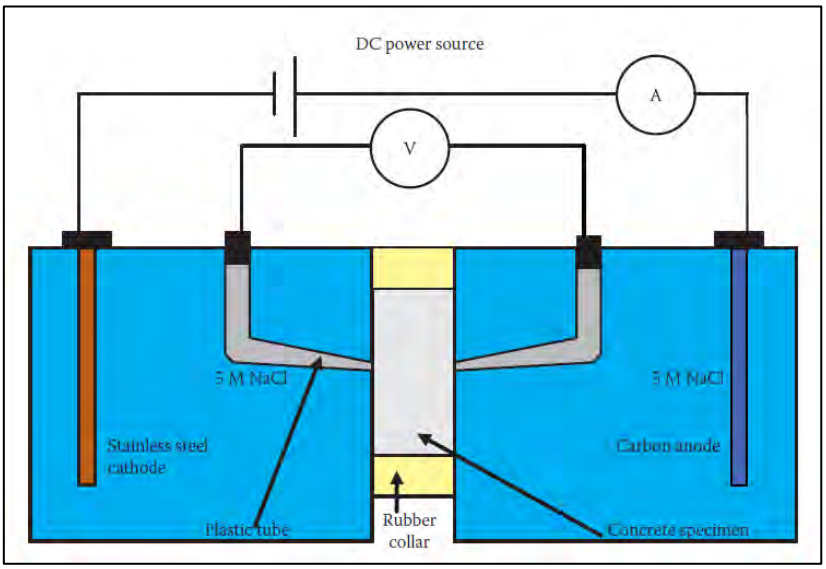

Figure 3-9: Schematic of the chloride conductivity index test apparatus (after Beushausen and Alexander, 2010)

$$\sigma = \frac{It}{VA} \tag{3-8}$$

where	σ	-	chloride conductivity (mS/cm)
	I	-	current (mA)
	t	-	specimen thickness (cm)
	V	-	voltage
	A	-	cross-sectional area (cm^2)

3.8.3 Oxygen permeability index

Permeation is the movement, under an externally applied pressure, of fluid through a pore structure that is saturated in that same fluid. The Oxygen Permeability test used in the South

African Durability Index was designed to measure the permeability of cover concrete. The test is carried out in a falling head permeameter, as illustrated in Figure 3-10, in which oxygen is pressurised against a surface of the sample and the rate of pressure decay measured, as permeation proceeds. An initial pressure of 100 kPa was used and the pressure decay was measure over a period of 6 hours. The plot of the log of the ratio between the original pressure and the instantaneous pressure versus time provides a linear relationship from which the parameters for the determination of the coefficient of permeability can be determined. The coefficient of permeability is determined by Equation 3-9.

$$k = \frac{\omega V g d}{RA\theta t} \ln \frac{P_0}{P} \quad \textbf{(3-9)}$$

Where
- k - coefficient of permeability (m/s)
- ω - molecular mass of permeating gas (kg/mol)
- V - volume of the pressure cylinder (m^3)
- g - acceleration due to gravity (m/s^2)
- d - sample thickness (m)
- R - universal gas constant (Nm/K mol)
- A - cross-sectional area of specimen
- θ - absolute temperature (K)
- t - time (s)
- P_0 - pressure at start of test (kPa)
- P - pressure at time t (kPa)

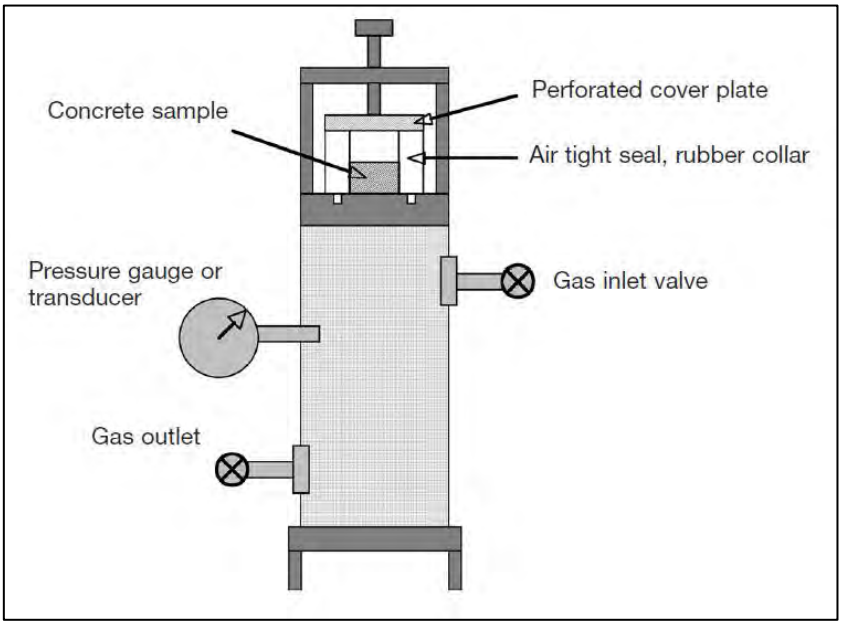

Figure 3-10: Schematic of the oxygen permeability index test apparatus (after Ballim, Alexander and Beushausen, 2009)

The coefficient of permeability is typically in the order of 10^{-10} or smaller. The oxygen permeability index is of a form that is more attractive and easier to use and is found by taking the negative log of the coefficient of permeability as as shown in Equation 3-10.:

$$OPI = -\log_{10} k \quad \textbf{(3-10)}$$

3.9 Carbonation

The durability index tests served to characterise the penetrability of the concrete in terms of various transport properties. Whilst each transport property contributes to the concrete's penetrability, deleterious agents usually penetrate the concrete through a combination of the transport mechanisms. Furthermore, there is chemical interaction between the products of hydration and the deleterious substances which can result in changes in the microstructure of the concrete and thereby influence both the penetrability and the susceptibility of the concrete to the action of deleterious agents. As such characterisation of the individual transport mechanisms can only give an indication of the potential for the concrete to be penetrated by that mechanism. The rate at which the concrete will be penetrated by a substance cannot be inferred from them. Thus accelerated carbonation tests were therefore conducted to determine the practical implications of the experimental variations.

The cubes were placed in the carbonation chamber at a temperature of 20 ± 2 °C, relative humidity of 65 ± 5 % and a carbon dioxide concentration of 2.0 ± 0.2 %. The carbonation chamber used was a LEEC GA2010 Cell Culture Standard 150 litre incubator, which can control carbon dioxide concentration from 0 to 20 % at ± 0.1 %. The LEEC chamber is depicted in Figure 3-11. The chamber can be heated to 37 °C but when the heating function is not used it operates at around 5 °C above the ambient temperature. Thus the temperature was regulated at 20 ± 2 °C by pumping cooled water through a cooing coil inside the LEEC chamber. The water was pumped from a bucket in an adjacent refrigerator to an inlet valve at the head of the LEEC chamber by a 1 m head aquarium pump. The water returned through a pipe running from the outlet valve at the head of the LEEC chamber back to the bucket. The relative humidity was controlled by placing a tray containing a litre of water saturated in sodium nitrite in the LEEC chamber.

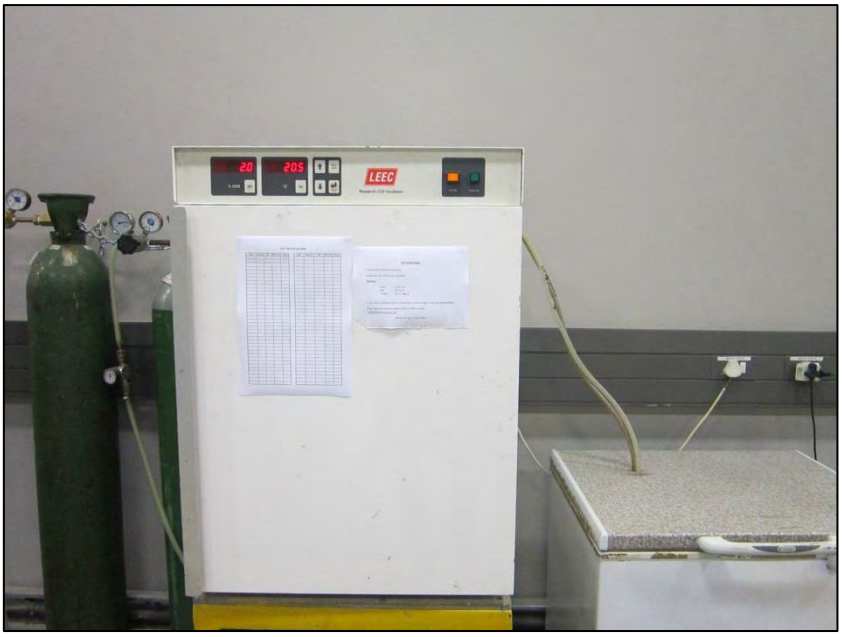

Figure 3-11: LEEC GA2010 carbonation chamber with adjacent refrigeration unit

The carbonation depth was taken at 30 and 60 days. The testing involved slicing the sample parallel and at a distance of 10 mm from an unexposed surface. The cut surface was sprayed with 1 % phenolphthalein solution and the thickness of the layer of different colour measured with Vernier callipers. Three readings, one in the centre and one on either side, were taken along each carbonated edge.

3.10 Experimental repeatability

As is discussed in detail in Section 4.3, the compressive strength results ranged between 42.9 and 47.1 MPa, a range of 4.2 MPa. This narrow range was taken as sufficient confirmation of the repeatability of the material and test specimen preparation procedure. The South African Durability Index Test Methods give repeatable results (Alexander, Mackechnie & Ballim, 2001; Mackechnie, 1997)

3.11 Summary

This chapter presented the experimental method used in this research. The experimental design indicated the requirement of maintaining constant aggregate packing density in all tests. A particle packing model – the Modified Toufar Model – was used to determine the packing density of the test aggregates and the aggregate mix proportions to achieve this packing density. This method has been detailed. The sample constituent materials and their

respective proportions were given in the mix design. Durability index tests and carbonation tests were used to characterise the concrete penetrability and durability. The procedures followed in carrying out these tests have been described.

In total, 18 different mixes were tested. The variables of the mixes were the fineness modulus (FM) and the coefficient of uniformity of the fine aggregate and the fineness modulus of the coarse aggregate which dictated whether the overall aggregate grading was gap or continuous. FM and C_u used because they characterise two different aspects of an aggregate grading. The former describes the average particle size whilst the latter gives an indication of the slope of the grading curve. For the fine aggregate FM was varied between 1.5 and 3.0, where the limits were selected with consideration of SANS 1083:2013 and ASTM C33. For all fine aggregates, 100 % of particles were smaller than 4.75 mm and 5 % was smaller than 75 μm. This physically restricted the range of C_u which varied between 3.3 and 6.8.

4. Results

4.1 Introduction

The laboratory experiments that formed part of this research included four different tests. Three were tests that are used in the South African Durability Index (DI) Approach, consisting of the oxygen permeability index (OPI), water sorptivity index (WSI) and chloride conductivity index (CCI) tests. In particular these were used to characterise the transport mechanisms of permeability, sorptivity and conductivity, which is related to diffusivity. The fourth test used was the accelerated carbonation test which provided a measure of the rate of penetration of carbon dioxide. These test methods are described in Chapter 3. This chapter presents and discusses the results.

The Chapter begins with an evaluation of the consistency of the test specimens through the average cube strength. Thereafter the results of each of the four abovementioned tests are presented. For each an overview of the results, including descriptive statistics, is presented. Thereafter the specific effects of tested aggregate properties of fineness modulus (FM), coefficient of uniformity (C_u) and the overall grading are analysed. At the end of each section there is a discussion on the respective test parameter. At the end of the chapter a final discussion is presented which considers the link between the results for each of the parameters and raises some general considerations regarding sample sizes.

4.1.1 Correlation and regression analysis

Correlation and regression analyses were employed to determine effects of FM and C_u on the measured parameters. Correlation analysis was used to determine whether there was a significant relationship between either FM or C_u and the measured parameters. This involved the calculation of the correlation coefficient r, as represented in Equation (4-1), where x_i is the measured parameter at level i and $\bar{x}$ is the average of the measured parameter over all test levels, whilst y_i is the value of the controlled variable at level i and $\bar{y}$ is average of the controlled variable over all test levels, with controlled variables being either FM or C_u.

r is the correlation coefficient ranging from -1 to 1 and describes the linear relationship where negative values indicate a inversely proportionate relationship and positive values describe a directly proportionate relationship. Values close to -1 or 1 indicate that date points are centred around a definite line (ie there is strong relationship between the two variables) whilst

a value close to zero indicates a large scatter. R^2 (which is the same as r^2) is the coefficient of determination, which specifically indicates the goodness of fit of the fitted linear relationship. Since it was necessary to know whether a change in the controlled variable resulted in an increase or decrease in penetrability, it was beneficial to use r rather than R^2.

Cohen (1988) suggests that $|r| < 0.3$ indicates little correlation. With a low correlation, there is little relationship between the variables of interest which means that a regression analysis is not of value. The correlation analysis was therefore used as an indicator of whether or not to perform a regression analysis, where, if $|r| < 0.3$, a regression analysis was deemed unnecessary.

$$r = \frac{\sum(x_i - \bar{x})(y_i - \bar{y})}{\sqrt{\sum(x_i - \bar{x})^2 \sum(y_i - \bar{y})^2}} \quad \textbf{(4-1)}$$

Through visual assessment of Figures 4-5, 4-8, 4-10 and 4-13 it was concluded that linear regression analysis was more appropriate than any higher order regression. The linear regression analysis was conducted using the method of least squares. An example calculation using this method is presented in Appendix E. The general formula derived through the regression is given in Equation (4-2), where $\hat{y}$ is the estimate of the property of interest, β_0 is a constant and β_1 and β_2 are parameters that indicate the magnitude of the influence of FM and C_u respectively.

$$\hat{y} = \beta_0 + \beta_1(FM) + \beta_2(C_u) \quad \textbf{(4-2)}$$

4.1.2 Hypothesis tests

Hypothesis testing provided a useful tool to compare the means of tested properties between samples ($\mu_{C1} = \mu_{C2}$) with different overall aggregate grading, being either continuous (C1) or gap (C2). The t-test was applied to properties which are known to have a normal distribution and was chosen because samples consisted of 4 specimens each. The following hypothesis was tested:

$H_0 : \mu_{C1} = \mu_{C2}$
$H_1 : \mu_{C1} \neq \mu_{C2}$
Significance level: 5 %

4.2 Relationship between FM and y_1

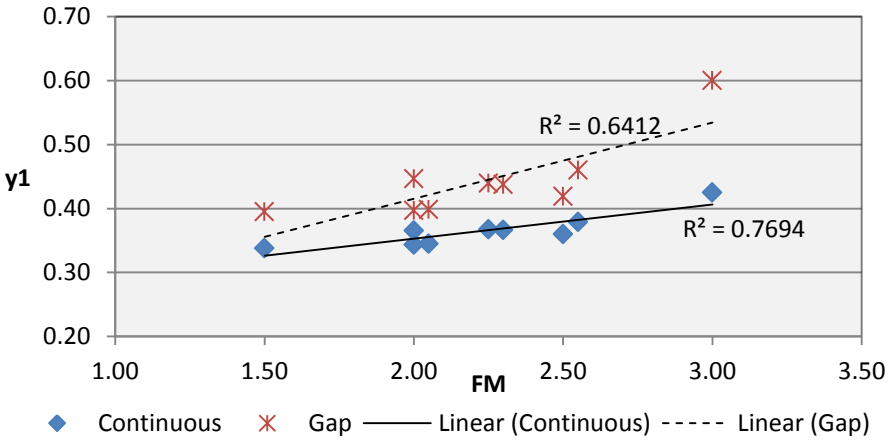

Figure 4-1: Relationship between FM and y_1 at different overall aggregate gradings

Figure 4.1 shows the coefficient of determination for the linear relationship between y_1 and FM. With increasing aggregate coarseness, there was a greater amount of fine aggregate required to maintain the same packing density. For continuous graded aggregate $R^2 = 0.7694$ and for gap graded aggregate $r^2 = 0.641$. Thus the correlation coefficients (the square root of the coefficient of determination) for the relationship between FM and y_1 are $r = 0.877$ and $r = 0.801$ for the continuous and gap graded aggregates respectively. y_1 for the gap graded aggregate at FM = 3.00 appears to be unusually distant from the fitted line, with a difference of around 0.07. However, y_1 for the gap graded aggregate at FM = 2.50 is equally distant from the fitted line and the next greatest difference between the observed and the fitted value for gap graded aggregate was around 0.05 units at an FM of 1.50. Thus it was concluded that there was no outliers.

To test whether the observed correlations were statistically significant a hypothesis test was conducted, where ρ is the correlation coefficient for the population.

$H_0 : \rho = 0$
$H_1 : \rho \neq 0$
Significance level: 5%

It was found that at a 5 % significance level, $r > 0.602$ is statistically significant. Since $r > 0.602$for both continuous and gap graded aggregates, they fall into the rejection region and thus the null hypothesis is rejected. It is concluded that there is a linear relationship between FM and y_1. Any variations that were found to coincide with changes in FM could be attributed either directly to the changes in FM or to the variation in y_1 which is directly linked

to FM. By considering these two variables together, the complexity of the analysis was reduced.

The continuously graded aggregate had CFM = 8.37 and the gap graded aggregate had a CFM = 9.03. From Figure 4-1 it is evident that the gap grading demanded a higher y_1 with each of the fine aggregates, indicating that the relationship observed between FM and y_1 above, holds for coarse aggregates. This makes sense as the larger average particle size yields greater voids to be filled by fine aggregate.

The C&CI Method for concrete mix design incorporates Equation (4-3), which says that with increased FM, greater amounts of fine aggregate are required. Here, M_a is the mass of coarse aggregate, CBD is the compacted bulk density of the coarse aggregate, K is a factor relating to the maximum aggregate size and the workability of the concrete (Addis & Goodman, 2009). The finding above reaffirms the basis for this method.

$$M_a = CBD(K - 0.1FM) \quad \textbf{(4-3)}$$

4.3 28 day compressive strength

The 28 day compressive strength was determined as a measure of repeatability and to ensure that batching, mixing and compaction were carried out correctly. The compressive strength results are presented in Table 4-1 and Figure 4-2.

From Table 4-1 and Figure 4-2 the following observations were made:

i. The highest observed mean strength was 47.1 MPa for mix C2F2 and lowest was 39.0 MPa for mix C1F8, giving a range of 7.2 MPa.
ii. The range between the two lowest strengths – mixes C1F8 and C1F4 – was 3.3 MPa which is 41 % of the range between the highest and lowest strengths.
iii. The mean strength across all samples with a continuous grading was 44.03 MPa and across samples with gap grading was 45.50 MPa.
iv. The highest CoV was 5.43 %, for mix C1F7. The lowest CoV was 0.40 % for mix C2F7. After C2F7 the highest CoV was 3.74 % for mix C2F4.

The box plot in Figure 4-3 indicates that the mean strength found for sample C1F8 is within 3 inter-quartile ranges of the lower quartile and is thus not depicted as an outlier (If it were outside of this range it would be represented as a point beyond the tip of the "whisker"). However, the plot of the observed strength distribution vs. the expected standardised normal distribution indicates that the strength results generally follow a normal distribution apart

from that of C1F8 which is a clear outlier. On this basis, along with the large difference between the strength of C1F8 and that of C1F4 which was the next lowest observed strength, sample C1F8 was rejected. The remainder of the analyses omitted the results for this sample.

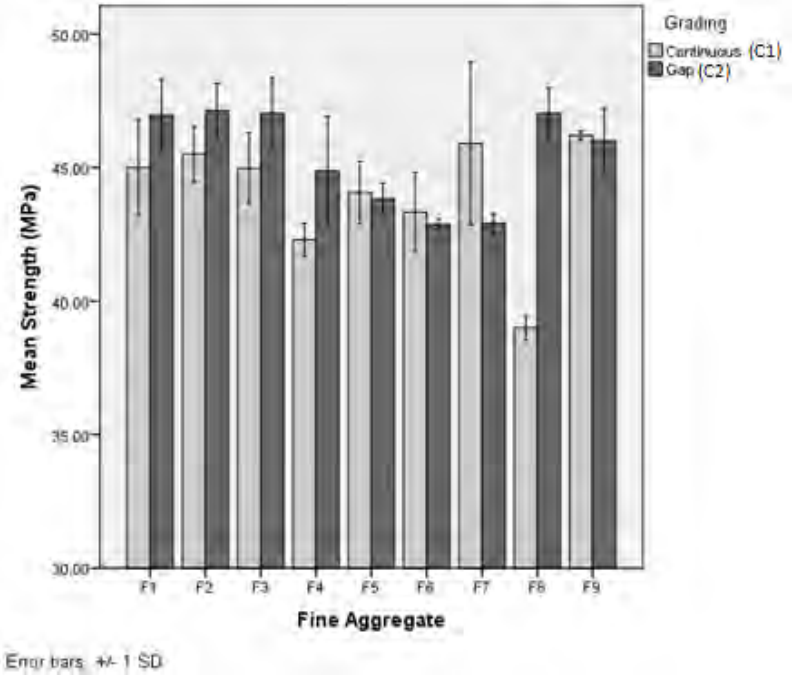

Figure 4-2: 28 day cube strengths for all test concretes

Table 4-1: 28 day cube strength results

Mix	Average mass (kg)	Average density (kg/m^3)	Average strength (MPa)	Std. Deviation (MPa)	CoV (%)
C1F1	2.36	2362	45.0	1.47	3.27
C1F2	2.33	2326	45.5	0.85	1.86
C1F3	2.33	2330	45.0	1.09	2.42
C1F4	2.35	2352	42.3	0.50	1.17
C1F5	2.30	2301	44.1	0.94	2.14
C1F6	2.34	2337	43.3	1.22	2.82
C1F7	2.36	2358	45.9	2.49	5.43
C1F8	2.33	2334	39.0	0.37	0.96
C1F9	2.34	2337	46.2	0.14	0.31
C2F1	2.33	2327	47.0	1.10	2.33
C2F2	2.33	2327	47.1	0.83	1.77
C2F3	2.36	2362	47.0	1.10	2.33
C2F4	2.29	2294	44.9	1.68	3.74
C2F5	2.35	2352	43.8	0.48	1.09
C2F6	2.31	2313	42.9	0.17	0.40
C2F7	2.34	2341	42.9	0.29	0.69
C2F8	2.33	2325	47.0	0.77	1.64
C2F9	2.35	2354	46.0	0.99	2.15

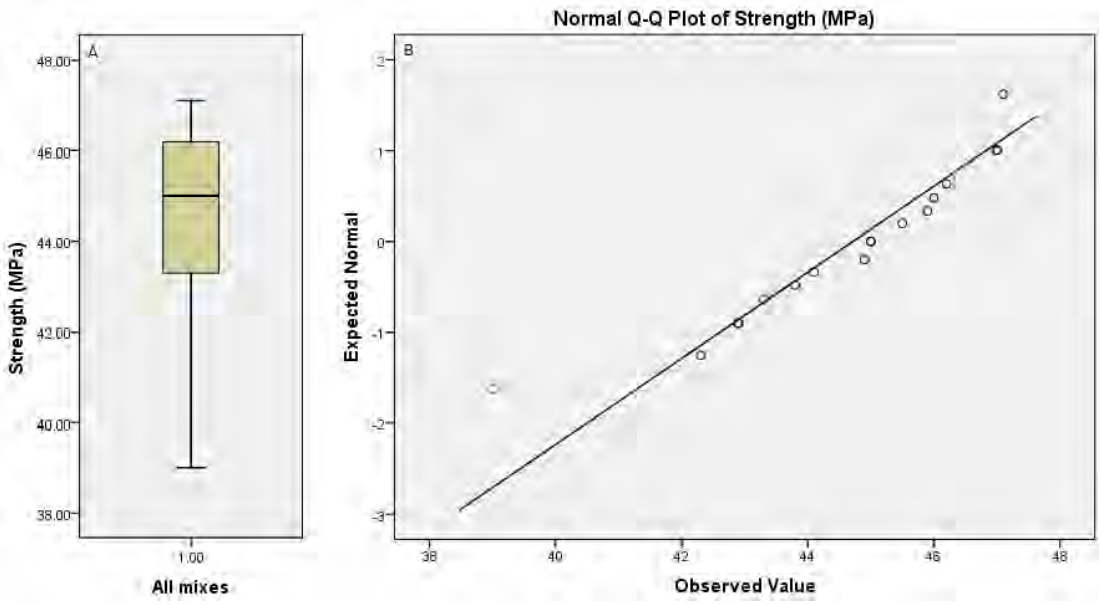

Figure 4-3: (A) Box plot of strength results and (B) a Q-Q plot of the expected standardised normal distribution vs. the observed distribution of strength results

4.4 Oxygen permeability index

This section presents and discusses the results obtained from the oxygen permeability index tests.

4.4.1 Descriptive statistics

The descriptive statistics on the oxygen permeability index (OPI) data are presented in Table 4-2 and the means are plotted on a bar chart presented in Figure 4-4.

Observations made from the descriptive statistics and Figure 4-4 are:-

i. With changes in fine aggregate, the OPI of concretes with continuously graded aggregate ranged between 10.10 for C1F4 (FM = 2.05, C_u = 6.0) and 10.51 for C1F1 (FM = 1.50, C_u = 4.3), a range of 0.41. For concretes with gap grading, OPI varied from 10.07 for C2F3 (FM = 2.00, C_u = 4.4) to 10.80 for C2F2 (FM = 2.00, C_u = 3.3), a range of 0.73.

ii. The mean OPI of the mixes made with a continuous grading was 10.32 and the mean OPI of the mixes made with gap grading was 10.40.

iii. The greatest differences in OPI observed between samples in which only the coarse aggregate was varied was 0.44 which was for concretes with fine aggregate F2.

Table 4-2: Descriptive statistics for OPI data

Mix	Number of specimens tested	Mean	Std. Deviation	Minimum	Maximum	CoV (%)
C1F1	4	10.51	0.18	10.38	10.78	1.73
C1F2	4	10.36	0.16	10.20	10.56	1.58
C1F3	4	10.34	0.08	10.25	10.43	0.78
C1F4	4	10.10	0.20	9.84	10.28	2.01
C1F5	4	10.42	0.09	10.31	10.51	0.84
C1F6	4	10.16	0.30	9.78	10.46	3.00
C1F7	4	10.31	0.19	10.15	10.58	1.87
C1F9	4	10.34	0.16	10.14	10.53	1.56
C2F1	4	10.46	0.15	10.28	10.62	1.39
C2F2	4	10.80	0.17	10.63	11.00	1.58
C2F3	4	10.07	0.12	9.95	10.24	1.21
C2F4	4	10.36	0.13	10.17	10.45	1.25
C2F5	4	10.42	0.17	10.23	10.61	1.62
C2F6	4	10.36	0.30	9.93	10.61	2.87
C2F7	4	10.21	0.13	10.07	10.38	1.31
C2F8	4	10.67	0.10	10.53	10.73	0.89
C2F9	4	10.51	0.27	10.21	10.86	2.54

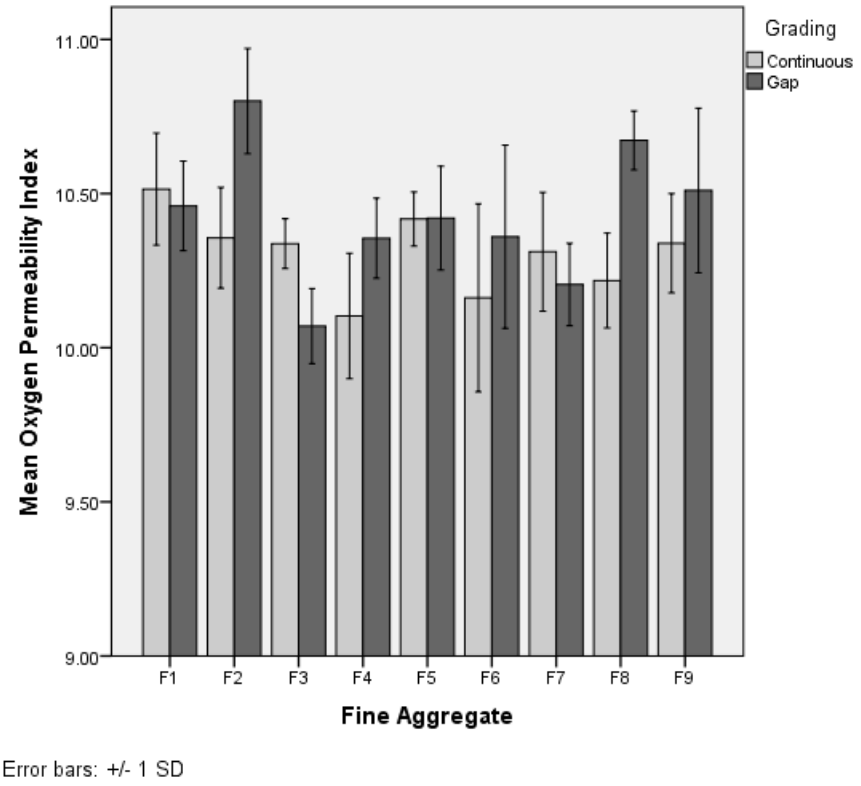

Figure 4-4: OPI results for different coarse and fine aggregates

iv. There were 9 fine aggregates that were tested in two different concretes; one concrete for each of the two coarse aggregates C1 and C2. For three of these pairs the higher OPI was observed in the concrete with coarse aggregate C1. With the exclusion of C1F8, there were 5 pairs where the higher OPI was observed with C2. Thus in general a gap grading gave a higher OPI.

v. The three concretes for which a greater OPI was observed with C1, were those with fine aggregates F1 (FM = 1.50, C_u = 4.3), F3 (FM = 2.00, C_u = 4.4) and F7 (FM = 2.50, C_u = 5.6). Both the FM and C_u values of these are widely spread amongst the tested values ($1.50 \leq FM \leq 3.00$; $3.3 \leq C_u \leq 6.0$) of each, indicating no particular pattern in distribution.

vi. The CoV ranged from 0.78 to 3.00 % for continuously graded aggregate and from 0.89 to 2.87 % for gap graded aggregate. A CoV greater than 2.00 % is considered high for lab conditions (Alexander, 2013, Pers. Comm.). Four mixes had CoV greater than 2.00 %. These were C1F4 (2.01 %), C1F6 (3.00 %), C2F6 (2.87 %) and C2F9 (2.54 %). The two greatest CoV values were observed for mixes with fine aggregate F6 which had the greatest coefficient of uniformity (C_u = 6.8). This is explored further in Section 4.4.2.

4.4.2 Influence of changes in fine aggregate on OPI

In Section 4.4.1 it was observed that changes in fine aggregate resulted in a change in OPI of as much as 0.73. This is equivalent to a difference in the coefficient of permeability of more than half an order of magnitude. Furthermore there was a high degree of variation in the CoV between samples with different fine aggregates. However, it is now necessary to distinguish whether the observed differences were a result of changes in FM or C_u or both. This section explores the influence of FM and C_u on the OPI and the variance of OPI.

Correlation between FM and C_u and OPI

The method used to understand the influence of FM and C_u on the OPI was correlation and regression analysis. The former determined whether there was a relationship between either of the fine aggregate characteristics and the OPI. If a relationship was established the regression analysis was used to determine the strength of the influence that the fine aggregate characteristics had on the OPI.

Figure 4-5 presents the observed OPI values against FM and C_u independently. For example, in the bottom left corner the relationship between FM (increasing from left to right on the x-

axis) and OPI (increasing from bottom to top on the y-axis). The figure is symmetric about the diagonal from the top left corner to the bottom right corner.

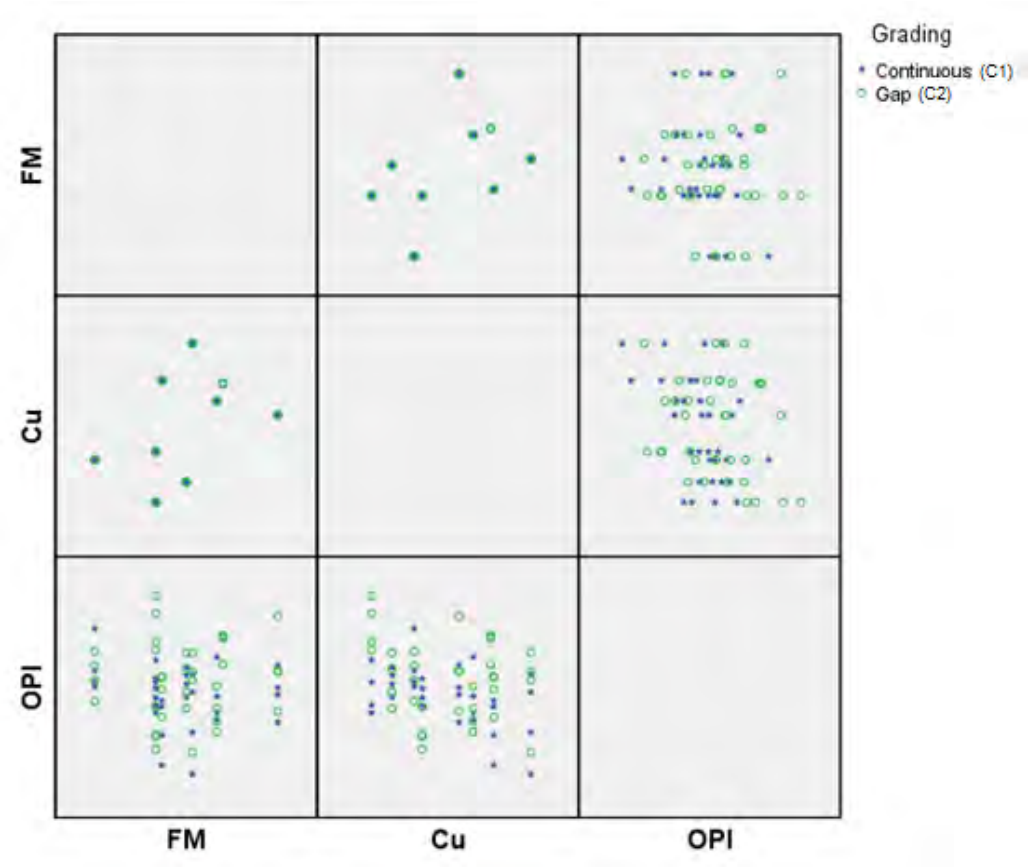

Figure 4-5: Matrix scatter plot showing the influence of FM and Cu on OPI with different aggregate gradings

For both OPI vs. FM and OPI vs. C_u the correlation coefficient r was determined for concretes with each of the coarse aggregates. These are presented in Table 4-3.

Table 4-3: Correlation coefficients r between OPI and Cu and FM

Correlation coefficients r		
Grading	**OPI vs. FM**	**OPI vs. C_u**
Continuous (C1)	-0.171	-0.472
Gap (C2)	0.067	-0.198

Observations

For OPI vs. FM:- r was negative for continuously graded aggregate and positive for gap graded aggregate. This indicates that when FM increased for the continuous grading OPI decreased and for gap grading it increased. This change either indicates that the influence of FM was linked to the overall grading or that OPI was not affected by FM. For both aggregate gradings, $-0.3 < r < 0.3$. It is therefore concluded that variations in FM had no meaningful influence on OPI.

For OPI vs. C_u:- The absolute value or r for OPI vs. C_u was greater than that for OPI vs. FM at all aggregate gradings. This indicates that there was a stronger relationship in the former. The greatest value of the correlation coefficient was r = -0.472. This was deemed strong enough ($r < -0.3$ or $r > 0.3$) to warrant a regression analysis between OPI and C_u.

Regression analysis for OPI vs. C_u

The correlation coefficients for OPI vs. C_u suggest that there might be a relationship between C_u and OPI. This was studied further by way of linear regression analysis using the method of least squares. The regression analysis solved for the β_i parameters (i = 0, 1, 2) in Equation (4-2). Since negligible correlation was found between FM and OPI, $\beta_1 = 0$.

Table 4-4: OPI vs. Cu regression analysis results

Grading	Parameter	Value	t	Significance
Continuous (C1)	β_0	10.742	72.359	0.000
	B_2	-0.086	-2.929	0.006
Gap (C2)	β_0	10.668	51.121	0.000
	B_2	-0.048	-1.177	0.247

The β_i values are presented in Table 4-4. The values of these parameters on a t-distribution were determined, from which the significance level was determined. A confidence interval of 95% was used in the analysis of the results. Thus the β_i was concluded to be meaningful (ie: $|\beta_i| > 0$ where the significance was less than 5 % (ie: significance < 0.05).

For continuously graded aggregate $\beta_2 = -0.086$ and for gap graded aggregate $\beta_2 = -0.048$. Of the two only the former was found to be significant at a 5 % level.

C_u influence on OPI variance

Section 4.4.1 highlighted that for both aggregate gradings the greatest CoV was observed with fine aggregate F6 which had the greatest C_u of all of the fine aggregates tested. This suggested that the variance at each test level may have been linked to C_u. To investigate this further the standard deviation was plotted against C_u for each grading, as shown in Figure 4-6(A). In Figure 4-6(B) the same relationship is plotted but with the omission of the concretes made with F6.

In Figure 4-6(A) an upward trend was observed for both continuously and gap graded concretes. However, there was little linear correlation with $R^2 = 0.493$ for continuous grading and $R^2 = 0.071$ for gap grading. When the same relationship was plotted without the samples with F6, the trend line for the former became flatter and for the latter its slope became

negative, as shown in Figure 4-6(B). It is therefore concluded that in general the standard deviation, and therefore variance, in OPI results was not dependent on C_u.

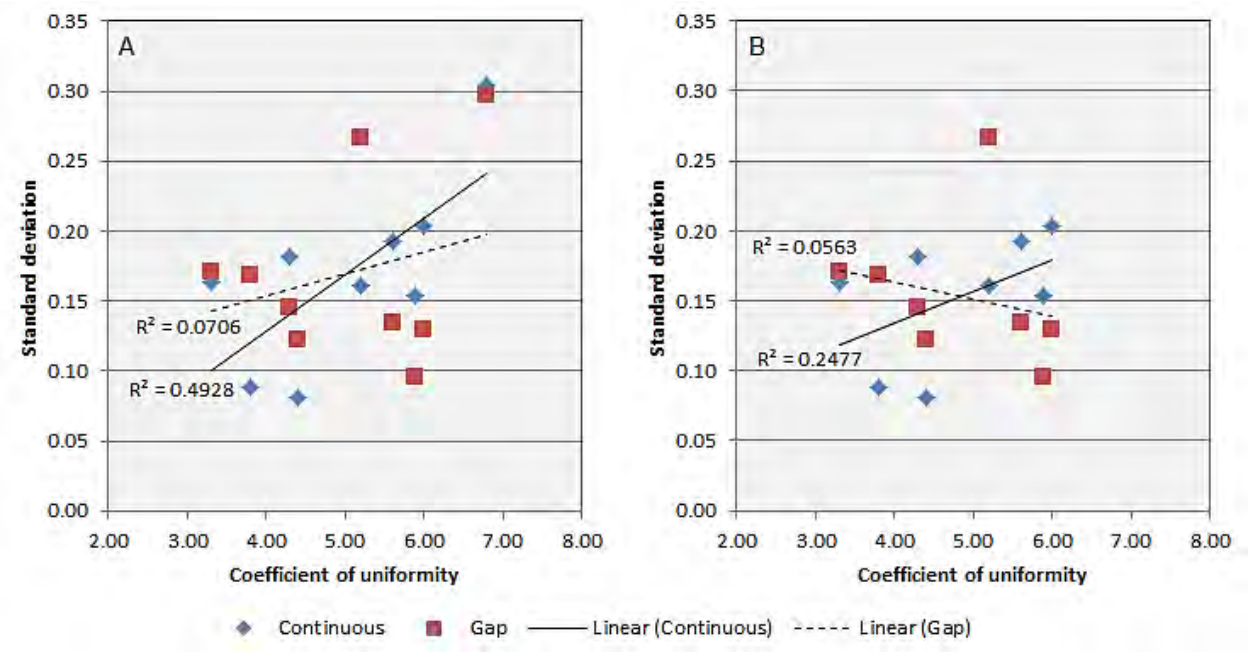

Figure 4-6: Plots of standard deviation vs. coefficient of uniformity for different coarse aggregates with (A) and without (B) mixes with F6

4.4.3 Effects of overall aggregate grading on OPI

In Figure 4-4, when comparing the concretes made with the same fine aggregates but different coarse aggregates, the continuously graded aggregate had a higher OPI three times out of nine. Five of the six pairs in which the concrete with gap graded aggregate had a higher OPI had a difference between the higher and the lower OPI greater than 0.1, whereas for the remaining 3 the difference was greater than 0.1 only once. In other words, where greater differences were observed, the gap graded aggregate usually yielded the higher OPI.

A hypothesis test was conducted, as presented in Section 4.1.2, to further investigate the relationship between overall aggregate grading and OPI. A sample calculation showing the t-test procedure is presented in Appendix E. The results are summarised in Table 4-5 where it is observed that, with a significance level of 5 % ($\alpha = 0.05$), the null hypothesis can be rejected three times out of 9 compared mixes.

Table 4-5: t-test results for comparison of OPI means between samples with different coarse aggregates

Fine aggregate			Equal variance	t-value	Significant at α=0.05 (Y/N)
Code	FM	C_u			
F1	1.50	4.3	Yes	-0.46	No
F2	2.00	3.3	Yes	3.75	Yes
F3	2.00	4.4	Yes	-3.66	Yes
F4	2.05	6.0	Yes	2.09	No
F5	2.25	3.8	Yes	0.03	No
F6	2.30	6.8	Yes	0.93	No
F7	2.50	5.6	Yes	-0.91	No
F8	2.55	5.9	Yes	5.03	Yes
F9	3.00	5.2	Yes	1.10	No
*All			Yes	1.93	No

*Calculated with the exclusion of F8 based on findings in Section 4.2.

Of the mixes that were compared, the most significant t-statistic was obtained for concretes with fine aggregate F8 but in Section 4.3 it was observed that there was likely to have been an error in the production of concrete C1F8. Thus the comparison at F8 is not considered further here, leaving only two pairs in which the mean OPIs were statistically different. Furthermore the null hypothesis cannot be rejected when comparing all samples (excluding those with F8) at once. Thus the differences in overall aggregate grading were deemed not to have had a significant influence on OPI.

4.4.4 Discussion of OPI results

Evaluation of results

The variations observed in OPI values of different samples appear to be small, particularly when considered as a percentage increase or decrease between samples. However, OPI is the negative log of the permeability coefficient and thus a unit change in OPI represents an order of magnitude change in the permeability coefficient. Mehta and Monteiro (1993) note that a change in the permeability of hydrated cement paste of around 90×10^{-11} has been observed with a decrease in capillary porosity from 40 to 30 percent, whilst a similar reduction in capillary porosity at lower fractions of capillary porosity results in significantly smaller changes in permeability. As will be presented later, the porosity was found to be significantly lower. Thus it is unlikely that the abovementioned phenomenon was a factor.

A variation in fine aggregate resulted in a maximum difference in OPI of 0.73, whilst a maximum difference of 0.45 was observed for samples with different coarse aggregates. This compares with a difference of around as much as 1.0 with the variation of water/binder ratio from 0.4 to 0.6, and a difference of 0.5 with the use of different extenders, as observed by

Heiyantuduwa (2008). The descriptive statistics thus suggest that variation in fine aggregate is of greater concern than coarse aggregate with regard to OPI and that variation in aggregate grading requires less consideration than of other input parameters, particularly water/binder ratio, by a designer striving to improve OPI.

The 0.73 difference in OPI was observed between samples C2F2 and C2F3 where the only variable that changed was C_u. Barring this pair of samples the next largest difference between any two samples of the same coarse aggregate was 0.46. Thus there was an unusually high difference between the OPI of C2F2 and C2F3. Visual inspection of the samples did not reveal any notable differences. Furthermore, Section 4.3 gave an indication that the mix proportioning was correct for these mixes. Thus there is no sound basis for the exclusion of samples C2F2 or C2F3 from the analysis of the OPI results.

Relationship between FM and OPI

It was found that there was little correlation between FM and OPI with $r = -0.171$ the most significant correlation coefficient. As a basis for conducting a regression analysis, the relationship needed to have $|r| \geq 0.3$. Thus it is concluded that FM had no significant influence on OPI, and no regression analysis was necessary.

Relationship between C_u and OPI

In the case with the greatest correlation between C_u and OPI, $r = -0.472$. This warranted a regression analysis of the relationship between the two where β_2 was the calculated coefficient for C_u. It was found that $\beta_2 = -0.086$ for continuous graded aggregate and $\beta_2 = -0.048$ for gap graded aggregate.

At $\beta_2 = -0.086$, for a unit increase in OPI, C_u would need to be reduced by 11.6 units. Put a different way, with a 3.5 unit decrease in C_u, which is the range between the maximum and minimum C_u values tested and which is representative of the range of C_u that may be used in practice, there may be an increase in OPI of 0.3. This reaffirms that the fine aggregate is of less concern with regard to permeability than binder type and content and the water/binder ratio, as indicated earlier in Section 4.4.4.

The increase in permeability with increasing C_u may be explained by tortuosity. With an increasing D_{60} in particular, there is a larger proportion of larger particles which attract greater amounts of bleed water which locally increases the water/cement ratio at their surface, thereby increasing the extent of porosity in the ITZ. Thus with an increase in C_u there was an increase in permeability – as indicated by the decrease in OPI.

Relationship between overall grading and OPI

In Section 4.4.1 it was observed that gap graded aggregates generally gave a higher OPI than continuously graded aggregates. This may be explained by the y_1 value. Comparing the coarse aggregates alone: The greater distribution of particles in coarse aggregate C1 (the coarse aggregate that gave rise to an overall aggregate with a continuous grading) gave it a greater particle packing efficiency than C2 which was more uniformly graded. Thus to achieve the same overall packing density in aggregate blends, a greater proportion of fine aggregate had to be blended with C2 than with C1. This meant that for each fine aggregate, y_1 for coarse aggregate C2 was greater than y_1 for coarse aggregate C1.

With a greater y_1 there is a greater content of each of the particle sizes within the range of sizes that constitute fine aggregate. Thus at each level of fine aggregate, the gap graded aggregate had a greater content of 75 μm particles than the continuously graded aggregate. Particles of 75 μm and smaller refine the pore structure by way of the filler effect, particularly in the region of the ITZ, and thereby reduce concrete permeability.

Statistical analysis of the results revealed that the difference in OPI that derived from changes in aggregate grading were not statistically significant. However, as a result of the small sample sizes, the statistical analysis tended to give a large range for the acceptance of the null hypothesis, with the result that there would need to be a large difference between compared means for the null hypothesis to be rejected. None-the-less, it cannot be concluded that changes in coarse aggregate resulted in a statistically significant difference in OPI. But the results do suggest that, in general, use of coarse aggregates that give an overall gap grading yields higher OPI values than concretes with continuously graded aggregates.

It may be beneficial to conduct further experiments into this relationship with larger sample sizes whereby a statistical analysis would be more reflective of the true relationship.

4.4.5 Summary

From analysis of the OPI results, the following key findings were made:

i. With $|r| < 0.3$, there was negligible correlation between OPI and FM.
ii. Between C_u and OPI, in concretes with continuous grading, $r = -0.472$, where an increase in C_u of 3.5 units caused a decrease in OPI 0.3 units. This was attributed primarily to the increase in D_{60} which, as a result of a greater level of localised bleeding which causes a greater water/binder ratio at the aggregate surface, causes a greater porosity in the ITZ. However, this effect was less than the effects that water/binder ratio and binder type and content have been observed to have on OPI.

There was little correlation between the same two parameters in concretes with a gap grading.

iii. An overall gap graded aggregate tends to give a higher OPI than a continuously graded aggregate. This is explained by the fact that for a given fine aggregate, the coarse aggregate that gave an overall gap graded aggregate (C1) demanded a greater y_1 than was necessary in the continuously graded aggregate in order to achieve a particular packing density. Thus at each level of fine aggregate, the gap graded aggregate had a greater content of 75 μm particles than the continuously graded aggregate. Particles of 75 μm and smaller refine the pore structure by way of the filler effect, particularly in the region of the ITZ, and thereby reduce concrete permeability.

4.5 Water sorptivity index

4.5.1 Descriptive statistics

The descriptive statistics on the water sorptivity index (WSI) data are presented in Table 4-6 and the means are plotted on a bar chart presented in Figure 4-7.

Table 4-6: Descriptive statistics for WSI data

Mix	Number of specimens tested	Mean ($mm/hr^{0.5}$)	Std. Deviation ($mm/hr^{0.5}$)	Minimum ($mm/hr^{0.5}$)	Maximum ($mm/hr^{0.5}$)	CoV (%)
C1F1	4	6.80	1.35	5.39	8.47	19.92
C1F2	4	6.20	0.48	5.85	6.91	7.77
C1F3	4	6.42	0.71	5.61	7.20	11.02
C1F4	4	6.15	0.85	5.01	6.91	13.76
C1F5	4	6.15	0.44	5.59	6.60	7.07
C1F6	4	6.59	0.61	5.82	7.09	9.25
C1F7	4	5.82	0.38	5.41	6.26	6.51
C1F9	4	6.34	0.50	5.64	6.83	7.92
C2F1	4	7.19	2.21	4.98	9.14	30.74
C2F2	4	5.06	0.74	4.39	6.03	14.55
C2F3	4	6.62	0.75	5.71	7.54	11.31
C2F4	4	6.20	0.35	5.75	6.55	5.57
C2F5	4	5.65	0.46	5.09	6.11	8.18
C2F6	4	6.43	0.48	6.03	7.10	7.51
C2F7	4	6.73	0.62	5.82	7.25	9.28
C2F8	4	5.44	0.43	5.06	5.99	7.99
C2F9	4	5.37	0.39	4.88	5.72	7.21

Observations made from the descriptive statistics Table 4-6 and Figure 4-7 are:-

i. With changes in fine aggregate, the WSI of concretes with continuously graded aggregate ranged from 5.82 mm/hr$^{0.5}$ for C1F7 (FM = 2.50, C_u = 5.6) and 7.21 mm/hr$^{0.5}$ for C1F8 (FM = 2.55, C_u = 5.9), a range of 1.39 mm/hr$^{0.5}$. If C1F8 is rejected based on the findings of Section 4.3, the highest WSI for a continuously graded aggregate was 6.80 mm/hr$^{0.5}$ for C1F1 (FM = 1.50, C_u = 4.3), giving a range of 0.98 mm/hr$^{0.5}$. For concretes with gap grading, WSI varied from 5.06 mm/hr$^{0.5}$ for C2F2 (FM = 2.00, C_u = 3.3) to 7.19 mm/hr$^{0.5}$ for C2F1 (FM = 1.50, C_u = 4.3), a range of 2.13 mm/hr$^{0.5}$.

ii. Neglecting samples with C8, the largest change observed from a change in grading was with fine aggregate F2 where the WSI was 1.14 mm/hr$^{0.5}$ greater for the continuously graded C1F2, for which WSI = 6.20 mm/hr$^{0.5}$ than the gap graded C2F2, for which WSI = 5.06 mm/hr$^{0.5}$. There was an inconsistent relationship between grading and WSI. The continuously graded aggregate had the higher WSI 5 times and the gap graded 4 times.

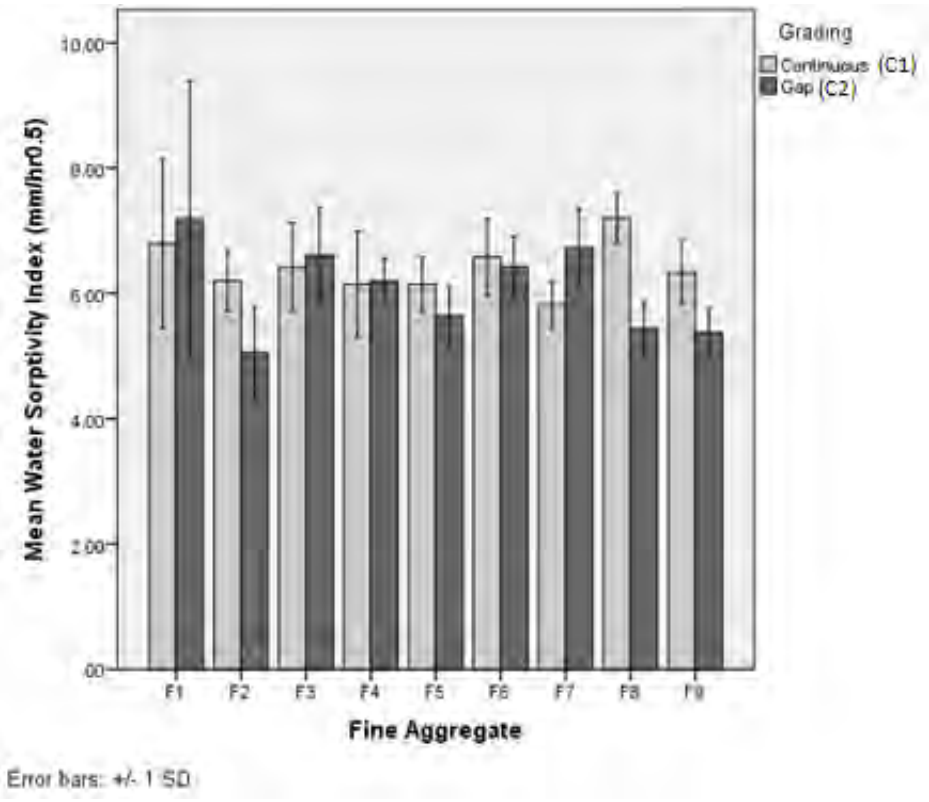

Figure 4-7: WSI results for different coarse and fine aggregates

iii. The mean WSI of the mixes made with a continuous grading was 6.31 mm/hr$^{0.5}$ and the mean WSI of the mixes made with gap grading was 6.15 mm/hr$^{0.5}$ (excluding mixes with fine aggregate F8).

iv. With the exception of samples containing fine aggregate F1, the standard deviation ranged between 0.38 mm/hr$^{0.5}$ and 0.85 mm/hr$^{0.5}$. However samples C1F1 and C2F1 had s = 1.35 mm/hr$^{0.5}$ and s = 2.21 mm/hr$^{0.5}$ respectively.

4.5.2 Effects of variations in fine aggregate

In Section 4.5.1 it was observed that changes in fine aggregate resulted in a change in WSI of 2.13 mm/hr$^{0.5}$ which was a 42 % difference between the minimum to the maximum value. Furthermore there was a high degree of variation in the standard deviation between samples with different fine aggregates. This section explores the influence of FM and C_u on the WSI and the variance of WSI.

The method used to understand the influence of FM and C_u on the WSI was correlation and regression analysis. The former determined whether there was a relationship between either of the fine aggregate characteristics and the WSI. If a relationship was established the regression analysis was used to determine the strength of the influence that the fine aggregate characteristics had on the WSI.

Correlation between FM and C_u and WSI

Table 4-7 presents the correlation coefficients. Of the four correlation coefficients, $|r| > 3$ only once, indicating that the variations in fine aggregate in general had little influence on WSI.

Table 4-7: Correlation coefficients between WSI and Cu and FM

Correlation Coefficients		
Grading	WSI vs. FM	WSI vs. C_u
Continuous (C1)	-0.186	0.004
Gap (C2)	-0.342	0.144

For WSI vs. FM:- Conversely to the OPI, it was FM rather than C_u that had the more distinct relationship with WSI. For both continuous and gap graded aggregate the correlation coefficients were negative between OPI and FM. However the correlation was low, with the

greatest correlation being r = -0.342. The correlation between WSI and FM was strong enough (r < -0.3 or r > 0.3) to warrant a regression analysis between the two.

For WSI vs. C_u:- As noted above, WSI had a weaker relationship with C_u than with FM, which was converse to the finding for OPI. The correlation coefficient was positive for both continuously and gap graded aggregate, indicating that with an increase in C_u there was generally an increase in WSI. However, given that -0.3 < r < 0.3 for both gap and continuous graded aggregates, it is concluded that there was no significant relationship between WSI and C_u.

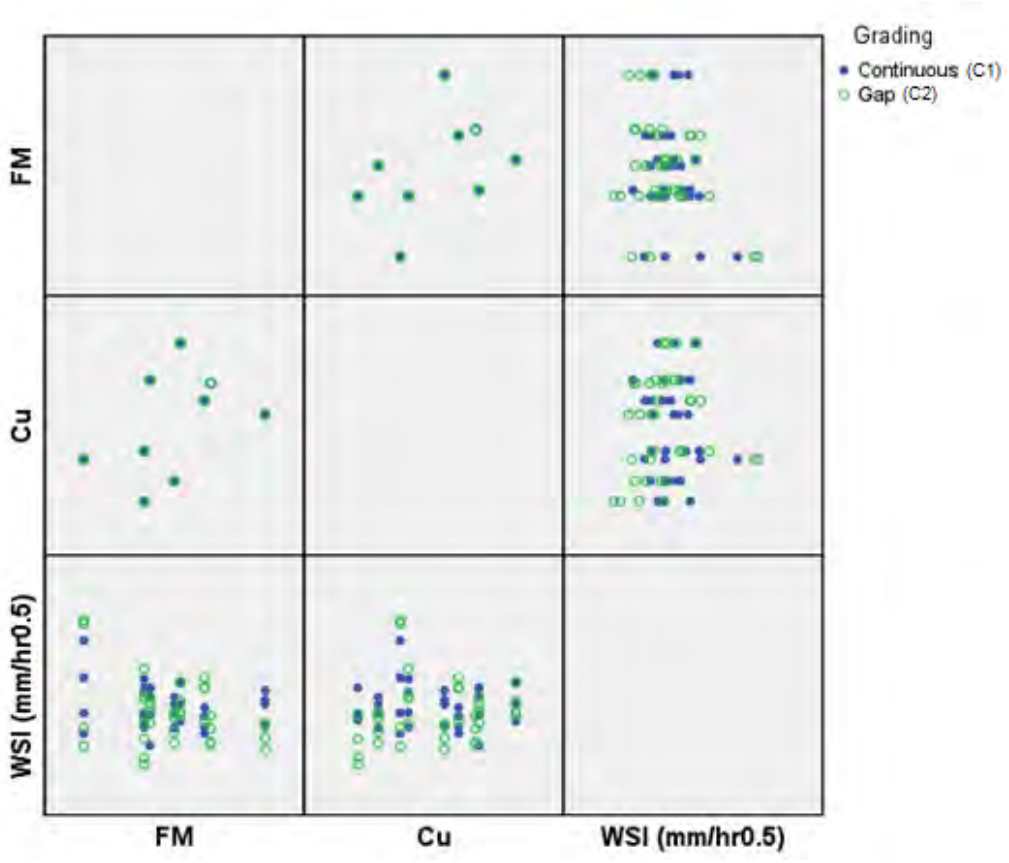

Figure 4-8: Matrix scatter plot showing the influence of FM and Cu on WSI at different aggregate gradings

Regression analysis for WSI vs. FM

The correlation coefficients for WSI vs. FM suggest that there be a relationship between WSI and FM. This was studied further by way of linear regression analysis using the method of least squares. An example calculation with this method is presented in Appendix E. The general formula for the regression is given in Equation (4-2). The regression coefficients are presented in Table 4-8 where $\beta_2 = 0$ because of the small correlation between WSI and C_u.

Table 4-8: WSI vs. FM regression analysis results

Grading	Parameter	Value	t	Significance
Continuous (C1)	β_0	7.000	10.329	0.000
	β_1	-0.315	-1.039	0.307
Gap (C2)	β_0	8.056	8.498	0.000
	β_1	-0.885	-2.123	0.041

For continuously graded aggregate β_1 = -0.315 and for gap graded aggregate β_1 = -0.885. Of the two only the latter was found to be significant at a 5 % level. The results are discussed further in Section 4.5.4.

4.5.3 Effects of variations in coarse aggregate

In Figure 4-7, there was no distinct trend in which one grading gave a higher WSI than the other. The continuous grading gave a higher WSI 5 times out of nine. If concrete C1F8 is excluded based on the findings of Section 4.3, both the continuous and the gap graded samples had a higher WSI 4 times, suggesting that coarse aggregate grading had no significant influence on WSI. Furthermore, as shown in Table 4-9, when ranking the difference between the WSI of samples with different coarse aggregates from largest to smallest, the continuously and the gap graded aggregates are roughly equally distributed.

Table 4-9: Ranking of the differences observed in the WSI values and the grading that caused the greater WSI

Rank	Fine aggregate	Grading for greater WSI	WSI difference
1	F2	Continuous (C1)	1.14
2	F9	Continuous (C1)	0.97
3	F7	Gap (C2)	0.90
4	F5	Continuous (C1)	0.50
5	F1	Gap (C2)	0.39
6	F3	Gap (C2)	0.20
7	F6	Continuous (C1)	0.16
8	F4	Gap (C2)	0.06

To further investigate the observed relationship between WSI and grading the mean WSI for concretes with the same fine aggregate but different overall aggregate grading were compared by way of a hypothesis test, as described in Section 4.1.2. A sample calculation showing the t-test procedure is presented in Appendix E. The results are summarised in Table 4-10 where it is observed that, with $\alpha = 0.05$, the null hypothesis can be rejected only three times out of 9

compared mixes. The most significant t-statistic was t = 6.037 found between the WSI of concretes with fine aggregate F8. This was almost double the next highest t-statistic (t = 3.050 for F9) which reaffirms that there may have been an error with the production of concrete C1F8 as highlighted in Section 4.3. The remainder of the discussion in this section excludes concretes with fine aggregate F8.

Table 4-10: t-test results for comparison of WSI means between samples with different coarse aggregates

Fine aggregate			Equal variance	t-value	Significant at α=0.05 (Y/N)
Code	FM	Cu			
F1	1.50	4.3	No	0.299	No
F2	2.00	3.3	Yes	-1.917	Yes
F3	2.00	4.4	Yes	0.380	No
F4	2.05	6.0	Yes	0.122	No
F5	2.25	3.8	Yes	-1.619	No
F6	2.30	6.8	Yes	-0.399	No
F7	2.50	5.6	Yes	2.474	No
F8	2.55	5.9	Yes	-6.037	Yes
F9	3.00	5.2	Yes	-3.050	Yes
All*			Yes	-1.087	No

*Calculated with the exclusion of F8 based on findings in Section 4.2.

t = -1.087 for the t-test conducted across all samples, suggesting that the continuously graded aggregate generally yielded a higher WSI. However, this statistic was not significant at the 5 % level. Furthermore, of the accepted samples, there were only two occasions where the null hypothesis was rejected with statistically significant differences in WSI with a change in overall aggregate grading. In both cases it was the continuously graded aggregate that yielded higher WSI. The results are discussed further in Section 4.5.4.

4.5.4 Discussion of WSI results

Evaluation of results

The maximum range between the WSI of any two sample groups was 1.91 mm/hr$^{0.5}$. In other research, variation in water/binder ratio was found to give a difference in WSI of up to approximately 5.5 mm/hr$^{0.5}$ and variation in extender type and content a difference of approximately 3.5 mm/hr$^{0.5}$ (Heiyantuduwa, 2008). Furthermore, differences in curing conditions have been found to alter WSI by up to approximately 5.5 mm/hr$^{0.5}$ (Alexander, et al., 2001). The observed maximum variations in WSI of 1.14 mm/hr$^{0.5}$ from variations in overall aggregate grading and 2.13 mm/hr$^{0.5}$ from variations in fine aggregate are therefore relatively low. Thus it can be concluded that in performance based design, water/binder ratio, extender type and content and curing method are of greater concern than aggregate fineness

modulus, coefficient of uniformity and the average particle size of the coarse aggregate at a given maximum particle size.

The water sorptivity index and oxygen permeability index tests were conducted on the same sets of samples. It is therefore expected that the OPI results correspond to some degree with the WSI results. For example a sample with a high OPI should have a low WSI. However, there was no distinct correlation between the two properties. This result is not unique to this study. Nganga (2009) found a lack of connection between OPI and WSI results. Whilst both characteristics depend on the size and interconnectivity of the pores of the concrete, WSI, being a measure of sorptivity, is far more sensitive to the size and shape of the pores.

The CoV exhibited by the continuously and gap graded aggregates with a FM of 1.5, namely sample groups C1F1 and C2F1, were 19.92 % and 30.74 % respectively. Stanish et al. (2006) observed a CoV of 18 % in WSI results between samples tested in the same lab and a CoV of 26 % between samples tested in different labs. Thus, in particular the CoV of C2F1 was of concern. Samples C1F1 and C2F1 were tested separately of each other, but in the same run as other sample groups which exhibited lower, more average variance. Furthermore, through visual inspection the test samples appeared to not to have any notable inconsistencies. Thus the elevated variance in WSI found in these two sample groups can sensibly be attributed to the fine aggregate. The fineness modulus of these samples, at 1.5, was the lowest of all tested sample groups. Thus they had the highest proportion of sub-300 μm and sub-150 μm particles. Furthermore, sample C2F1 had a larger CoV than C1F1. It also had a larger y_1. It therefore had a greater proportion of all fine aggregate sizes, including the sub-75 μm fraction. The exact mechanism through which these particle sizes influenced the variance cannot be determined here. However, interparticle forces which occur between particles of sizes smaller than 125 μm, as discussed in the research of Fennis (2012), may hold the answer. These forces, which include van der Waals forces, electrical double layer forces and steric forces, would have been most prevalent in these two sample groups. The forces may have been broken down to different extents during mixing and this variability could have translated in microstructural differences in the samples.

Relationship between FM and WSI

In the case with the greatest correlation between FM and OPI, $r = -0.342$. Since $|r| > 0.3$, a regression analysis of the relationship was warranted. In the regression analysis the parameter of interest was β_1 – the magnitude by which the WSI increased with a unit increase in FM. It was found that $\beta_1 = -0.315$ for continuous graded aggregate and $\beta_1 = -0.885$ for gap graded aggregate.

The inverse relationship between WSI and FM may be explained by the linear, proportional relationship between FM and y_1 as presented in Section 4.2; that is, as FM increased, so did the proportion of the total aggregate constituted of fine aggregate (y_1) in order to maintain constant aggregate packing density. Since the proportion of the fine aggregate passing the 75 μm sieve, as a percentage of the fine aggregate, was held constant at 5 % throughout, an increase in y_1 resulted in an increase in the total content of sub-75 μm particles in the total aggregate. Particles in this size range refine the pore structure and improve the ITZ properties through the fine filler effect, which may be reflected by WSI.

At $\beta_1 = -0.885$, for a unit decrease in WSI, FM would need to be increased by 1.13 units. Put differently, with a 2.3 unit increase in FM, which is the range between the maximum and minimum FM values tested and which is representative of the range of FM that may be used in practice, there may be a decrease in WSI of 2.03 $mm/hr^{0.5}$. This reaffirms that in concrete performance based design, water/binder ratio, extender type and content and curing method are of greater concern than fineness modulus.

Relationship between C_u and WSI

It was found that there was little correlation between C_u and OPI with $r = -0.171$ being the most significant correlation coefficient. As a basis for conducting a regression analysis, the relationship needed to have $|r| \geq 0.3$. Thus it is concluded that C_u had no significant influence on OPI. A regression analysis for this relationship was not necessary.

Relationship between overall aggregate grading and WSI

The descriptive statistics did not show a distinct trend in the relationship between aggregate grading and WSI. With the exclusion of fine aggregate F8, the gap graded and the continuously graded aggregates each yielded the higher WSI four times. Ranking the observed differences showed there was a similar spread of high and low differences in the WSI of concretes with different coarse aggregates between cases where the higher WSI was observed with gap grading and cases where the higher WSI was observed with continuous grading. If the larger differences were observed exclusively with one particular coarse aggregate, this would have suggested that the overall aggregate grading influenced the WSI. A closer look at the relationship through the results of the t-test showed that there were only two occasions where there was a statistically significant difference between the WSI of the continuously graded and the gap graded aggregates. In both cases it was the gap graded aggregate that gave the lower WSI. Furthermore the t-test conducted across all samples shows that, in general, gap graded aggregates gave a lower WSI but this t-statistic was not significant at the 5 % level.

It is concluded that using overall gap graded aggregates gives reduced sorptivity compared to continuously graded aggregate. However the benefit is small when compared to the improvements that can be achieved through the use of a lower water/binder ratio and the introduction of a mineral admixture to the mix.

4.5.5 Summary

From analysis of the WSI results, the following key findings were made:

i. Between FM and WSI, r = -0.342 in concretes with gap grading where an increase in FM of 2.3 units caused a decrease in WSI of 2.03 mm/hr$^{0.5}$. With an increase in FM there was a decrease in WSI. This was explained by the relationship between FM and y_1 whereby, in order to maintain constant packing density, as FM increased, so did y_1. As a result there was a greater proportion of particles of 75 μm and smaller, which refine the pore structure, particularly in the region of the ITZ. However, this effect was less than the effect that water/binder ratio has been observed to have on WSI in other research. There was little correlation between the same two parameters in concretes with a continuous grading.
ii. With $|r| < 0.3$, there was negligible correlation between WSI and C_u.
iii. Variation of overall aggregate grading had a small influence on WSI.

4.6 Chloride conductivity index

4.6.1 Descriptive statistics

The descriptive statistics on the chloride conductivity index (CCI) data are presented in Table 4-11 and the means are plotted on a bar chart presented in Figure 4-9.

Observations made from the descriptive statistics and Figure 4-9 are:-

i. C1F8 had a CCI of 1.24 mS/cm and C1F4 had a CCI of 1.12 mS/cm. These were the two highest CCIs observed and appeared to be outliers. Based on the findings of Section 4.3, the result for C1F8 can be rejected. The range between the CCI for C1F4 and C2F4 which had a CCI of 0.85 mS/cm, was 0.27 mS/cm. This was 69 % greater than the next highest range between CCI values of concretes made with the same fine aggregate but different overall gradings (0.16 mS/cm). Given that the CCI for C2F4 was similar to those of concretes with the same overall aggregate grading and similar fine aggregate properties, the result for C1F4 was rejected.

Table 4-11: Descriptive statistics for CCI data

Mix	Number of specimens tested	Mean (mS/cm)	Std. Deviation (mS/cm)	Minimum (mS/cm)	Maximum (mS/cm)	CoV (%)
C1F1	4	0.58	0.09	0.47	0.69	15.57
C1F2	4	0.88	0.20	0.69	1.14	23.17
C1F3	4	0.61	0.09	0.52	0.73	14.74
C1F4	4	1.12	0.12	0.98	1.27	10.74
C1F5	4	0.97	0.13	0.82	1.10	13.59
C1F6	4	0.90	0.07	0.81	0.99	8.31
C1F7	4	0.90	0.11	0.80	1.04	12.38
C1F8	4	1.24	0.14	1.09	1.44	11.66
C1F9	4	0.85	0.16	0.72	1.08	18.49
C2F1	4	0.69	0.04	0.62	0.71	6.36
C2F2	4	0.83	0.07	0.74	0.92	8.84
C2F3	4	0.77	0.19	0.60	1.05	25.07
C2F4	4	0.85	0.03	0.81	0.87	3.33
C2F5	4	0.81	0.14	0.72	1.02	17.21
C2F6	4	0.97	0.08	0.91	1.09	8.54
C2F7	4	0.77	0.05	0.73	0.83	5.86
C2F8	4	0.81	0.15	0.69	1.02	19.04
C2F9	4	0.72	0.17	0.61	0.96	23.14

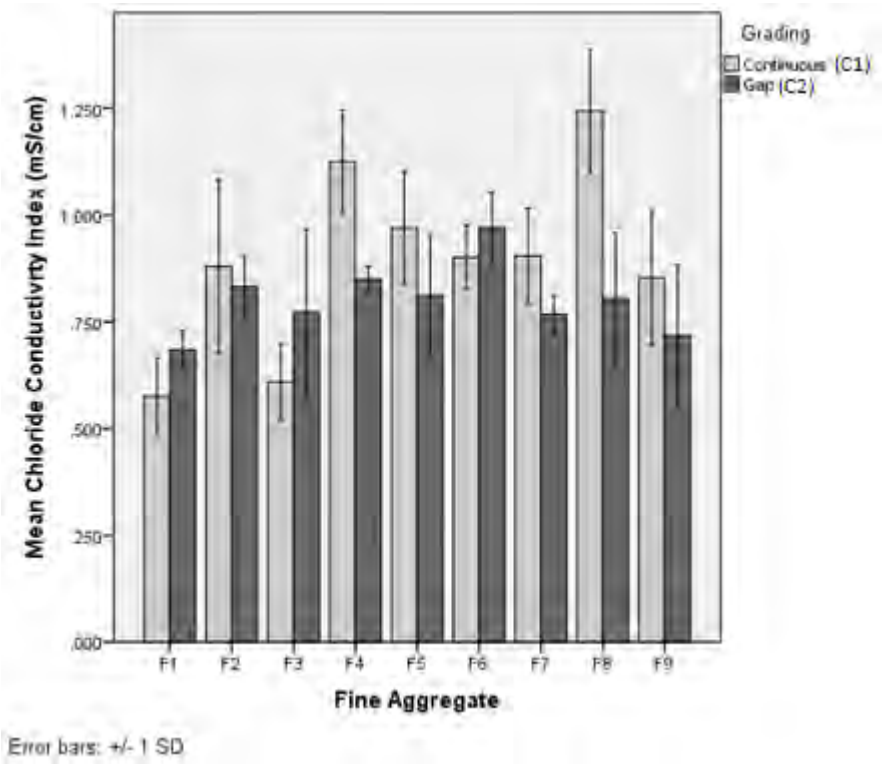

Figure 4-9: CCI results for different coarse and fine aggregates

ii. With the exclusion of samples C1F4 and C1F8, with changes in fine aggregate, the CCI of concretes with continuously graded aggregate ranged between 0.58 mS/cm for C1F1 (FM = 1.50, C_u = 4.3) and 0.97 mS/cm for C1F5 (FM = 2.25, C_u = 3.8), a range of 0.39 mS/cm. For concretes with gap grading, CCI varied from 0.69 mS/cm for C2F1 (FM = 1.50, C_u = 4.3) to 0.97 mS/cm for C2F6 (FM = 2.30, C_u = 6.8), a range of 0.28 mS/cm.

iii. The mean CCI of the mixes made with a continuous grading was 0.85 mS/cm and the mean CCI of the mixes made with gap grading was 0.80 mS/cm (excluding mixes with fine aggregate F8).

iv. There was a high degree of inconsistency in the CoV with a range between the highest and the lowest CoV was 21.74 %, where the highest CoV was 25.07 % for C2F3 and the lowest was 3.33 % for C2F4.

4.6.2 Effects of variations in fine aggregate

In Section 4.6.1 it was observed that changes in fine aggregate resulted in a change in CCI of as much as 0.39 mS/cm which is a 67 % increase from the lowest to the highest value. This section explores the influence of FM and C_u on the CCI.

The method used to understand the influence of FM and C_u on the CCI is correlation and regression analysis. The former determined whether there was a relationship between either of the fine aggregate characteristics and the CCI. If a relationship was established the regression analysis was used to determine the strength of the influence that the fine aggregate characteristics had on the CCI.

Table 4-12 presents the correlation coefficients, the calculation of which excluded the results for concretes C1F4 and C1F8. Of the four correlation coefficients, $|r| > 0.3$ only once, indicating that the variations in fine aggregate had very little influence on CCI. The highest correlation was between CCI and FM in samples with a continuous grading, where the value was $r = 0.488$. Since $|r| > 0.3$ the relationship between CCI and FM was investigated further by way of a regression analysis. Since $|r| < 0.3$ for the relationship between CCI and C_u for both continuously and gap graded aggregates it is concluded that C_u did not have a significant effect on CCI. No regression analysis was necessary for this relationship.

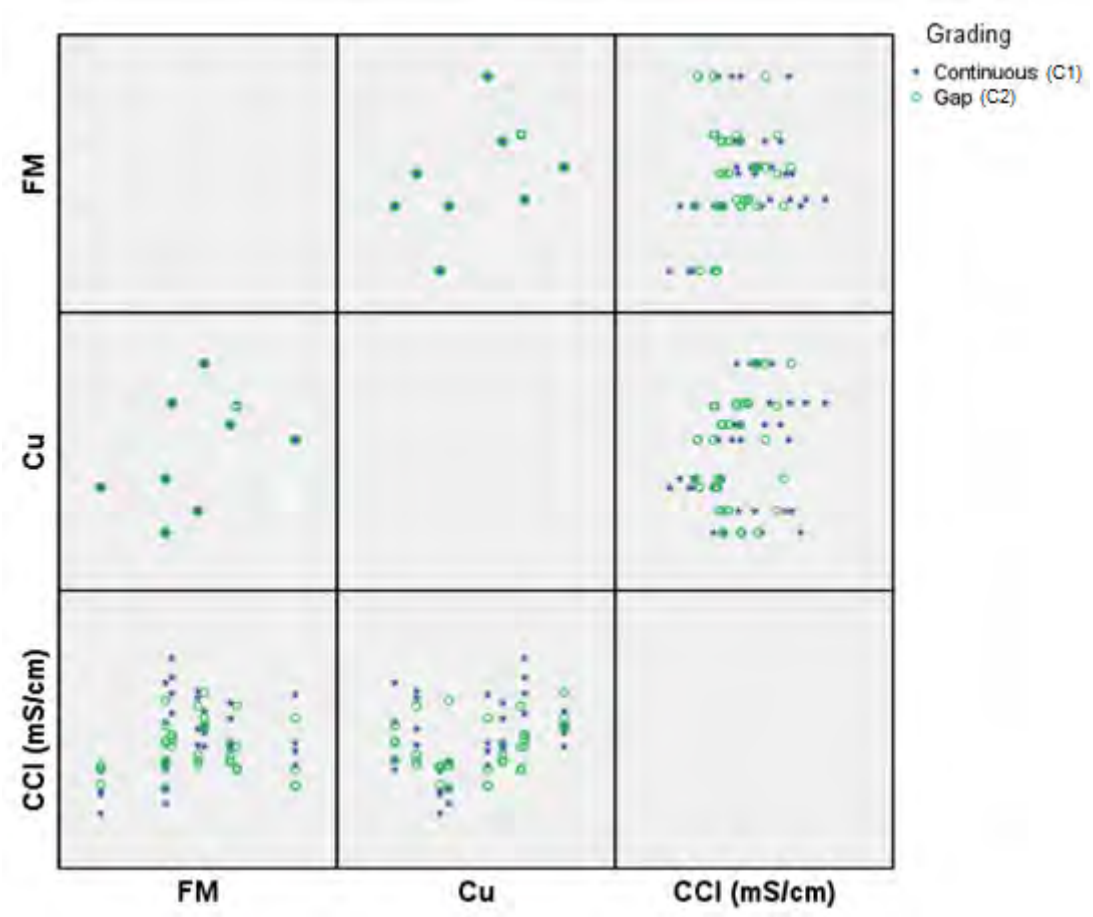

Figure 4-10: Matrix scatter plot showing the influence of FM and Cu on CCI at different aggregate gradings

Table 4-12: Correlation coefficients between CCI and Cu and FM

Correlation Coefficients		
Grading	**CCI vs. FM**	**CCI vs. C_u**
Continuous (C1)	0.488	0.147
Gap (C2)	0.033	0.283

Regression analysis for CCI vs. FM

The correlation coefficients for CCI vs. FM suggest that there may be a relationship between CCI and FM. This was studied further by way of linear regression analysis using the method of least squares. An example calculation with this method is presented in Appendix E. The general formula for the regression is given in Equation (4-2). The regression coefficients are presented in Table 4-13.

Table 4-13: CCI vs. FM regression analysis results

Grading	Parameter	Value	t	Significance
Continuous (C1)	β_0	0.355	2.173	0.039
	β_1	0.206	2.851	0.008
Gap (C2)	β_0	0.778	6.226	0.000
	β_1	0.010	0.191	0.850

For continuously graded aggregate $\beta_1 = 0.206$ and for gap graded aggregate $\beta_1 = 0.010$. Of the two only the former was found to be significant at a 5 % level.

4.6.3 Effects of variations in coarse aggregate

The descriptive statistics presented in Section 4.6.1 indicated that the concretes with a continuously graded aggregate tended to have a greater CCI. The effects of the variations in coarse aggregate were investigated further by way of t-tests between pairs of samples of the same fine aggregate. The results of all of the t-tests are presented in Table 4-14. A sample calculation showing the t-test procedure is presented in Appendix E.

Table 4-14: t-test results for comparison of CCI means between samples with different coarse aggregates

Fine aggregate			Equal variance	t-value	Significant at α=0.05 (Y/N)
Code	FM	Cu			
F1	1.50	4.3	Yes	2.197	No
F2	2.00	3.3	Yes	-1.717	No
F3	2.00	4.4	Yes	0.716	No
F4	2.05	6.0	Yes	-4.433	Yes
F5	2.25	3.8	Yes	-1.644	No
F6	2.30	6.8	Yes	1.238	No
F7	2.50	5.6	No	-2.266	No
F8	2.55	5.9	Yes	-4.157	Yes
F9	3.00	5.2	Yes	-1.183	No
All*			Yes	-0.284	No

*Calculated with the exclusion of F8 based on findings in Section 4.2.

From Table 4-14 it is observed that, with an α of 0.05, the null hypothesis can be rejected only twice out of the eight pairwise comparisons made. The two instances are for concretes with fine aggregates F4 and F8, of which C1F4 and C1F8 were identified as possible outliers in Section 4.6.1. For these t = 4.433 and t = 4.157 respectively. The latter was 84 % greater than the next lowest t-value. This further validates the rejection of samples C1F4 and C1F8.

Table 4-15: Ranking of the differences observed in the mean CCI values and the grading that caused the greater WSI

Rank	Fine aggregate	Grading for greater CCI	CCI difference
1	F3	Gap (C2)	0.16
2	F5	Continuous (C1)	0.16
3	F7	Continuous (C1)	0.14
4	F9	Continuous (C1)	0.14
5	F1	Gap (C2)	0.11
6	F6	Gap (C2)	0.07
7	F2	Continuous (C1)	0.05

As shown in Table 4-15, when ranking the difference between the CCI of samples with different coarse aggregates from largest to smallest, the continuously and the gap graded aggregates are more or less equally distributed.

4.6.4 Discussion of CCI results

Evaluation of results

The maximum observed difference between CCI of different concretes was 0.54. It has been found that a change in water/binder ratio from 0.4 to 0.6 can reduce the CCI by as much as approximately 0.7 mS/cm and variations in extender type and content has been found to cause a difference of as much as 1.2 mS/cm (Heiyantuduwa, 2008). Thus, relative to the parameters of water/binder ratio and extender type and content, variations of FM, C_u and coarse aggregate within the studied limits had a less significant effect on CCI. Thus it can be concluded that, when the performance parameter is CCI, within the limits studied, the designer should give greater consideration to factors of water/binder ratio and extender type and content than to FM and CFM when targeting a performance level.

The high CoV observed for some of the samples was a concern. In an inter-laboratory experiment the CoV observed by Stanish et al. (2006) in CCI test results ranged from 5.2 % to 13.5 %. 9 of the 18 concretes tested in this experiment had CoV > 13.5 % in CCI results. Table 4-16 shows the properties of the 6 concretes with the highest CoV in CCI results. It is observed that the high CoV values were spread amongst samples of different gradings and values of FM and C_u, indicating that there was no particular property that yielded a high variance. Figure 4-11 is a plot of the standard deviation in relation to the test run order, with different shades indicating samples that were tested in the same session. It is evident that the test run order did not have an influence on the variance.

Table 4-16: Properties of 6 concretes that exhibited the greatest CoV in CCI

Rank	Mix	Grading	FM	C_u	Std. Dev. $((mS/cm)^{0.5})$	CoV (%)
1	C2F3	Gap	2.00	4.4	0.19	25.07
2	C1F2	Continuous	2.00	3.3	0.20	23.17
3	C2F9	Gap	3.00	5.2	0.17	23.14
4	C2F8	Gap	2.55	5.9	0.15	19.04
5	C1F9	Continuous	3.00	5.2	0.16	18.49
6	C2F5	Gap	2.25	3.8	0.14	17.21

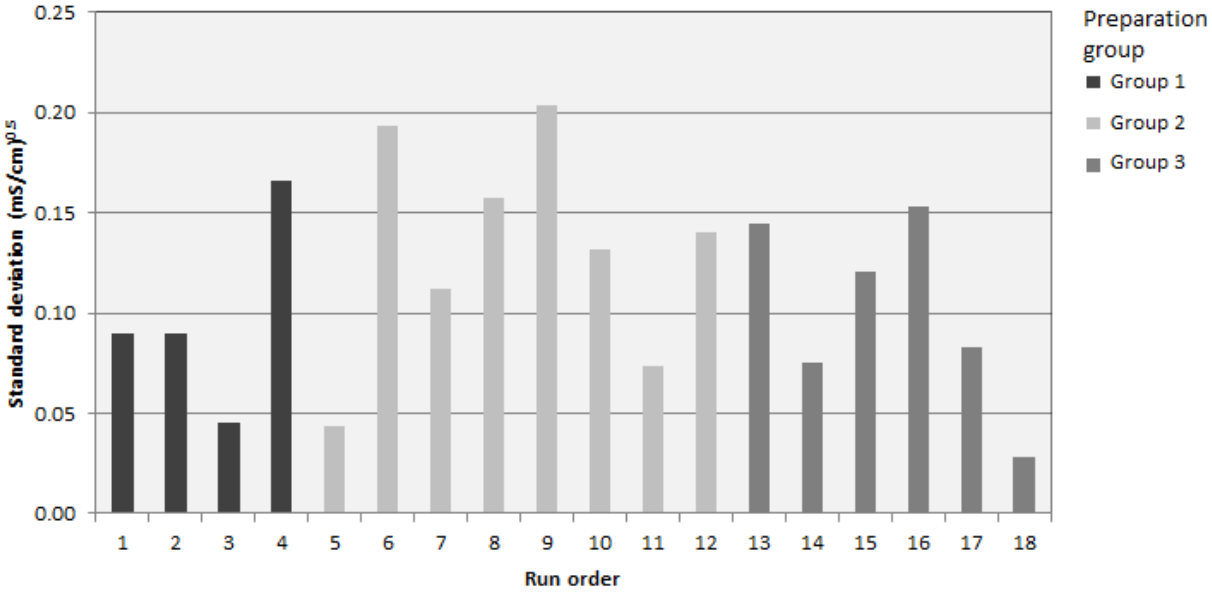

Figure 4-11: Standard deviation vs. run order for CCI results

Relationship between FM and CCI

r = 0.488 was the greatest correlation between FM and CCI. A regression analysis was conducted to further study the relationship. The strongest influence FM had on CCI was in concrete with a continuously graded aggregate where $\beta_1 = 0.206$, which was significant at the 5 % level. Practically this means that for an increase in FM of 2.3 – the range between maximum and minimum allowable FM as specified in SANS 1083:2013 – there would be a corresponding increase in CCI of 0.47 mS/cm. This reaffirms the observation earlier in Section 0 that water/binder ratio and binder type and content are more critical to the CCI.

An increased FM represents an increase in the coarseness of the aggregate and therefore, given that finer aggregate, particularly the material in the size fraction smaller than 75 µm, refines the pore structure and reduces the penetrability of the cement paste, it would be expected that a reduced fineness modulus would lead to a reduced CCI. However, it is noted that with all changes in FM the fraction of the fine aggregate smaller than 75 µm was held

constant at 5 %. Thus it is more likely that the relationship observed between CCI and FM is explained by tortuosity. With decreasing coarseness at constant packing density, there is an increasing amount of particles and thus a greater tortuosity of the flow path through the concrete which yields a lower CCI. Furthermore, larger particles attract a greater amount of bleed water which results in a localised increase in water/cement ratio at the aggregate particle surface and thus a greater porosity in the region of the ITZ.

Relationship between C_u and CCI

For the relationship between C_u and CCI in samples with continuous grading r = 0.147 and in samples with gap grading r = 0.283. Since $|r| < 0.300$ in both cases it is concluded that there was negligible correlation between C_u and CCI.

Relationship between overall aggregate grading and CCI

The descriptive statistics indicated that concretes C1F4 and C1F8 had particularly high CCI values of 1.12 mS/cm and 1.24 mS/cm respectively. The latter was rejected based on the strength results as presented in Section 4.3 which indicated that C1F8 was an outlier which may have resulted from an error in its production. Given that the range between the CCI of C1F4 and C2F4 was 69 % greater than the next highest range between concretes of the same fine aggregate but different overall grading, and that C2F4 had a CCI similar to that of the concretes with the same overall grading and similar fine aggregates, the CCI of C1F4 was deemed an outlier.

Of the remaining 7 acceptable pairs of results, there was an even split, whereby in 4 of the pairs the higher CCI was observed with a continuous grading, suggesting that different gradings had no particular influence on CCI. Furthermore, ranking the observed differences showed the differences both of higher and lower magnitude were spread evenly between the two coarse aggregates. If the larger differences were observed exclusively with one particular coarse aggregate, this would have suggested that the overall aggregate grading influenced the CCI.

The statistical analysis reaffirmed the rejection of the CCI result for concrete C1F4. With the exclusion of fine aggregates F4 and F8 the t-statistic, which factored in CCI values for each of the fine aggregates, indicated that the gap graded aggregate yielded a lower CCI. However, this difference was not significant at the 5 % level. It is therefore concluded that there is a modest improvement in the chloride conductivity index through use of gap graded aggregates rather than continuously graded aggregates. However this is minimal compared to the improvements attained through the use of lower water/binder ratios and the introduction of mineral admixtures to the mix.

4.6.5 Summary

From analysis of the CCI results, the following key findings were made:

i. Between FM and CCI, $|r| > 0.3$ in concretes with continuous grading indicating a significant correlation. As FM increased, an increase in CCI was observed. This was attributed to the increase in the average particle size which, as a result of a greater level of localised bleeding which causes a greater water/binder ratio at the aggregate surface, causes a greater porosity in the ITZ. Furthermore, with a greater average aggregate particle size there is a lower level of tortuosity which allows for easier passage of a penetrating substance. However, this effect was less than the effects that water/binder ratio and binder type and content have been observed to have on CCI in other research. There was little correlation between the same two parameters in concretes with a gap grading.
ii. With $|r| < 0.3$, there was negligible correlation between CCI and C_u.
iii. Overall aggregate grading had a small influence on CCI.

4.7 Carbonation

Accelerated carbonation tests were conducted to determine the concrete resistance to ingress of carbon dioxide. Carbonation depth was recorded at 30 and 60 days. The rate of carbonation was too slow to make out discernable trends after 30 days. This prompted a calibration of the carbonation chamber where it was found that the CO_2 concentration was 0.5 %, although the digital display on the chamber indicated 2.0 %. A gas meter was used to gauge the CO_2 concentration thereafter and the concentration was increased to 2.0 %. Since there were no discernable trends at 30 days it was concluded that no carbonation took place due to the low CO_2 concentrations. The readings that were taken at 60 days were therefore considered to be equivalent to the 30 day accelerated carbonation depth. The analysis of the accelerated carbonation test results looks exclusively at these results and therefore speaks in terms of the 30 day accelerated carbonation results.

It is noted that the carbonation depths were generally very low and due consideration must be given to this before using these results as a basis for any deductions.

4.7.1 Descriptive statistics

The descriptive statistics for the accelerated carbonation data are presented in Table 4-17 and the means are plotted on a bar chart presented in Figure 4-12.

Observations made from the 30 day accelerated carbonation descriptive statistics and Table 4-17 are:-

i. Concrete C1F8 was rejected on the basis of the findings presented in Section 4.3. The largest carbonation depth observed was 3.1 mm for C2F7. The observed carbonation depth for C1F7 was 1.6 mm, which was 1.5 mm less than that of C2F7. This range is 89 % greater than the next largest range between carbonation depths of concretes of the same fine aggregate but different overall grading. The result for C2F7 was therefore rejected.

Table 4-17: Descriptive statistics for 30 day accelerated carbonation depth

Mix	Number of readings taken	Mean (mm)	Std. Deviation (mm)	Minimum (mm)	Maximum (mm)	CoV (%)
C1F1	12	1.6	0.4	1.2	2.5	21.7
C1F2	12	1.7	0.3	1.3	2.3	16.8
C1F3	12	1.7	0.3	1.2	2.2	17.9
C1F4	12	2.4	0.3	1.9	3.0	14.1
C1F5	12	2.0	0.3	1.4	2.4	15.6
C1F6	12	1.7	0.4	1.1	2.4	25.4
C1F7	9	1.6	0.4	1.0	2.0	22.6
C1F9	12	2.0	0.3	1.4	2.3	16.6
C2F1	12	1.4	0.3	0.7	2.0	22.6
C2F2	12	1.2	0.2	1.0	1.5	15.6
C2F3	12	1.9	0.3	1.4	2.3	16.4
C2F4	12	1.8	0.3	1.3	2.4	18.8
C2F5	12	1.6	0.3	1.3	2.2	17.3
C2F6	12	2.3	0.4	1.8	3.1	17.2
C2F7	12	3.1	0.4	2.6	3.8	12.1
C2F8	12	2.0	0.3	1.6	2.5	13.1
C2F9	12	2.8	0.5	1.8	3.8	18.9

ii. With the exclusion of the rejected samples: The largest difference between two samples with continuous grading was 0.8 mm. This was between C1F1 (FM = 1.50, C_u = 4.3) and C1F6 (FM = 2.30, C_u = 6.8), both of which had a carbonation depth of 1.6 mm and C1F4 (FM = 2.05, C_u = 6.0) which had a carbonation depth of 2.4 mm. The largest difference between two samples with gap grading was 1.6 mm. This was between C2F2 (FM = 2.00, C_u = 3.3) and C2F9 (FM = 3.00, C_u = 5.2), which had carbonation depths of 1.2 mm 2.8 mm respectively.

iii. The mean carbonation depth of the mixes made with a continuous grading was 1.8 mm and for mixes made with gap grading was 2.0 mm.

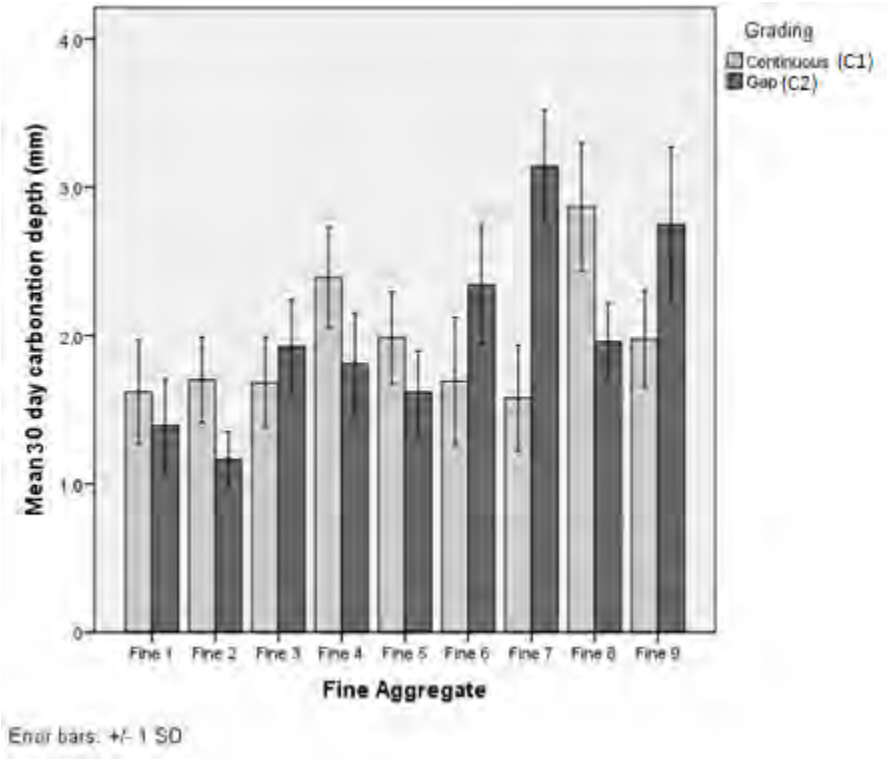

Figure 4-12: 30 day accelerated carbonation results for different coarse and fine aggregates

4.7.2 Effects of variations in fine aggregate

This section studies the effects that variations in FM and C_u had on the carbonation rate. It was observed in Section 4.7.1 that the changes in fine aggregate yielded a maximum difference in 30 day carbonation depth of 1.6 mm – an increase of 130 % from the lowest to the highest reading. This section aims to determine whether this change was in fact a result of changes in FM or C_u.

The method used to understand the influence of FM and C_u on the carbonation depth is correlation and regression analysis. The former determined whether there was a relationship between either of the fine aggregate characteristics and the carbonation depth. If a relationship was established the regression analysis was used to determine the strength of the influence that the fine aggregate characteristics had on the carbonation depth. Figure 4-13 shows a matrix scatter plot of the results with relation to FM and to C_u separately.

Table 4-18 presents the correlation coefficients, the calculation of which excluded the results for concretes C2F7 and C1F8. There was a weak correlation between carbonation depth and both FM and C_u ($|r| < 0.3$ for both) for samples with a continuous grading. There was a strong correlation between carbonation depth and both FM and C_u ($|r| > 0.3$ for both) for samples with a gap grading. The strong correlations observed for gap graded samples prompted a regression analysis to further investigate the relationships between carbonation and both FM and C_u.

Table 4-18: Correlation coefficients between carbonation depth and C_u and FM

Correlation Coefficients		
Grading	**30 day carbonation depth vs. FM**	**30 day carbonation depth vs. Cu**
Continuous (C1)	0.132	0.144
Gap (C2)	0.638	0.529

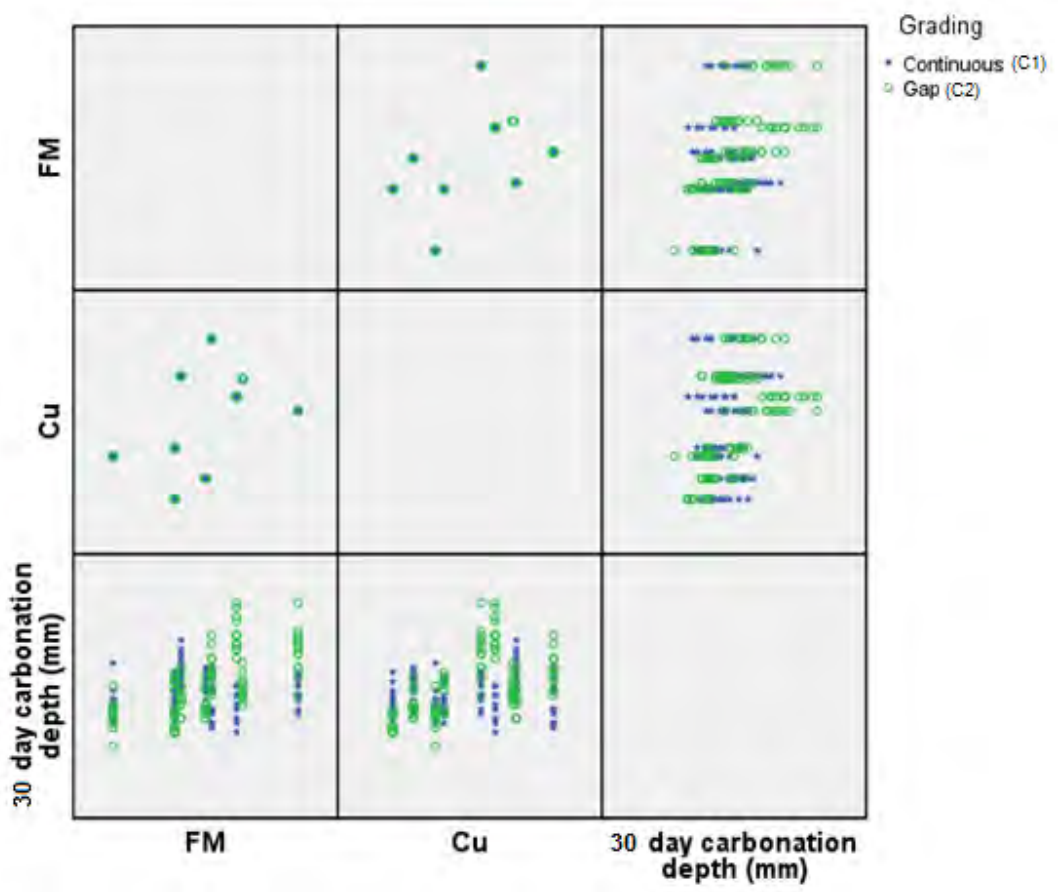

Figure 4-13: Matrix scatter plot showing the influence of FM and Cu on carbonation depth at different aggregate gradings

Regression analysis for CCI vs. FM

The correlation coefficients for carbonation depth vs. both FM and C_u, particularly in concretes with gap grading, suggest that the rate of carbonation may have depended on both factors. This was studied further by way of linear regression analysis using the method of least squares. An example calculation with this method is presented in Appendix E. The general formula for the regression is given in Equation (4-2). The regression coefficients are presented in Table 4-19.

Table 4-19: Carbonation depth vs. FM and C_u regression analysis results

Grading	Parameter	Value	t	Significance
Continuous (C1)	β_0	1.425	5.419	0.000
	β_1	0.093	0.826	0.411
	β_2	0.042	1.002	0.319
Gap (C2)	β_0	-0.949	-3.203	0.002
	β_1	0.866	6.657	0.000
	β_2	0.203	4.231	0.000

Table 4-19 shows that the effects of both C_u and FM on the carbonation rate were greater with gap graded aggregate rather than continuously graded aggregate. Furthermore it is seen that the estimated coefficients β_1 and β_2 were both statistically significant at the 5 % level only for the gap graded aggregate. These results are discussed further in Section 4.7.4.

4.7.3 Effects of variations in coarse aggregate

The effects of the variations in coarse aggregate were tested by way of t-tests between pairs of samples of the same fine aggregate. The results of all of the t-tests are presented in Table 4-20. A sample calculation showing the t-test procedure is presented in Appendix E.

Table 4-20: t-test results for comparison of 60 day accelerated carbonation depth between samples with different coarse aggregates

Fine aggregate			Equal variance	t-value	Significance (%)	Significant at α=0.05 (Y/N)
Code	FM	Cu				
F1	1.50	4.3	Yes	1.653	0.113	No
F2	2.00	3.3	Yes	5.444	0.000	Yes
F3	2.00	4.4	Yes	-1.916	0.068	No
F4	2.05	6.0	Yes	4.223	0.000	Yes
F5	2.25	3.8	Yes	3.046	0.006	Yes
F6	2.30	6.8	Yes	-3.822	0.001	Yes
F7	2.50	5.6	Yes	-9.579	0.000	Yes
F8	2.55	5.9	No	6.264	0.000	Yes
F9	3.00	5.2	Yes	-4.370	0.000	Yes
All*			No	0.260	0.795	No

*Calculated with the exclusion of F8 based on findings in Section 4.2 and F2 based on the findings of Section 4.7.1.

From Table 4-20 it is observed that there were only two pairs in which the comparison showed that the means were not different at the 5 % significance level. These were pairs with fine aggregate F1 and F3.

The overall comparison was conducted with the exclusion of sample pairs with fine aggregates F2 and F8. This was based on the findings of Sections 4.7.1 and 4.3 which validated the rejection of samples C2F7 and C1F8 respectively.

Of the seven valid pairs of samples, the concretes with continuously graded aggregate had the greater carbonation depth 3 times or 43 % of the time.

Whilst seven of the nine individual comparisons showed significant differences between mean carbonation depths, the overall comparison had a t-value of 0.795 which was not significant at the 5 % level. These findings are discussed in Section 4.7.4.

4.7.4 Discussion of carbonation results

Effects of FM and C_u on the rate of carbonation

A significant correlation was found for the relationship between carbonation depth at 30 days and both FM and C_u for samples with gap graded aggregate but with continuously graded aggregate there was little correlation with either of these properties. A regression analysis was conducted which indicated that with gap grading, for a 1 mm decrease in accelerated carbonation depth at 30 days, there would need to be reduction in the FM of 1.15 units or a reduction in the C_u of 4.93 units. With FM realistically changing within a range of 2.30 units and C_u within a range of 3.5 units, this indicates that the FM is of greater concern with regard to carbonation rate. However, the low level of correlation found in the continuously graded samples between carbonation depth and both FM and C_u suggests that permeability may have little relation to fine aggregate grading.

Relationship between overall aggregate grading and carbonation rate

In examining the relationship between carbonation depth and overall aggregate grading, it was observed that 7 of the 9 compared concretes had significantly different mean carbonation depths. However, the comparison of the mean of all samples showed no significant difference. This is a result of the fact that, of the 7 pairs of compared carbonation depths, the continuously graded aggregate yielded the greater depth of carbonation 4 times. Thus there was not a distinct relationship between grading and the rate of penetration of CO_2. It is therefore concluded that overall grading has a negligible effect on concrete penetrability.

4.7.5 Summary

From analysis of the 30 day carbonation results, the following key findings were made:

i. In concretes with a gap grading there was a correlation between FM and 30 day carbonation depth of r = 0.638 and between C_u and 30 day carbonation depth, r = 0.529. The regression analysis indicated that in the case of gap graded aggregates variation in FM had a greater effect than changes in C_u. However, there was no correlation between either FM or C_u and 30 day carbonation depth in concretes with continuously graded aggregate. It is therefore concluded that fine aggregate has little influence on concrete penetrability.

ii. The change in overall grading from continuous to gap grading through variation of the coarse aggregate FM resulted in a greater 30 day carbonation depth 3 times and a lower depth 4 times, out of 7 valid comparisons. The inconsistency in this relationship leads to the conclusion that penetrability of the concrete was not linked to overall aggregate grading.

4.8 Summary discussion

The research looked at the influence of aggregate properties, namely the FM and C_u of fine aggregate as well as the overall aggregate grading as determined by the FM of the coarse aggregate, on concrete potential durability and penetrability. Table 4-21 presents the level of the tested properties that gave the best performance in each parameter. FM was tested in the range between 1.5 and 3.0 and C_u was tested in the range between 3.3 to 6.8. In Table 4-21, low and high represent the lower and higher values within these ranges respectively. Where there is no comment given there was no distinct relationship found between the durability parameter and the test variable. Table 4-21 shows that an overall gap graded aggregate generally gave a better performance across all parameters, as opposed to a continuous grading.

The comparative influence of fine aggregate grading characterised in terms of FM and C_u, as well as that of overall aggregate grading, relative to the influence of variation of water/binder ratio and variation of binder type and content is presented in Table 4-22. It is observed that the aggregate grading in terms of each of the considered characterisations has the least influence across all of the durability indices. This is discussed further in Sections 4.8.1 and 4.8.2.

Table 4-21: The level of the tested aggregate property that leads to better performance in the indicated parameters

Aggregate property	OPI	WSI	CCI	Carbonation depth
FM	-	Increase	Decrease	Decrease
Cu	Decrease	-	-	Decrease
Overall Grading	Gap	Gap	Gap	Gap

Table 4-22: Comparison of the effects of water/binder ratio, binder type and content and aggregate grading on potential durability

Property	Change	OPI	WSI ($mm/hr^{0.5}$)	CCI (mS/cm)
Change in w/b ratio	0.4 - 0.6	-1.00	5.50	0.70
Change in binder type and content*	-	0.50	3.50	1.20
Fineness modulus †	1.5 - 3.0	-	-2.03	0.47
Coefficient of uniformity †	3.3 - 6.8	-0.30	-	-
Grading	Continuous - Gap	0.45	-1.14	-0.16

*These values are magnitude only

†Where no value is given, there was no meaningful effect found

4.8.1 Fine aggregate and concrete penetrability

For OPI, little correlation was found with FM. It was found that in the most extreme case – which was with samples with a continuous overall grading – a reduction in OPI of 0.3 would result from an increase in C_u of 3.5, where an increase in C_u of this magnitude covers the range of C_u values that may be acceptably used in practice, given the limits on FM imposed by various standards. This is a smaller change of OPI than that which may result from changes in water/binder ratio within practical limits, as well as binder type and content. The observed relationship was attributed primarily to the greater D_{60} that accompanies an increased C_u. Larger particles attract a greater amount of bleed water which increases the extent of porosity in the region of the ITZ.

For WSI, in the most extreme case – which was with samples with a continuous overall grading – a reduction in WSI of 2.03 $mm/hr^{0.5}$ would result from an increase in FM of 3.5, where an increase in FM of this magnitude covers the range of FM values that may be acceptably used in practice given the limits on FM imposed by various standards. This is a smaller change of WSI than that which may result from changes in water/binder ratio within practical limits, as well as binder type and content. The observed relationship was a result of the fact that with an increasing FM there is an increasing y_1 necessary to maintain constant packing density. With an increase in y_1 there is a greater content of particles smaller than 75 µm. These particles refine the pore structure, particularly in the region of the ITZ. There was little correlation between WSI and C_u.

For CCI, in the most extreme case – which was with samples with a continuous overall grading – an increase in CCI of 0.47 mS/cm would result from an increase in FM of 3.5, where an increase in FM of this magnitude covers the range of FM values that may be acceptably used in practice given the limits on FM imposed by various standards. This is a

smaller change of CCI than that which may result from changes in water/binder ratio within practical limits, as well as binder type and content. The observed relationship was a result of the increased tortuosity that results from a decreased FM at constant packing density, which causes greater obstruction of the flow path through the concrete. The observed relationship was further attributed to the fact that larger particles attract a greater amount of bleed water which increases the extent of porosity in the region of the ITZ.

In cases where test parameters had a correlation with FM, there were two cases where a decrease in FM resulted in improved performance and one where improvements were gained through increasing FM. A decrease was found to give reductions in CCI and carbonation depth. This correlation between the results for CCI and carbonation are to be expected given that carbonation rate depends on permeability and that CCI is a measure of conductivity which is related to diffusibility by way of Equation 3-7 and the diffusion coefficient is related to the permeability coefficient by way of Equation 2-1. Furthermore, it is plausible that the WSI and CCI react differently to a particular change, as was observed with changes in FM, since sorptivity is dictated, to a far greater extent, by pore geometry. Thus the observed trends are acceptable. However, given the different influences on different properties, a particular FM – high or low – cannot be prescribed here. If properties are to be improved through the selection of an FM, the requirements must be determined based on the application and whether it is sorption or permeation and diffusion that are of concern.

4.8.2 Coarse aggregate and concrete penetrability

OPI results showed that gap grading tended to yield a lower permeability. WSI results showed that the gap grading generally lead to a lower sorptivity and CCI results showed that the gap grading generally lead to a lower conductivity. Thus, with regards to the variations in coarse aggregate, the durability index results generally agreed with one another.

The observed relationships – whereby gap graded aggregates yielded concrete with greater potential durability and lower permeability – may be explained as follows: The greater distribution of particles in coarse aggregate C1 (the coarse aggregate that gave rise to an overall aggregate with a continuous grading) gave it a greater particle packing efficiency than C2 which was more uniformly graded. Thus to achieve the same overall packing density in aggregate blends, a greater proportion of fine aggregate had to be blended with C2 than with C1. This meant that for each fine aggregate, y_1 for coarse aggregate C2 was greater than y_1 for coarse aggregate C1, with a correspondingly greater amount of 75 μm material which refined the pore structure and yielded less particle friction which improved consolidation. Penetrability was thus reduced.

Statistically there was little difference in the mean measured values of each of the durability indices between samples of different overall aggregate gradings in each of the measured parameters. Furthermore, the variations that were observed are less than those that were observed by Heiyantuduwa (2008) which resulted from variations in water/binder ratio within practical limits, as well as variations in binder type and content. Thus it is concluded that the selection of aggregates with an overall gap grading rather than those with an overall continuous grading will give improved durability. However, the benefits are small and a designer should consider the water/binder ratio and the selection of a mineral admixture ahead of aggregate grading when a lower penetrability is desired.

4.8.3 FM as a grading characterising parameter

FM had little correlation with measured parameters 5 times out of 8, with considerable correlation with WSI with gap graded aggregate, with CCI with continuous graded aggregate and with carbonation in samples with gap graded aggregate. Furthermore there was a different relationship between FM and WSI to that between FM and both CCI and carbonation. Thus it is concluded that FM is not an effective parameter in characterising aggregate grading when mix design centres on durability.

4.8.4 C_u as a grading characterising parameter

C_u had little correlation with measured parameters 6 times out of 8, with considerable correlation only with OPI with use of continuously graded aggregates and with carbonation with use of gap graded aggregates. With this low level of correlation with potential durability and permeability, C_u is an ineffective parameter with which to characterise aggregate grading for aggregate specification in durability focused mix design.

4.8.5 Aggregate grading and packing density

In the literature review presented in Chapter 2 it was found that greater aggregate packing densities yield better durability. As it has been concluded that C_u and FM had no influence on potential durability and permeability and overall aggregate grading had a small influence, it is concluded that aggregate packing density remains of primary importance and thus the importance of aggregate grading lies in the influence it has on aggregate packing density.

4.8.6 Evaluation of results and test methods

The test samples consisted of 4 specimens. With such small sample sizes it was difficult to draw conclusions on observed trends. Furthermore, the variance in the results was often very high when compared to the results of other research using the same method, which contributed to the uncertainty in the observations. In addition the increments of both FM and C_u were smaller than what may have been necessary to study the relationships in question. The research may have been more conclusive had fewer samples with a greater number of specimens been used.

4.9 Conclusions from results

Following the experimental work and the analysis of results the following conclusions can be drawn:

- The modified Toufar packing model was used to determine the volume fractions y_1 and y_2, of fine and coarse aggregate respectively, necessary to achieve the same aggregate packing density in each mix. It was found that there was a directly proportional relationship between the FM of fine aggregate and the required value of y_1. A similar relationship was observed between coarse aggregate FM and y_1 which meant that a greater y_1 was required for an overall gap graded aggregate which was created by using a coarse aggregate with a greater coarse aggregate FM.
- Both coarse and fine aggregate was crushed greywacke. The particle size distribution of the fine aggregates was varied to achieve different values of FM and C_u. The FM of the coarse aggregate was varied to achieve different overall aggregate grading. Besides the aggregate, the mix designs were based on commonly used proportions. Apart from mix C1F8, the compressive strengths obtained were as expected and showed that the mixing, casting and curing were done correctly. Mix C1F8 was rejected on the basis of its low strength.
- OPI was found to have some correlation with C_u in concretes with continuously graded aggregates. With an increase in C_u there was an increase in permeability, indicated by a decrease in OPI. This was attributed primarily to the increase in D_{60} which, as a result of a greater level of localised bleeding which causes a greater water/binder ratio at the aggregate surface, causes a greater porosity in the ITZ. However, this effect was significantly less than the effects that water/binder ratio and binder type and content have been observed to have on OPI. Variation of FM had little practical influence on OPI.
- WSI was found to have some correlation with FM in concretes with gap graded aggregates. With an increase in FM there was a decrease in WSI. This was explained by

the relationship between FM and y_1 whereby, in order to maintain constant packing density, as FM increased, so did y_1. As a result there was a greater proportion of particles of 75 μm and smaller, which refines the pore structure, particularly in the region of the ITZ. Variation of C_u had little influence on WSI.

- CCI was found to have some correlation with FM in concretes with continuously graded aggregates. As FM increased, an increase in CCI was observed. This was attributed to the increase in the average particle size which, as a result of a greater level of localised bleeding leading to a greater water/binder ratio at the aggregate surface, causes a greater porosity in the ITZ. Furthermore, with a greater average aggregate particle size there is a lower level of tortuosity which allows for easier passage of a penetrating substance. Variation of C_u had little influence on CCI.
- The depth of carbon dioxide penetration at thirty days of accelerated carbonation indicated that there was a relationship between penetrability in concretes with gap graded aggregate. However, the concrete with continuously graded aggregate showed no correlation between carbonation depth and both FM and C_u. It was therefore concluded that the fine aggregate grading, in terms of both FM and C_u, had no meaningful effect on the penetrability as measured by carbon dioxide penetration.
- Gap graded aggregates yielded better performance in all of the measured parameters. This is explained as follows: The greater distribution of particles in coarse aggregate C1 (the coarse aggregate that gave rise to an overall aggregate with a continuous grading) gave it a greater particle packing efficiency than C2 which was more uniformly graded. Thus to achieve the same overall packing density in aggregate blends, a greater proportion of fine aggregate had to be blended with C2 than with C1. This meant that for each fine aggregate, y_1 for coarse aggregate C2 was greater than y_1 for coarse aggregate C1, with a correspondingly greater amount of 75 μm material which refines the pore structure and thereby reduces penetrability.
- With each of the DI parameters where there was some observed correlation with either FM or C_u, the sensitivity of the DI parameter to changes in aggregate grading was less than the sensitivity of the same parameters to changes in water/binder ratio and OPI and CCI were less sensitive to changes in FM and C_u than to changes in binder type and content.

5. Conclusions and Recommendations

5.1 Summary

Repair of concrete structures accounts for expenditure of 3 to 5 % of GNP in some countries. The foremost mechanism of concrete deterioration is corrosion of steel reinforcement. A performance based approach to concrete mix design is being adopted whereby designers strive to achieve the optimum level of performance in outcomes such as durability, specific to the application. In this dissertation, a detailed literature review presented an overview of concrete durability with attention given to the influence of concrete aggregate on concrete durability. The literature review was concluded with a review of aggregate packing models. Conclusions drawn for the literature review are given below.

The aggregate grading that is 'ideal' for concrete is a function of the purpose and of the concrete in both its plastic and hardened states. In fact, there is no 'ideal' grading, despite great research efforts on the topic (Grieve, 2009b). It is understood that near maximum packing density is usually optimum for strength and durability (Powers, 1961; Alexander and Mindess, 2005) and that there is a strong link between grading and packing density (Johansen & Andersen, 1991; de Larrard, 2001) as well as workability (Andersen, 1990). As such, mix proportioning guidelines both in the USA and South Africa attempt to achieve the greatest packing density for a given combination of coarse and fine aggregates.

However, there are other properties that are influenced by the aggregate particle size distribution which have been found to affect concrete properties, including durability. These include the extent of the porosity in the interfacial transition zone and tortuosity which determines the complexity of the flow path of a permeating fluid through the concrete (Mehta and Monteiro, 2006). Neither the extent of the effects of aggregate grading on these factors, nor the implications these have on concrete properties, are fully understood.

5.1.1 Methods of characterising aggregate grading

A grading curve describes the distribution of particle sizes. The curve is typically of a complex shape that may, at best, be represented by a step-wise function. However, this would be complex and cumbersome, and therefore not suited for use in aggregate specification. A good characterising parameter accurately describes the changes that influence the performance outcomes whilst being simple.

Two pieces of information contained within a grading curve are the average particle size and the grading type, being uniform or continuous. The former may be characterised by the fineness modulus (FM) whilst the latter may be characterised by the coefficient of uniformity (C_u).

A limiting range for the allowable FM is given in USA and South African standards as a means to ensure that the fine aggregate is not too fine – leading to poor workability – or too coarse – leading to harshness and segregation. Furthermore, guidelines on concrete mix proportioning use FM as a means to determine the volume fractions of coarse and fine aggregate for optimum packing density. However, the relationship between each of the two parameters and concrete durability is not understood and they may serve as a means to better understand the influence of aggregate grading on the durability of concrete.

5.1.2 Laboratory experiments

The main purpose of the research was to determine the relationship, if any, between aggregate grading and concrete durability. This was done by way of laboratory experiments where the aggregate packing density was held constant and where the parameters of interest were FM and C_u of the fine aggregate as well as the overall aggregate grading – being gap or continuously graded – which was controlled through the FM of the coarse aggregate. Each of nine different fine aggregates (F1 to F9) was combined with each of two coarse aggregates (C1 & C2), for a total of 18 different aggregate samples (C1F1 to C2F9).

The Modified Toufar Model (MTM) was used to estimate the aggregate packing density in concretes with different aggregate samples. The packing density for each combination of different coarse and fine aggregate was determined at different volume fractions of fine (y_1) and coarse (y_2) aggregate, as a percentage of total aggregate volume. This allowed for the selection of coarse and fine aggregate volume fractions in each aggregate sample such that each sample had the same aggregate packing density.

The durability index tests, including the oxygen permeability index, water sorptivity index and the chloride conductivity index, were conducted to characterise concrete potential durability and carbonation tests were conducted to characterise concrete permeability.

5.2 Conclusions from research

Overall, potential durability, as measured by the durability index tests, and the concrete permeability, as measured by the accelerated carbonation tests, had little relationship with both FM and C_u. With each of these variables generally having less of an influence on the

potential durability than water/binder ratio and binder type and content, it is concluded that aggregate grading as characterised by FM and C_u is of less importance than, and should thus not receive as much consideration, as water/binder ration and the selection of binder type and content when designing concrete to achieve a particular durability.

Across all tests overall gap graded aggregate tended to give better performance that overall continuously graded aggregates. It is concluded that the selection of aggregates with an overall gap grading rather than those with an overall continuous grading will give improved durability. However, the benefits are small and a designer should consider the water/binder ratio and the selection of a mineral admixture ahead of aggregate grading when a lower penetrability is desired.

There were 4 tests and two different overall gradings. Thus there were a total of 8 different test runs which could identify whether variations in fine aggregate, either by change in FM or by C_u, had an influence on concrete penetrability. Of 8, FM had a fair correlation with a durability parameter three times (37.5 % of the time) and C_u had a fair correlation twice (25 % of the time). It is therefore concluded that both FM and C_u have little effect on the penetrability of concrete. As a result of this finding it can be concluded that FM and C_u are not useful parameters for the characterisation of aggregate grading for use in durability-focused performance-based design.

It was found that gap graded aggregates tended to yielded better performance in the measured parameters than continuously graded aggregates. It is therefore concluded that the practice in South Africa, whereby gap graded aggregates are commonly used, is of greater benefit to durability than the practice of using continuously graded aggregates as found in the United States and Western Europe. However the benefit is small and in general does not warrant incurring added cost in the name of obtaining gap graded aggregates. Water/binder ratio and binder type and content remain of greater concern when designing concrete to achieve a particular level of durability.

Since it has been shown that concrete penetrability has little relationship with FM it can be concluded that the current use of FM in SANS 1083: 2013 and ASTM C33 need not be reconsidered on account of concrete durability requirements. Furthermore, with the small correlation found between concrete penetrability and C_u, C_u is not a useful parameter for characterising grading for purposes of durability-focused, performance-based design and thus it need not be considered further for this application.

Greater aggregate packing densities yield better durability. As it has been concluded that C_u and FM had no influence on potential durability and permeability and overall aggregate grading had a small influence, it is concluded that aggregate packing density remains of

primary importance and thus the importance of aggregate grading lies in the influence it has on aggregate packing density.

5.3 Recommendations

It is difficult to characterise the grading curve with a single parameter. The grading curve holds a large amount of information which cannot all be accounted for by a single value. This research set out to identify whether there was a particular piece of information from the grading curve that was of relevance to concrete durability. The research looked at three different pieces of information contained in the grading curve, namely the average particle size (FM), the slope of the distribution (C_u) and the overall grading profile (gap or continuous). Of these, only overall aggregate grading was found to have an effect, which was not statistically significant and less than effects of variations in water/binder ratio and binder type and content, as observed by other researchers. As such the following recommendations are made with regard to the selection of aggregate grading:

- Overall aggregate grading may be considered when optimising the durability in concrete mix design. However, aggregate grading requires less attention than water/binder ratio and binder type and content.
- Aggregate packing density is more critical than any other aggregate grading related property with regard to concrete durability. Thus in the selection of concrete aggregate, it is important to select a grading to achieve near maximum packing density in order to maximise durability.

For the durability index tests samples of four specimens were used, in accordance with the guidelines (Alexander, Mackechnie & Ballim, 1999). However, there was a large amount of variability in the experimental results. It is widely accepted that 30 specimens is the minimum to obtain an accurate representation. With the small sample size that was used the high variability introduces uncertainty into the observations. It is therefore recommended that the experiments be repeated with greater sample sizes.

References

Addis, B. & Goodman, J., 2009. Concrete mix design, In: G. Owens, ed. *Fulton's concrete technology.* Midrand: C&CI, pp. 219-228.

Aim, R. & Goff, P., 1967. Effet de paroi dans les empilements desordonnes de spheres et application a la porosite de melanges binaires. *Powder technology,* Volume 1, pp. 281-290.

Alexander, M., MacKechnie, J. & Ballim, Y., 1999. *Research monograph 2: Guide to the use of durability indexes for achieving durability in concrete structures.* Cape Town: University of Cape Town.

Alexander, M., Mackechnie, J. & Ballim, Y., 2001. Use of durability inexes to achieve durable cover concrete in reinforced concrete structures. In: S. Mindess & J. Skalney, eds. *Materials science of concrete VI.* Westerville: The American Ceramic Society, pp. 483-512.

Alexander, M. & Mindess, S., 2005. *Aggregates in concrete.* Oxon: Taylor and Francis.

Andersen, P., 1990. *Control and monitoring of concrete production (PhD thesis).* Copenhagen: The Technical University of Denmark.

Anderson, J. & Johansen, V., 1993. *SHRP-C-334: A guide to determining the optimal gradation of concrete aggregates,* Washington D.C.: National Research Council.

Austen, J., 1939. Methods of representing distribution of particle size. *Industrial and engineering chemistry,* 11(6), pp. 334-339.

Ballim, Y., Alexander, M. & Beushausen, H., 2009. Durability of concrete. In: G. Owens, ed. *Fulton's concrete technology.* Midrand: C&CI, pp. 155-188.

Bentur, A. & Cohen, M., 1987. Effect of Condensed Silica Fume on the Microstructure of the Interfacial Zone in Portland Cement Mortars. *Journal of the American Ceramic Society,* 70(10), pp. 738-743.

Bentz, D., Stutzman, P. & Garboczi, E., 1992. Experimental and simulation studies of the interfacial zone in concrete. *Cement and concrete research,* Volume 22, pp. 891-902.

beton, C. E.-I. d., 1982. Durability of concrete structures: State of the art report. *Bulletin d'information Paris,* Volume 148, p. 328.

Cohen, J. 1988. *Statistical power analysis for the behavioural sciences*, Hillside, New Jersey.

Czernin, W., 1980. *Cement chemistry and physics for civil engineers.* 2nd ed. Wiesbaden: Bauverlag.

de Larrard, F., 1999. *Concrete mixture proportioning: A scientific approach.* Oxon: Taylor & Francis.

de Larrard, F. & Sedran, T., 1994. Packing of aggregates: An alternative tool to determine the optimal aggregate mix. *Cement and Concrete Research,* Volume 24, pp. 997-1009.

Dhir, R.K., McCarthy, M.J. & Paine, K.A., 2005, Engineering property and structural design relationships for new and developing concretes, Materials and Structures, 38(275) pp. 1-9.

Diamond, S. & Huang, J., 2001. The ITZ in concrete - a different view based on image analysis and SEM observations. *Cement and concrete composites,* Volume 23, pp. 179-188.

Elsharief, A., Cohen, M. & Olek, J., 2003. Influence of aggregate size, water cement ratio and age on the microstructure of the interfacial transition zone. *Cement and concrete research,* Volume 33, pp. 1837-1849.

Feldman, R. & Sereda, P., 1970. A new model of hydrated cement and its paracticle implications. *Engineering Journal (Canada),* 53(8/9), pp. 53-59.

Fennis, S., Walraven, J.C. & den Uijl, J.A. 2012. Compaction-interaction packing model:regarding the effect of fillers in concrete mixture design. *Materials and Structures*, Volume 46, Issue 3, pp. 463-478.

Fennis, S., 2011. *Design of ecological concrete by particle packing optimisation (PhD Thesis),* Delft: Technical University of Delft.

Fuller, W. & Thompson, S., 1907. The laws of proportioning concrete. *Transactions of the American Society of Civil Engineers,* Volume 59, pp. 67-143.

Galloway Jr., J., 1994. Grading, shape and surface properties. In: P. &. L. J. Klieger, ed. *Significance of tests and properties of concrete and concrete making materials.* Philedalphia: ASTM, pp. 401-410.

Golterman, P., Johansen, V. & Palbol, L., 1997. Packing of aggregates: an alternative tool to determine the optimal aggregate mix, *ACI Materials Journal*, 94(5): 435-443.

Grieve, G., 2009. Aggregates for concrete. In: G. Owens, ed. *Fulton's concrete technology.* Midrand: C&CI, pp. 25-61.

Grieve, G., 2009. Cementitious materials. In: G. Owens, ed. *Fulton's Concrete Technology.* Midrand: C&CI, pp. 1-14.

Halamickova, P., Detwiler, R., Bentz, D. & Garboczi, E., 1995. Water permeability and chloride ion diffusion in portland cement mortars: relationship to sand content and critical pore diameter. *Cement and concrete research,* 25(4), pp. 790-802.

Hearn, N. H. R. &. M. R., 1994. Pore structure and permeability. In: P. &. L. J. Klieger, ed. *Significance of tests and properties of concrete and concrete-making materials.* Philadelphia: American society for testing and materials, pp. 240-262.

Heiyantuduwa, R., 2008. *Service life modelling using the durability index approach,* Cape Town: University of Cape Town, Unpublished report.

Johansen, V. & Andersen, P., 1991. Particle packing and concrete properties. In: J. Skalney & S. Mindess, eds. *Materials science of concrete II.* Westerville: The American Ceramic Society, pp. 111-147.

Jones, M., Zheng, L. & Newlands, M., 2002. Comparison of particle packing models for proportioning concrete constituents for minimum voids ratio. *Materials and Structures,* Volume 35, pp. 301-309.

Kishitani, K., 1964. Uber die bestandigkeit von stahlbeton unter dem einfluss von CO2. *Zement - Kalk - Gips,* pp. 158-159.

Kumar V, S. & Santhanam, M., 2003. Particle packing theories and their application in concrete mixture proportioning. *The Indian Concrete Journal,* 77(9), pp. 1324-1331.

Mackechnie, J., 1997. *Research monograph 1: Predictions of reinforced concrete durability in the marine environment*, Cape Town: University of Cape Town.

Mackechnie, J., 1999. *Predictions of carbonation in concrete,* Cape Town: Unpublished.

McGeary, R., 1961. Mechanical packing of spherical particles. *Journal of American Ceramics Society,* 44(10), pp. 513-522.

Mehta, P. &. M. P., 1993. *Concrete: Structure, properties and materials.* 2nd ed. New Jersey: Prentice Hall.

Mehta, P. & Aitcin, P., 1990. *Microstructural basis of selection of materials and mix proportions for high-strength concrete.* Berkeley, American Concrete Institute, pp. 265-279.

Mehta, P. & Monteiro, P., 2006. *Concrete: Microstructure, properties and materials.* 3rd ed. New York: McGraw-Hill.

Meyer, A., Wierig, H.-J. & Husmann, K., 1967. *Carbonation of Concrete,* Berlin: Deutscher ausschuss fuer stahlbeton, Heft 182 Laboratorium der westfaelischen zementindustrie beckum.

Nanthagopalan, P. & Santhanam, M., 2012. An empirical approach for the optimisation of aggregate combinations for self-compacting concrete. *Materials and structures,* Volume 45, pp. 1167-1179.

National Stone Association (NSA), 1980. *Quality concrete with crushed stone aggregate.* Washington D.C.: National Stone Association.

Neves, R., Branco, F. & de Brito, J., 2011. Abouth the statistical interpretatipon of air permeability assessment. *Materials and Structures,* Volume 45, pp. 529-539.

Neville, A.M., 1995. Properties of Concrete. Harlow: Longman.

Nilsson, L., 2003. Durability concept; pore structure and transport processes. In: J. Newman & B. Choo, eds. *Advanced concrete technology: Concrete properties.* Oxford: Butterworth-Heinemann, pp. 8/1-8/29.

Nilsson, L. & Luping, T., 1995. Relations between different transport parameters. In: J. Krop & H. Hilsdorf, eds. *Performance criteria for concrete durability.* Paris: RILEM, pp. 15-32.

Nishi, T., 1962. *Outline of the studies regarding the neutralisation of alkali or carbonation of concrete.* Prague, RILEM.

Papadakis, V., Vayenas, C. & Fardis, M., 1991a. Physical and chemical characteristics affecting the durability of concrete. *ACI Materials Journal,* 88(2), pp. 186-196.

Papadakis, V., Vayenas, C. & Fardis, M., 1991b. Fundamental modellaing and experimental investigation of concrete carbonation. *ACI materials journal,* 88(4), pp. 363-373.

Ping, X., Beaudoin, J. & Brousseau, R., 1991. Effects of aggregate size on transition zone properties at the portland cement paste phase. *Cement and concrete research,* Volume 21, pp. 999-1005.

Powers, M. & Brownyard, T., 1947. Studies of the physical properties of hardened cement paste. *ACI Journal,* Volume 43, pp. 933-992.

Powers, T., 1968. *The properties of fresh concrete.* New York: Wiley & Sons.

Powers, T. & Brownyard, T., 1947. Studies of the physical properties of hardened cement paste. *Journal of the American Concrete Institute,* 18(6), pp. 669-712.

Reschke, T., 2000. Der Einfluss der Granulometrie der Feinstoffe auf die gefügeentwicklung und die Festigkeit von Beton VBT Verlag Bau+Technik GmbH. Düsseldorf.

Richardson, M., 2004. *Fundamentals of durable reinforced concrete.* Oxon: Taylor & Francis.

Rosin, P. & Rammler, E., 1933. The laws governing the fineness of powdered coal. *The Journal of the Institute of Fuel,* 109(12), pp. 29-36.

Roy, D. et al., 1993. *Concrete components packing handbook.* Waschington D.C.: National Research Council.

Roy, D., Scheetz, B.E. & Sillsbee, M.R. 1993. Processing of optimised cements and concretes via particle packing, *MRS Bulletin*, pp 45-49.

Salvoldi, B., 2010. *Modelling the carbonation of concrete using early age oxygen permeability index tests,* Cape Town: Unpublished.

Scrivener, K., 2000. Characterisation of the ITZ and its quantification by test methods. In: M. Alexander, et al. eds. *Engineering and transport properties of the interfacial transition zone in cementitios composites.* Paris: Rilem, pp. 3-15.

Scrivener, K. & Gartner, E., 1987. Microstructural gradients in cement paste around aggregate particles. In: S. Mindess & S. Shah, eds. *MRS Proceedings: Bonding in cementitious composites.* Pittsburgh: Materials Research Society.

Shacklock, B., 1959. *C&CA Technical report TRA/240: Comparison of gap- and continuously-graded concrete mixes,* Slough: Cement & Concrete Association.

Stovall, T., de Larrard, F. & Buil, M., 1986. Linear packing density model of grain mixtures. *Powder technology,* Volume 48, pp. 1-12.

Tattershall, G. & Banfill, P., 1983. *The rheology of fresh concrete.* Boston: Pitman Books Limited.

Thiery, M., Villain, G., Dangla, P. & Platret, G., 2007. Investigation of the carbonation front shape on cementitious materials: Effects of the chemical kinetics. *Cement and concrete research,* Volume 37, pp. 1047-1058.

Toufar, W., Born, M. & Klose, E., 1976. Beitrag zur optimierung der packungsdichte polydisperserkorniger systeme. *VEB Deutscher velag fur grunstoffindustrie,* pp. 29-44.

Toufar, W., Klose, E. & Born, M., 1977. Berechnung der packungsdichte von korngemischen. *Aufbereitungs-technik,* Volume 11, pp. 603-608.

United States Bureau of Reclamation (USBR), 1975. *Concrete Manual.* 8th ed. s.l.:USBR.

van Balen, K., 2005. Carbonation reaction of lime, kinetics at ambient temperature. *Cement and concrete research,* pp. 667-657.

White, T., 1991. Aggregate as a component of portland cement and asphalt concrete. In: R. Barksdale, ed. *The aggregate handbook.* Washington D.C.: National Stone Association, pp. 13/1-13/69.

Wierig, H., 1984. *Long time studies on the carbonation of concrete under normal outdoor exposure.* Hanover, RILEM, pp. 239-249.

Winslow, D., Cohen, M., Bentz, D., Snyder, K. & Garboczi, E., 1994. Percolation and pore structure in mortars and concrete. *Cement and concrete research,* Volume 24, pp. 25-37.

Winslow, D. & Liu, D., 1990. The pore structure of paste in concrete. *Cement and concrete research,* Volume 20, pp. 227-235.

Appendix A – Fine aggregate PSDs

Table A1: Sieve analysis for aggregate F1

F1			
Sieve aperture	Percentage passing	Percentage greater than	Percentage retained
(mm)	(%)	(%)	(%)
4.75	100	0	0
2.36	100	0	0
1.18	95	5	5
0.6	80	20	15
0.3	50	50	30
0.15	25	75	25
0.075	5	0	20
< 0.075			5
Σ		150	100.00
FM	1.50		
D60	0.40		
D10	0.09		
Cu	4.26		

Table A2: Sieve analysis for aggregate F2

F2			
Sieve aperture	Percentage passing	Percentage greater than	Percentage retained
(mm)	(%)	(%)	(%)
4.75	100	0	0
2.36	100	0	0
1.18	95	5	5
0.6	70	30	25
0.3	25	75	45
0.15	10	90	15
0.075	5	0	5
< 0.075			5
Σ		200	100
FM	2.00		
D60	0.50		
D10	0.15		
Cu	3.33		

Table A3: Sieve analysis for aggregate F3

F3			
Sieve aperture	Percentage passing	Percentage greater than	Percentage retained
(mm)	(%)	(%)	(%)
4.75	100	0	0
2.36	95	5	5
1.18	85	15	10
0.6	65	35	20
0.3	40	60	25
0.15	15	85	25
0.075	5	0	10
< 0.075			5
Σ		200	100.00
FM	2.00		
D60	0.50		
D10	0.11		
Cu	4.44		

Table A4: Sieve analysis for aggregate F4

F4			
Sieve aperture	Percentage passing	Percentage greater than	Percentage retained
(mm)	(%)	(%)	(%)
4.75	100	0	0
2.36	95	5	5
1.18	85	15	10
0.6	60	40	25
0.3	35	65	25
0.15	20	80	15
0.075	5	0	15
< 0.075			5
Σ		205	100.00
FM	2.05		
D60	0.60		
D10	0.1		
Cu	6.00		

Table A5: Sieve analysis for aggregate F5

F5			
Sieve aperture	Percentage passing	Percentage greater than	Percentage retained
(mm)	(%)	(%)	(%)
4.75	100	0	0
2.36	95	5	5
1.18	85	15	10
0.6	60	40	25
0.3	25	75	35
0.15	10	90	15
0.075	5	0	5
< 0.075			5
Σ		225	100.00
FM	2.25		
D60	0.57		
D10	0.15		
Cu	3.78		

Table A6: Sieve analysis for aggregate F6

F6			
Sieve aperture	Percentage passing	Percentage greater than	Percentage retained
(mm)	(%)	(%)	(%)
4.75	100	0	0
2.36	95	5	5
1.18	85	15	10
0.6	50	50	35
0.3	25	75	25
0.15	15	85	10
0.075	5	0	10
< 0.075			5
Σ		230	100.00
FM	2.30		
D60	0.77		
D10	0.1125		
Cu	6.81		

Table A7: Sieve analysis for aggregate F7

F7			
Sieve aperture	Percentage passing	Percentage greater than	Percentage retained
(mm)	(%)	(%)	(%)
4.75	100	0	0
2.36	90	10	10
1.18	75	25	15
0.6	50	50	25
0.3	25	75	25
0.15	10	90	15
0.075	5	0	5
< 0.075			5
Σ		250	100.00
FM	2.50		
D60	0.83		
D10	0.15		
Cu	5.55		

Table A8: Sieve analysis for aggregate F8

F8			
Sieve aperture	Percentage passing	Percentage greater than	Percentage retained
(mm)	(%)	(%)	(%)
4.75	100	0	0
2.36	95	5	5
1.18	85	15	10
0.6	35	65	50
0.3	20	80	15
0.15	10	90	10
0.075	5	0	5
< 0.075			5
Σ		255	100.00
FM	2.55		
D60	0.89		
D10	0.15		
Cu	5.93		

Table A9: Sieve analysis for aggregate F9

F9			
Sieve aperture	Percentage passing	Percentage greater than	Percentage retained
(mm)	(%)	(%)	(%)
4.75	100	0	0
2.36	85	15	15
1.18	60	40	25
0.6	35	65	25
0.3	15	85	20
0.15	5	95	10
0.075	5	0	0
< 0.075			5
Σ		300	100.00
FM	3.00		
D60	1.18		
D10	0.23		
Cu	5.24		

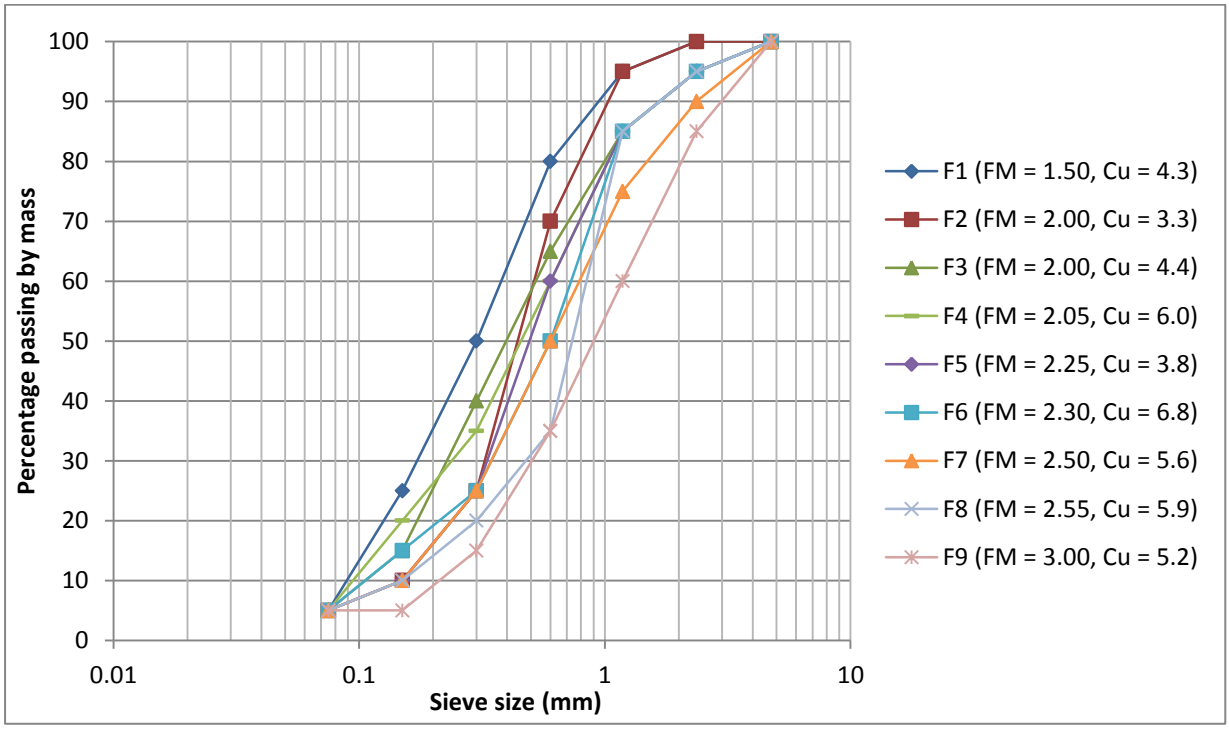

Figure A1: Grading curves for all tested fine aggregates

Appendix B – Rosin Rammler Data

Table B1: Calculation of Rosin-Rammler parameters for aggregate F1

F1						
Particle size - D (mm)	**Ln D**	**F (%)**	**R=1-F**	**1/R**	**ln(1/r)**	**ln(ln(1/r))**
4.75	1.56	100	0.00	-	-	-
2.36	0.86	100	0.00	-	-	-
1.18	0.17	95	0.05	20.00	3.00	1.10
0.60	-0.51	80	0.20	5.00	1.61	0.48
0.30	-1.20	50	0.50	2.00	0.69	-0.37
0.15	-1.90	25	0.75	1.33	0.29	-1.25
0.08	-2.59	5	0.95	1.05	0.05	-2.97

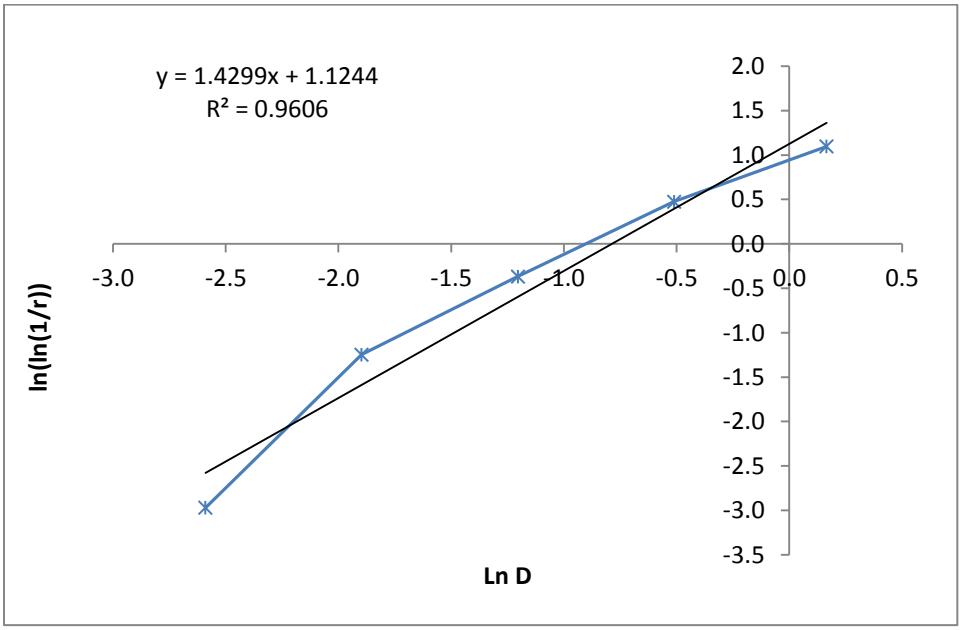

Figure B1: Rosin-Rammler curve for aggregate F1

Table B2: Characteristic diameter of aggregate F1

DISTRIBUTION PARAMETER	INTERCEPT	PACKING DENSITY	CHARACTERISTIC DIAMETER
n	**C**	**ϕ**	**D' (mm)**
1.430	1.124	0.596	0.46

Table B3: Calculation of Rosin-Rammler parameters for aggregate F2

F2						
Particle size - D (mm)	Ln D	F (%)	R=1-F	1/R	ln(1/r)	ln(ln(1/r))
4.750	1.56	100	0.00	-	-	-
2.360	0.86	100	0.00	-	-	-
1.180	0.17	95	0.05	20.00	3.00	1.10
0.600	-0.51	70	0.30	3.33	1.20	0.19
0.300	-1.20	25	0.75	1.33	0.29	-1.25
0.150	-1.90	10	0.90	1.11	0.11	-2.25
0.075	-2.59	5	0.95	1.05	0.05	-2.97

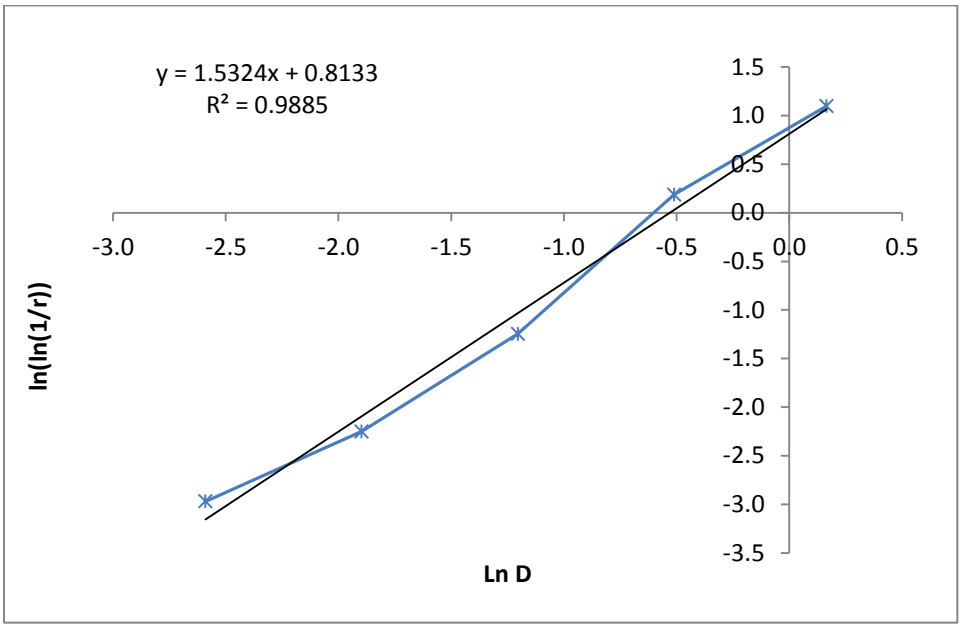

Figure B2: Rosin-Rammler curve for aggregate F2

Table B4: Characteristic diameter of aggregate F2

DISTRIBUTION PARAMETER	INTERCEPT	PACKING DENSITY	CHARACTERISTIC DIAMETER
n	C	ϕ	D' (mm)
1.532	0.813	0.571	0.59

Table B5: Calculation of Rosin-Rammler parameters for aggregate F3

F3						
Particle size - D (mm)	Ln D	F (%)	R=1-F	1/R	ln(1/r)	ln(ln(1/r))
4.750	1.56	100	0.00	-	-	-
2.360	0.86	95	0.05	20.00	3.00	1.10
1.180	0.17	85	0.15	6.67	1.90	0.64
0.600	-0.51	65	0.35	2.86	1.05	0.05
0.300	-1.20	40	0.60	1.67	0.51	-0.67
0.150	-1.90	15	0.85	1.18	0.16	-1.82
0.075	-2.59	5	0.95	1.05	0.05	-2.97

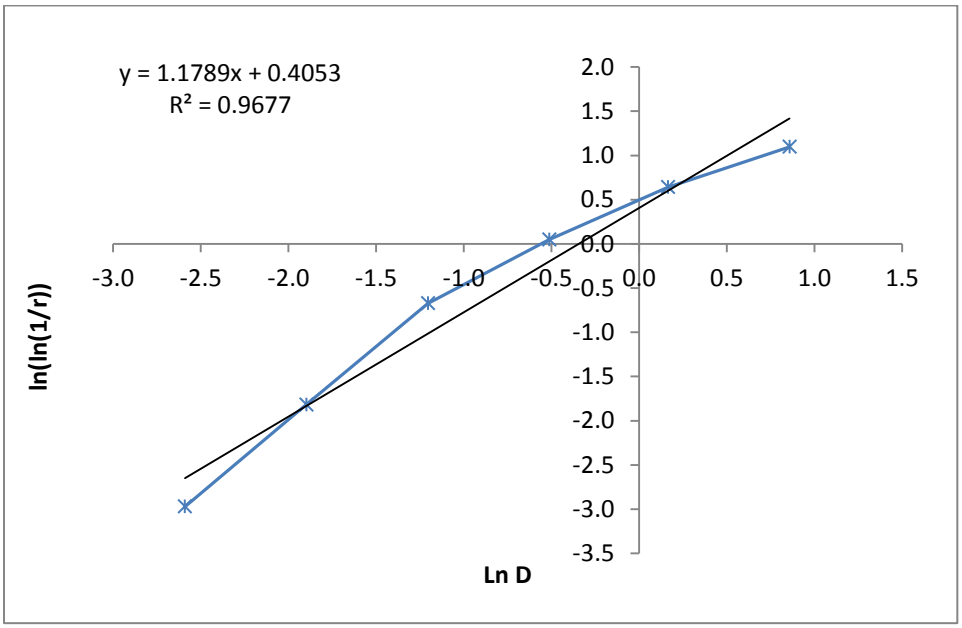

Figure B3: Rosin-Rammler curve for aggregate F3

Table B6: Characteristic diameter of aggregate F3

DISTRIBUTION PARAMETER	INTERCEPT	PACKING DENSITY	CHARACTERISTIC DIAMETER
n	C	ϕ	D' (mm)
1.179	0.404	0.611	0.71

Table B7: Calculation of Rosin-Rammler parameters for aggregate F4

F4						
Particle size - D (mm)	Ln D	F (%)	R=1-F	1/R	ln(1/r)	ln(ln(1/r))
4.750	1.56	100	0.00	-	-	-
2.360	0.86	95	0.05	20.00	3.00	1.10
1.180	0.17	85	0.15	6.67	1.90	0.64
0.600	-0.51	60	0.40	2.50	0.92	-0.09
0.300	-1.20	35	0.65	1.54	0.43	-0.84
0.150	-1.90	20	0.80	1.25	0.22	-1.50
0.075	-2.59	5	0.95	1.05	0.05	-2.97

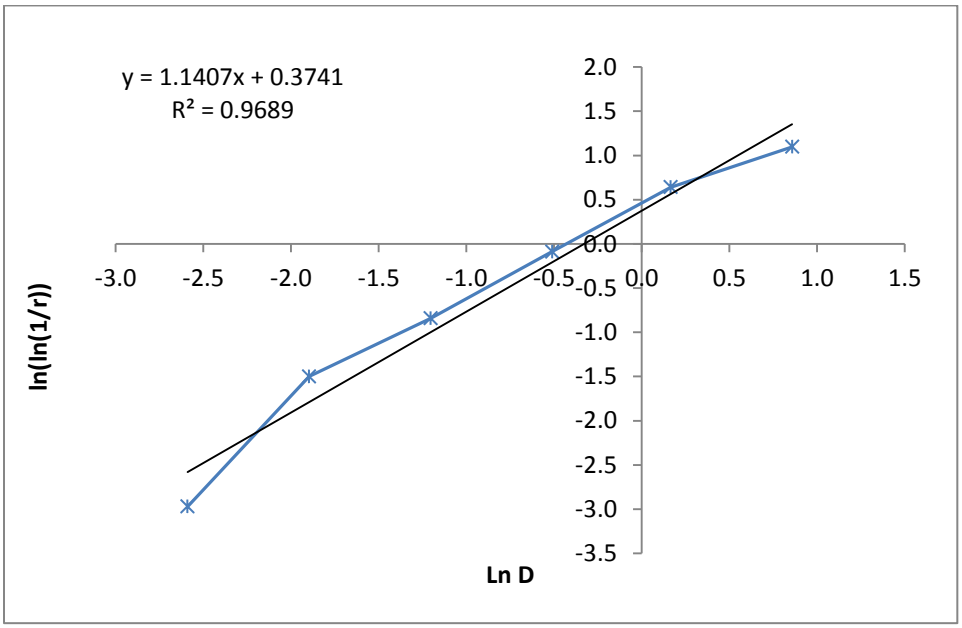

Figure B4: Rosin-Rammler curve for aggregate F4

Table B8: Characteristic diameter of aggregate F4

DISTRIBUTION PARAMETER	INTERCEPT	PACKING DENSITY	CHARACTERISTIC DIAMETER
n	C	ϕ	D' (mm)
1.141	0.374	0.610	0.72

Table B9: Calculation of Rosin-Rammler parameters for aggregate F5

F5						
Particle size - D (mm)	Ln D	F (%)	R=1-F	1/R	ln(1/r)	ln(ln(1/r))
4.750	1.56	100	0.00	-	-	-
2.360	0.86	95	0.05	20.00	3.00	1.10
1.180	0.17	85	0.15	6.67	1.90	0.64
0.600	-0.51	60	0.40	2.50	0.92	-0.09
0.300	-1.20	25	0.75	1.33	0.29	-1.25
0.150	-1.90	10	0.90	1.11	0.11	-2.25
0.075	-2.59	5	0.95	1.05	0.05	-2.97

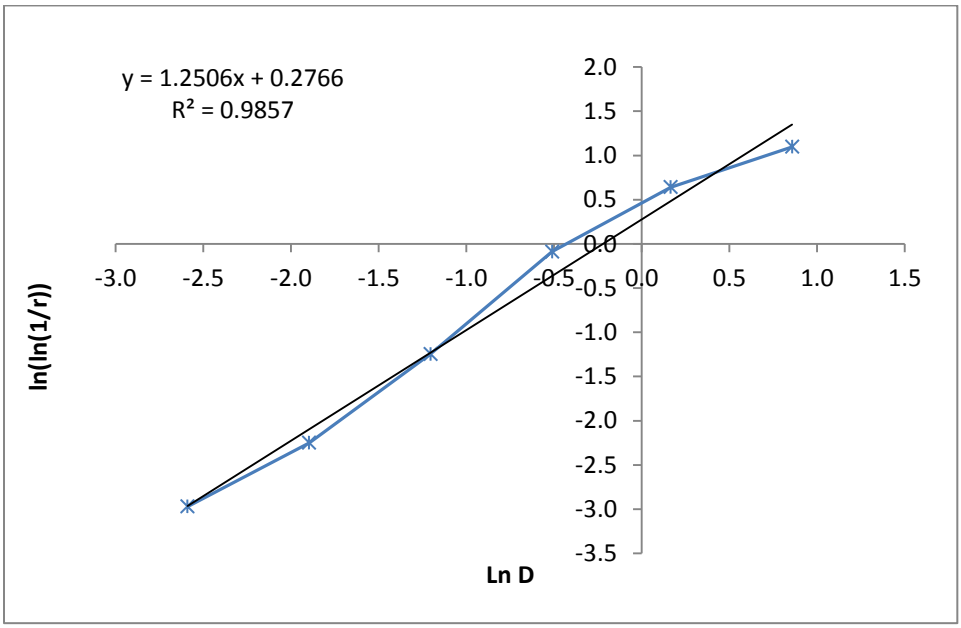

Figure B5: Rosin-Rammler curve for aggregate F5

Table B10: Characteristic diameter of aggregate F5

DISTRIBUTION PARAMETER	INTERCEPT	PACKING DENSITY	CHARACTERISTIC DIAMETER
n	C	ϕ	D' (mm)
1.251	0.277	0.585	0.80

Table B11: Calculation of Rosin-Rammler parameters for aggregate F6

F6						
Particle size - D (mm)	Ln D	F (%)	R=1-F	1/R	ln(1/r)	ln(ln(1/r))
4.750	1.56	100	0.00	-	-	-
2.360	0.86	95	0.05	20.00	3.00	1.10
1.180	0.17	85	0.15	6.67	1.90	0.64
0.600	-0.51	50	0.50	2.00	0.69	-0.37
0.300	-1.20	25	0.75	1.33	0.29	-1.25
0.150	-1.90	15	0.85	1.18	0.16	-1.82
0.075	-2.59	5	0.95	1.05	0.05	-2.97

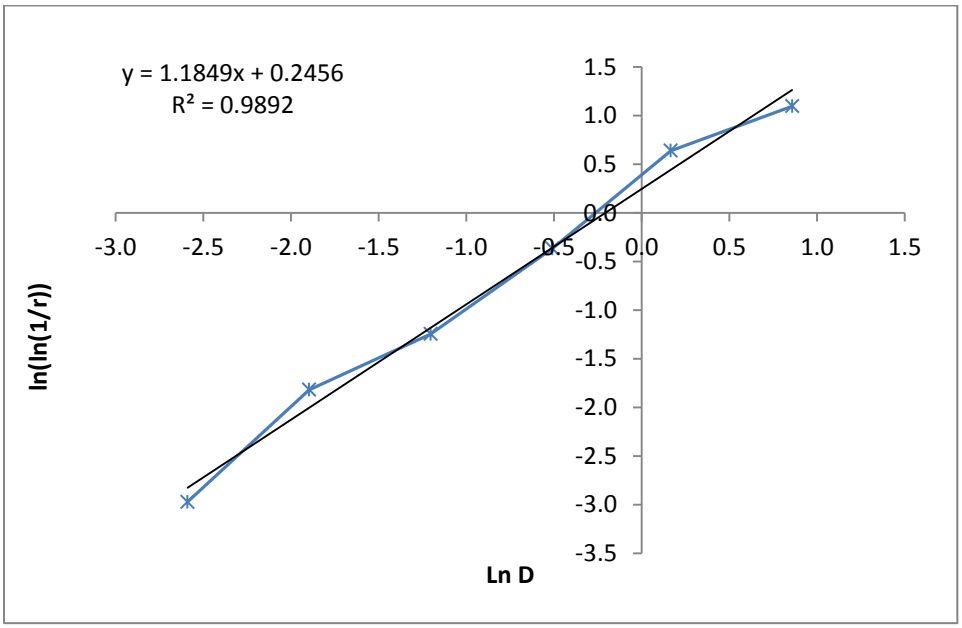

Figure B6: Rosin-Rammler curve for aggregate F6

Table B12: Characteristic diameter of aggregate F6

DISTRIBUTION PARAMETER	INTERCEPT	PACKING DENSITY	CHARACTERISTIC DIAMETER
n	C	ϕ	D' (mm)
1.185	0.246	0.587	0.81

Table B13: Calculation of Rosin-Rammler parameters for aggregate F7

F7						
Particle size - D (mm)	Ln D	F (%)	R=1-F	1/R	ln(1/r)	ln(ln(1/r))
4.750	1.56	100	0.00	-	-	-
2.360	0.86	90	0.10	10.00	2.30	0.83
1.180	0.17	75	0.25	4.00	1.39	0.33
0.600	-0.51	50	0.50	2.00	0.69	-0.37
0.300	-1.20	25	0.75	1.33	0.29	-1.25
0.150	-1.90	10	0.90	1.11	0.11	-2.25
0.075	-2.59	5	0.95	1.05	0.05	-2.97

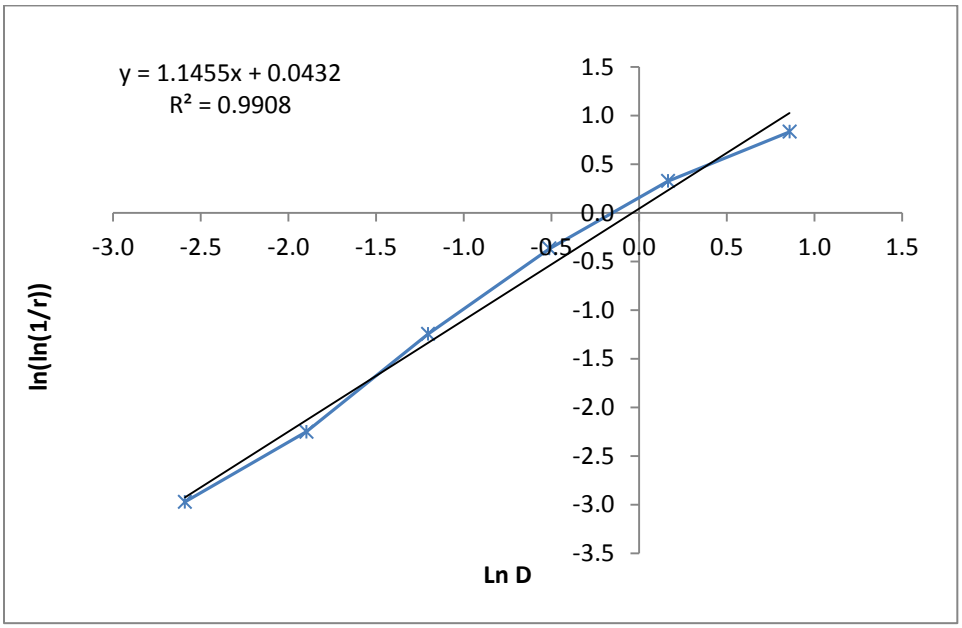

Figure B7: Rosin-Rammler curve for aggregate F7

Table B14: Characteristic diameter of aggregate F7

DISTRIBUTION PARAMETER	INTERCEPT	PACKING DENSITY	CHARACTERISTIC DIAMETER
n	C	ϕ	D' (mm)
1.146	0.043	0.607	0.96

Table B15: Calculation of Rosin-Rammler parameters for aggregate F8

F8						
Particle size - D (mm)	Ln D	F (%)	R=1-F	1/R	ln(1/r)	ln(ln(1/r))
4.750	1.56	100	0.00	-	-	-
2.360	0.86	95	0.05	20.00	3.00	1.10
1.180	0.17	85	0.15	6.67	1.90	0.64
0.600	-0.51	35	0.65	1.54	0.43	-0.84
0.300	-1.20	20	0.80	1.25	0.22	-1.50
0.150	-1.90	10	0.90	1.11	0.11	-2.25
0.075	-2.59	5	0.95	1.05	0.05	-2.97

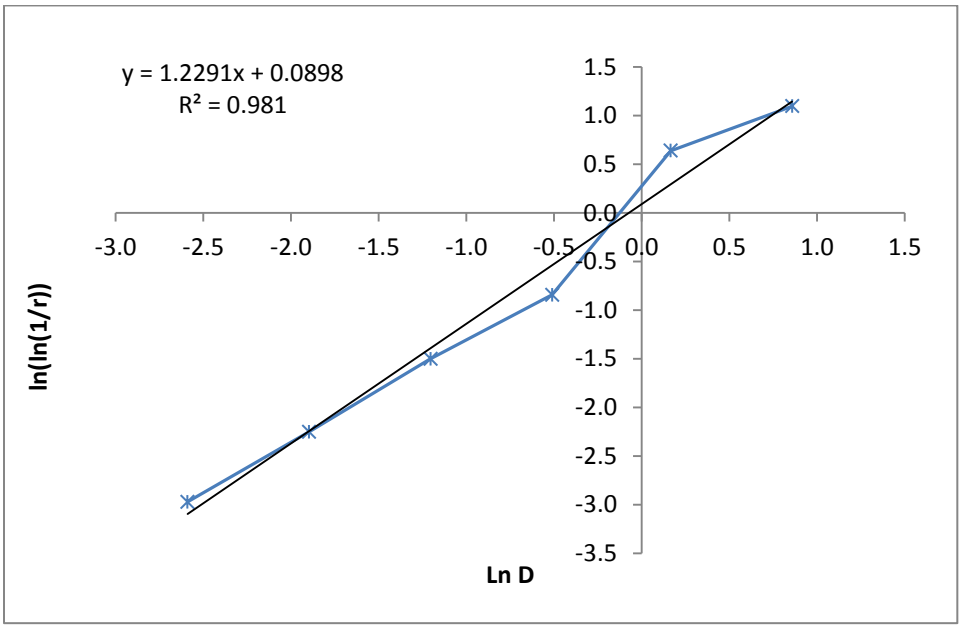

Figure B8: Rosin-Rammler curve for aggregate F8

Table B16: Characteristic diameter of aggregate F8

DISTRIBUTION PARAMETER	INTERCEPT	PACKING DENSITY	CHARACTERISTIC DIAMETER
n	C	ϕ	D' (mm)
1.229	0.090	0.581	0.93

Table B17: Calculation of Rosin-Rammler parameters for aggregate F9

F9						
Particle size - D (mm)	Ln D	F (%)	R=1-F	1/R	ln(1/r)	ln(ln(1/r))
4.750	1.56	100	0.00	-	-	-
2.360	0.86	85	0.15	6.67	1.90	0.64
1.180	0.17	60	0.40	2.50	0.92	-0.09
0.600	-0.51	35	0.65	1.54	0.43	-0.84
0.300	-1.20	15	0.85	1.18	0.16	-1.82
0.150	-1.90	5	0.95	1.05	0.05	-2.97
0.075	-2.59	5	0.95	1.05	0.05	-2.97

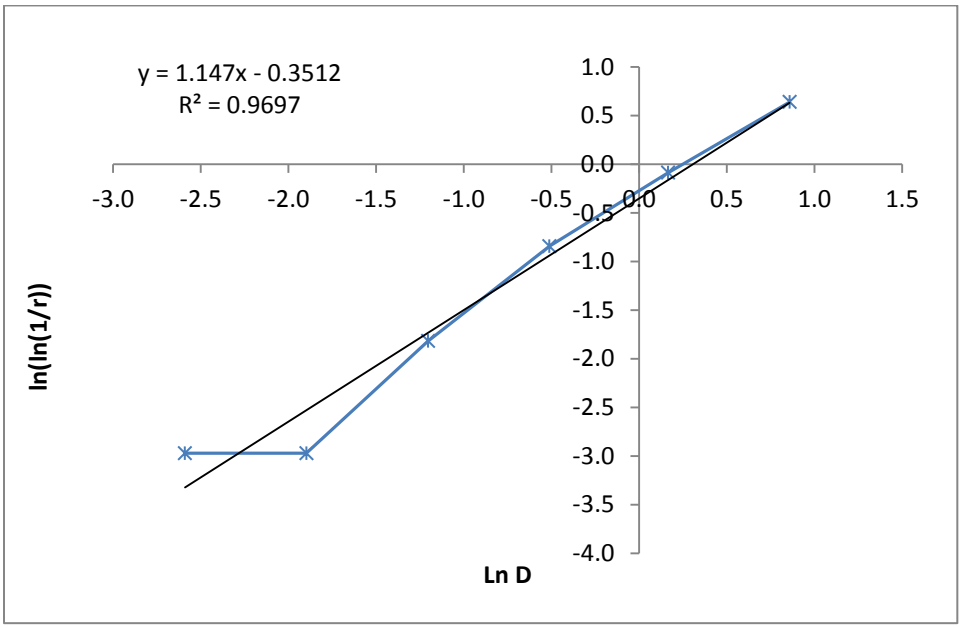

Figure B9: Rosin-Rammler curve for aggregate F9

Table B18: Characteristic diameter of aggregate F9

DISTRIBUTION PARAMETER	INTERCEPT	PACKING DENSITY	CHARACTERISTIC DIAMETER
n	C	ϕ	D' (mm)
1.229	0.090	0.581	0.93

Table B19: Calculation of Rosin-Rammler parameters for aggregate C1

Aggregate C1 (ASTM C33/57)						
Particle size - D (mm)	Ln D	F (%)	R=1-F	1/R	ln(1/r)	ln(ln(1/r))
37.50	3.62	100.00	0.00	-	-	-
26.50	3.28	100.00	0.00	-	-	-
19.00	2.94	86.21	0.14	7.25	1.98	0.68
13.20	2.58	54.06	0.46	2.18	0.78	-0.25
9.50	2.25	20.04	0.80	1.25	0.22	-1.50
6.70	1.90	2.38	0.98	1.02	0.02	-3.73
4.75	1.56	0.60	0.99	1.01	0.01	-5.11

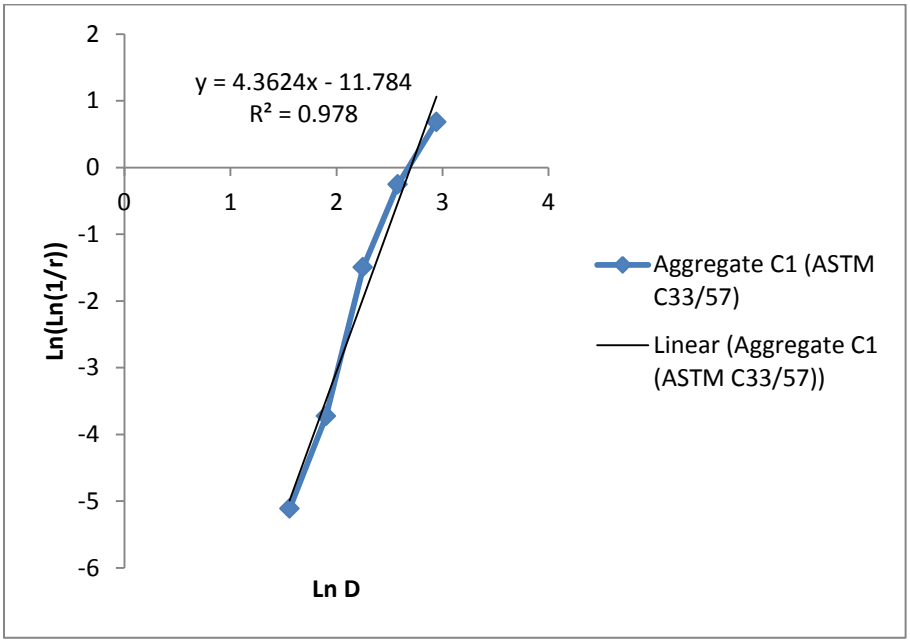

Figure B10: Rosin-Rammler curve for aggregate C1

Table B20: Characteristic diameter of aggregate C1

DISTRIBUTION PARAMETER	PACKING DENSITY	INTERCEPT	CHARACTERISTIC DIAMETER
n	ϕ	C	D' (mm)
4.362	0.486	-11.784	14.90

Table B21: Calculation of Rosin-Rammler parameters for aggregate C2

Aggregate C1 (ASTM C33/57)						
Particle size - D (mm)	Ln D	F (%)	R=1-F	1/R	ln(1/r)	ln(ln(1/r))
37.50	3.62	100.00	0.00	-	-	-
26.50	3.28	100.00	0.00	-	-	-
19.00	2.94	72.41	0.28	3.62	1.29	0.25
13.20	2.58	20.91	0.79	1.26	0.23	-1.45
9.50	2.25	3.14	0.97	1.03	0.03	-3.44
6.70	1.90	0.79	0.99	1.01	0.01	-4.84
4.75	1.56	0.00	1.00	1.00	0.00	-

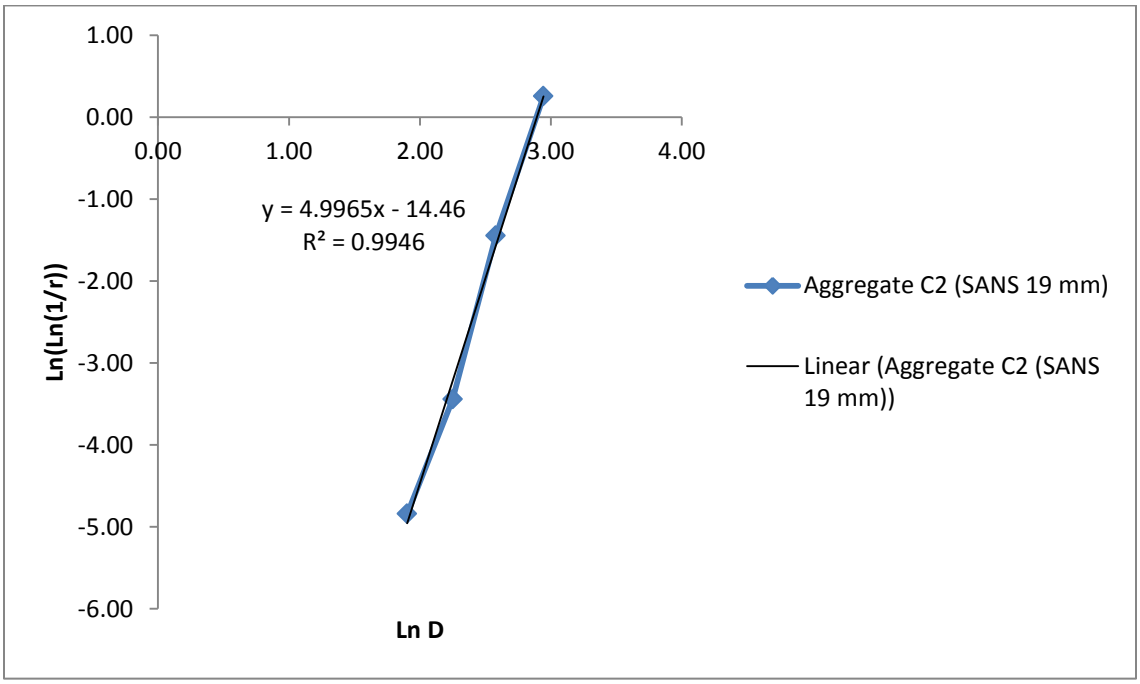

Figure B11: Rosin-Rammler curve for aggregate C2

Table B22: Characteristic diameter of aggregate C2

DISTRIBUTION PARAMETER	PACKING DENSITY	INTERCEPT	CHARACTERISTIC DIAMETER
n	ϕ	C	D' (mm)
4.997	0.458	-14.460	18.07

Appendix C – Coarse and fine aggregate packing densities

Table C1: Data from the experimental determination of the packing density of fine aggregates

		F1	F2	F3	F4	F5	F6	F7	F8	F9
PACKING MEASUREMENTS										
Distance between aggregate surface and top of bucket	mm	267	265	269	268	265	267	269	265	266
		267	265	268	268	266	266	268	265	266
		267	264	268	270	267	266	267	267	265
		268	266	268	267	264	266	268	266	265
		267	264	268	267	266	266	268	265	265
		266	264	268	267	267	266	269	267	267
		267	265	268	269	268	266	268	266	265
		269	264	268	269	265	267	269	265	266
		265	265	270	269	266	266	266	265	266
Average	**mm**	**267.00**	**264.67**	**268.33**	**268.22**	**266.00**	**266.17**	**268.00**	**265.67**	**265.67**
PACKING DENSITY CALCULATION										
Depth	mm	53.00	55.33	51.67	51.78	54.00	53.83	52.00	54.33	54.33
Area	mm2	107521	107521	107521	107521	107521	107521	107521	107521	107521
Volume	mm3	5698613	5949496	5555252	5567199	5806134	5788214	5591092	5841975	5841975
Mass	kg	9.00	9.00	9.00	9.00	9.00	9.00	9.00	9.00	9.00
Bulk density	kg/m3	1579.33	1512.73	1620.09	1616.61	1550.08	1554.88	1609.70	1540.57	1540.57
Unit weight	kg/m3	2650.00	2650.00	2650.00	2650.00	2650.00	2650.00	2650.00	2650.00	2650.00
Packing density	-	**0.5960**	**0.5708**	**0.6114**	**0.6100**	**0.5849**	**0.5867**	**0.6074**	**0.5813**	**0.5813**

Table C2: Data from the experimental determination of the packing density of coarse aggregates

		C1	C2
PACKING MEASUREMENTS			
Distance between aggregate surface and top of bucket	mm	250	256
		255	259
		251	255
		249	255
		253	253
		252	253
		249	254
		251	255
		249	255
Average	**mm**	**251.00**	**255.00**
PACKING DENSITY CALCULATION			
Depth	mm	69.00	65.00
Area	mm2	107521	107521
Volume	mm3	7418950	6988866
Mass	kg	9.00	9.00
Bulk density	kg/m3	1213.11	1287.76
Unit weight	kg/m3	2650.00	2650.00
Packing density	-	**0.4578**	**0.4859**

Appendix D – Modelled packing densities

Table D1: Modelled packing densities of aggregate C1F1

C1F1									
Fraction fine (y1)	0.1	0.2	0.3	0.4	0.5	0.6	0.7	0.8	0.9
Fraction coarse (y2)	0.9	0.8	0.7	0.6	0.5	0.4	0.3	0.2	0.1
ϕ1	0.5960	0.5960	0.5960	0.5960	0.5960	0.5960	0.5960	0.5960	0.5960
ϕ2	0.4859	0.4859	0.4859	0.4859	0.4859	0.4859	0.4859	0.4859	0.4859
kd	0.94	0.94	0.94	0.94	0.94	0.94	0.94	0.94	0.94
x	0.18	0.40	0.68	1.06	1.59	2.38	3.70	6.34	14.28
ks	0.14	0.32	0.53	0.71	0.84	0.92	0.97	0.99	1.00
ϕ	0.5288	0.5800	0.6359	0.6743	0.6887	0.6831	0.6653	0.6424	0.6186

Table D2: Modelled packing densities of aggregate C1F2

C1F2									
Fraction fine (y1)	0.1	0.2	0.3	0.4	0.5	0.6	0.7	0.8	0.9
Fraction coarse (y2)	0.9	0.8	0.7	0.6	0.5	0.4	0.3	0.2	0.1
ϕ1	0.5708	0.5708	0.5708	0.5708	0.5708	0.5708	0.5708	0.5708	0.5708
ϕ2	0.4859	0.4859	0.4859	0.4859	0.4859	0.4859	0.4859	0.4859	0.4859
kd	0.92	0.92	0.92	0.92	0.92	0.92	0.92	0.92	0.92
x	0.18	0.41	0.71	1.10	1.66	2.48	3.86	6.62	14.91
ks	0.15	0.34	0.55	0.72	0.85	0.93	0.97	0.99	1.00
ϕ	0.5277	0.5773	0.6292	0.6618	0.6707	0.6612	0.6414	0.6176	0.5935

Table D3: Modelled packing densities of aggregate C1F3

C1F3									
Fraction fine (y1)	0.1	0.2	0.3	0.4	0.5	0.6	0.7	0.8	0.9
Fraction coarse (y2)	0.9	0.8	0.7	0.6	0.5	0.4	0.3	0.2	0.1
ϕ1	0.6114	0.6114	0.6114	0.6114	0.6114	0.6114	0.6114	0.6114	0.6114
ϕ2	0.4859	0.4859	0.4859	0.4859	0.4859	0.4859	0.4859	0.4859	0.4859
kd	0.91	0.91	0.91	0.91	0.91	0.91	0.91	0.91	0.91
x	0.17	0.39	0.66	1.03	1.55	2.32	3.61	6.18	13.92
ks	0.14	0.32	0.52	0.70	0.83	0.92	0.97	0.99	1.00
ϕ	0.5279	0.5778	0.6331	0.6730	0.6906	0.6885	0.6740	0.6538	0.6322

Table D4: Modelled packing densities of aggregate C1F4

C1F4									
Fraction fine (y1)	0.1	0.2	0.3	0.4	0.5	0.6	0.7	0.8	0.9
Fraction coarse (y2)	0.9	0.8	0.7	0.6	0.5	0.4	0.3	0.2	0.1
ϕ1	0.6100	0.6100	0.6100	0.6100	0.6100	0.6100	0.6100	0.6100	0.6100
ϕ2	0.4859	0.4859	0.4859	0.4859	0.4859	0.4859	0.4859	0.4859	0.4859
kd	0.91	0.91	0.91	0.91	0.91	0.91	0.91	0.91	0.91
x	0.17	0.39	0.66	1.03	1.55	2.32	3.62	6.20	13.95
ks	0.14	0.32	0.52	0.70	0.83	0.92	0.97	0.99	1.00
ϕ	0.5279	0.5777	0.6327	0.6723	0.6895	0.6873	0.6727	0.6524	0.6308

Table D5: Modelled packing densities of aggregate C1F5

C1F5									
Fraction fine (y1)	0.1	0.2	0.3	0.4	0.5	0.6	0.7	0.8	0.9
Fraction coarse (y2)	0.9	0.8	0.7	0.6	0.5	0.4	0.3	0.2	0.1
ϕ1	0.5849	0.5849	0.5849	0.5849	0.5849	0.5849	0.5849	0.5849	0.5849
ϕ2	0.4859	0.4859	0.4859	0.4859	0.4859	0.4859	0.4859	0.4859	0.4859
kd	0.90	0.90	0.90	0.90	0.90	0.90	0.90	0.90	0.90
x	0.18	0.40	0.69	1.08	1.62	2.42	3.77	6.46	14.55
ks	0.15	0.33	0.54	0.71	0.84	0.92	0.97	0.99	1.00
ϕ	0.5270	0.5755	0.6274	0.6618	0.6736	0.6673	0.6502	0.6285	0.6062

Table D6: Modelled packing densities of aggregate C1F6

C1F6									
Fraction fine (y1)	0.1	0.2	0.3	0.4	0.5	0.6	0.7	0.8	0.9
Fraction coarse (y2)	0.9	0.8	0.7	0.6	0.5	0.4	0.3	0.2	0.1
ϕ1	0.5867	0.5867	0.5867	0.5867	0.5867	0.5867	0.5867	0.5867	0.5867
ϕ2	0.4859	0.4859	0.4859	0.4859	0.4859	0.4859	0.4859	0.4859	0.4859
kd	0.90	0.90	0.90	0.90	0.90	0.90	0.90	0.90	0.90
x	0.18	0.40	0.69	1.07	1.61	2.42	3.76	6.45	14.50
ks	0.15	0.33	0.54	0.71	0.84	0.92	0.97	0.99	1.00
ϕ	0.5269	0.5755	0.6275	0.6621	0.6744	0.6684	0.6515	0.6301	0.6079

Table D7: Modelled packing densities of aggregate C1F7

C1F7									
Fraction fine (y1)	0.1	0.2	0.3	0.4	0.5	0.6	0.7	0.8	0.9
Fraction coarse (y2)	0.9	0.8	0.7	0.6	0.5	0.4	0.3	0.2	0.1
ϕ1	0.6074	0.6074	0.6074	0.6074	0.6074	0.6074	0.6074	0.6074	0.6074
ϕ2	0.4859	0.4859	0.4859	0.4859	0.4859	0.4859	0.4859	0.4859	0.4859
kd	0.88	0.88	0.88	0.88	0.88	0.88	0.88	0.88	0.88
x	0.17	0.39	0.67	1.04	1.56	2.33	3.63	6.23	14.01
ks	0.14	0.32	0.53	0.70	0.83	0.92	0.97	0.99	1.00
ϕ	0.5267	0.5749	0.6278	0.6657	0.6821	0.6801	0.6665	0.6474	0.6271

Table D8: Modelled packing densities of aggregate C1F8

C1F8									
Fraction fine (y1)	0.1	0.2	0.3	0.4	0.5	0.6	0.7	0.8	0.9
Fraction coarse (y2)	0.9	0.8	0.7	0.6	0.5	0.4	0.3	0.2	0.1
ϕ1	0.5813	0.5813	0.5813	0.5813	0.5813	0.5813	0.5813	0.5813	0.5813
ϕ2	0.4859	0.4859	0.4859	0.4859	0.4859	0.4859	0.4859	0.4859	0.4859
kd	0.88	0.88	0.88	0.88	0.88	0.88	0.88	0.88	0.88
x	0.18	0.41	0.70	1.08	1.63	2.44	3.79	6.50	14.64
ks	0.15	0.33	0.54	0.72	0.84	0.92	0.97	0.99	1.00
ϕ	0.5263	0.5739	0.6244	0.6574	0.6685	0.6620	0.6451	0.6240	0.6021

Table D9: Modelled packing densities of aggregate C1F9

C1F9									
Fraction fine (y1)	0.1	0.2	0.3	0.4	0.5	0.6	0.7	0.8	0.9
Fraction coarse (y2)	0.9	0.8	0.7	0.6	0.5	0.4	0.3	0.2	0.1
ϕ1	0.5813	0.5813	0.5813	0.5813	0.5813	0.5813	0.5813	0.5813	0.5813
ϕ2	0.4859	0.4859	0.4859	0.4859	0.4859	0.4859	0.4859	0.4859	0.4859
kd	0.83	0.83	0.83	0.83	0.83	0.83	0.83	0.83	0.83
x	0.18	0.41	0.70	1.08	1.63	2.44	3.79	6.50	14.64
ks	0.15	0.33	0.54	0.72	0.84	0.92	0.97	0.99	1.00
ϕ	0.5244	0.5694	0.6167	0.6478	0.6588	0.6536	0.6388	0.6199	0.6002

Table D10: Modelled packing densities of aggregate C2F1

C2F1									
Fraction fine (y1)	0.1	0.2	0.3	0.4	0.5	0.6	0.7	0.8	0.9
Fraction coarse (y2)	0.9	0.8	0.7	0.6	0.5	0.4	0.3	0.2	0.1
ϕ1	0.5960	0.5960	0.5960	0.5960	0.5960	0.5960	0.5960	0.5960	0.5960
ϕ2	0.4578	0.4578	0.4578	0.4578	0.4578	0.4578	0.4578	0.4578	0.4578
kd	0.95	0.95	0.95	0.95	0.95	0.95	0.95	0.95	0.95
x	0.16	0.35	0.61	0.94	1.42	2.12	3.31	5.67	12.75
ks	0.13	0.29	0.49	0.67	0.80	0.90	0.96	0.99	1.00
ϕ	0.4991	0.5487	0.6063	0.6528	0.6765	0.6780	0.6640	0.6424	0.6188

Table D11: Modelled packing densities of aggregate C2F2

C2F2									
Fraction fine (y1)	0.1	0.2	0.3	0.4	0.5	0.6	0.7	0.8	0.9
Fraction coarse (y2)	0.9	0.8	0.7	0.6	0.5	0.4	0.3	0.2	0.1
ϕ1	0.5708	0.5708	0.5708	0.5708	0.5708	0.5708	0.5708	0.5708	0.5708
ϕ2	0.4578	0.4578	0.4578	0.4578	0.4578	0.4578	0.4578	0.4578	0.4578
kd	0.94	0.94	0.94	0.94	0.94	0.94	0.94	0.94	0.94
x	0.16	0.37	0.63	0.99	1.48	2.22	3.45	5.92	13.31
ks	0.13	0.30	0.50	0.68	0.82	0.91	0.96	0.99	1.00
ϕ	0.4982	0.5465	0.6012	0.6422	0.6601	0.6571	0.6405	0.6177	0.5937

Table D12: Modelled packing densities of aggregate C2F3

C2F3									
Fraction fine (y1)	0.1	0.2	0.3	0.4	0.5	0.6	0.7	0.8	0.9
Fraction coarse (y2)	0.9	0.8	0.7	0.6	0.5	0.4	0.3	0.2	0.1
ϕ1	0.6114	0.6114	0.6114	0.6114	0.6114	0.6114	0.6114	0.6114	0.6114
ϕ2	0.4578	0.4578	0.4578	0.4578	0.4578	0.4578	0.4578	0.4578	0.4578
kd	0.92	0.92	0.92	0.92	0.92	0.92	0.92	0.92	0.92
x	0.15	0.35	0.59	0.92	1.38	2.07	3.22	5.52	12.43
ks	0.13	0.28	0.48	0.66	0.80	0.90	0.96	0.99	1.00
ϕ	0.4985	0.5471	0.6041	0.6519	0.6785	0.6836	0.6729	0.6539	0.6324

Table D13: Modelled packing densities of aggregate C2F4

C2F4									
Fraction fine (y1)	0.1	0.2	0.3	0.4	0.5	0.6	0.7	0.8	0.9
Fraction coarse (y2)	0.9	0.8	0.7	0.6	0.5	0.4	0.3	0.2	0.1
ϕ1	0.6100	0.6100	0.6100	0.6100	0.6100	0.6100	0.6100	0.6100	0.6100
ϕ2	0.4578	0.4578	0.4578	0.4578	0.4578	0.4578	0.4578	0.4578	0.4578
kd	0.92	0.92	0.92	0.92	0.92	0.92	0.92	0.92	0.92
x	0.15	0.35	0.59	0.92	1.38	2.08	3.23	5.54	12.46
ks	0.13	0.28	0.48	0.66	0.80	0.90	0.96	0.99	1.00
ϕ	0.4984	0.5470	0.6038	0.6513	0.6776	0.6824	0.6716	0.6526	0.6310

Table D14: Modelled packing densities of aggregate C2F5

C2F5									
Fraction fine (y1)	0.1	0.2	0.3	0.4	0.5	0.6	0.7	0.8	0.9
Fraction coarse (y2)	0.9	0.8	0.7	0.6	0.5	0.4	0.3	0.2	0.1
ϕ1	0.5849	0.5849	0.5849	0.5849	0.5849	0.5849	0.5849	0.5849	0.5849
ϕ2	0.4578	0.4578	0.4578	0.4578	0.4578	0.4578	0.4578	0.4578	0.4578
kd	0.92	0.92	0.92	0.92	0.92	0.92	0.92	0.92	0.92
x	0.16	0.36	0.62	0.96	1.44	2.17	3.37	5.77	12.99
ks	0.13	0.29	0.49	0.67	0.81	0.90	0.96	0.99	1.00
ϕ	0.4977	0.5452	0.5997	0.6423	0.6631	0.6632	0.6494	0.6288	0.6065

Table D15: Modelled packing densities of aggregate C2F6

C2F6									
Fraction fine (y1)	0.1	0.2	0.3	0.4	0.5	0.6	0.7	0.8	0.9
Fraction coarse (y2)	0.9	0.8	0.7	0.6	0.5	0.4	0.3	0.2	0.1
ϕ1	0.5867	0.5867	0.5867	0.5867	0.5867	0.5867	0.5867	0.5867	0.5867
ϕ2	0.4578	0.4578	0.4578	0.4578	0.4578	0.4578	0.4578	0.4578	0.4578
kd	0.91	0.91	0.91	0.91	0.91	0.91	0.91	0.91	0.91
x	0.16	0.36	0.62	0.96	1.44	2.16	3.36	5.76	12.95
ks	0.13	0.29	0.49	0.67	0.81	0.90	0.96	0.99	1.00
ϕ	0.4977	0.5452	0.5998	0.6426	0.6638	0.6643	0.6507	0.6303	0.6081

Table D16: Modelled packing densities of aggregate C2F7

C2F7									
Fraction fine (y1)	0.1	0.2	0.3	0.4	0.5	0.6	0.7	0.8	0.9
Fraction coarse (y2)	0.9	0.8	0.7	0.6	0.5	0.4	0.3	0.2	0.1
ϕ1	0.6074	0.6074	0.6074	0.6074	0.6074	0.6074	0.6074	0.6074	0.6074
ϕ2	0.4578	0.4578	0.4578	0.4578	0.4578	0.4578	0.4578	0.4578	0.4578
kd	0.90	0.90	0.90	0.90	0.90	0.90	0.90	0.90	0.90
x	0.15	0.35	0.60	0.93	1.39	2.08	3.24	5.56	12.51
ks	0.13	0.28	0.48	0.66	0.80	0.90	0.96	0.99	1.00
ϕ	0.4976	0.5449	0.6000	0.6457	0.6711	0.6758	0.6657	0.6478	0.6274

Table D17: Modelled packing densities of aggregate C2F8

C2F8									
Fraction fine (y1)	0.1	0.2	0.3	0.4	0.5	0.6	0.7	0.8	0.9
Fraction coarse (y2)	0.9	0.8	0.7	0.6	0.5	0.4	0.3	0.2	0.1
ϕ1	0.5813	0.5813	0.5813	0.5813	0.5813	0.5813	0.5813	0.5813	0.5813
ϕ2	0.4578	0.4578	0.4578	0.4578	0.4578	0.4578	0.4578	0.4578	0.4578
kd	0.90	0.90	0.90	0.90	0.90	0.90	0.90	0.90	0.90
x	0.16	0.36	0.62	0.97	1.45	2.18	3.39	5.81	13.07
ks	0.13	0.30	0.50	0.68	0.81	0.90	0.96	0.99	1.00
ϕ	0.4972	0.5440	0.5974	0.6386	0.6585	0.6582	0.6445	0.6243	0.6024

Table D18: Modelled packing densities of aggregate C2F9

C2F9									
Fraction fine (y1)	0.1	0.2	0.3	0.4	0.5	0.6	0.7	0.8	0.9
Fraction coarse (y2)	0.9	0.8	0.7	0.6	0.5	0.4	0.3	0.2	0.1
ϕ1	0.5813	0.5813	0.5813	0.5813	0.5813	0.5813	0.5813	0.5813	0.5813
ϕ2	0.4578	0.4578	0.4578	0.4578	0.4578	0.4578	0.4578	0.4578	0.4578
kd	0.86	0.86	0.86	0.86	0.86	0.86	0.86	0.86	0.86
x	0.16	0.36	0.62	0.97	1.45	2.18	3.39	5.81	13.07
ks	0.13	0.30	0.50	0.68	0.81	0.90	0.96	0.99	1.00
ϕ	0.4957	0.5405	0.5913	0.6305	0.6498	0.6505	0.6386	0.6205	0.6006

Appendix E – Sample statistical calculation

This section presents a sample calculation that shows the method by which the regression coefficient (r) and the correlation coefficients (β_0, β_1 and β_2) were determined. The sample calculation finds the correlation and regression coefficients for the relationship between C_u and OPI for the samples with continuously graded aggregate. The data used in the calculations is presented in the table below and the equations for calculation of the regression coefficient and regression analysis by way of least squares are presented in Equations A-1 and A-2 respectively.

Table E1: Calculation of input parameters for regression and correlation coefficients for samples with aggregate C1

$x\ (Cu)$	$y\ (OPI)$	x^2	y^2	xy	$(x_i - \bar{x})$	$(x_i - \bar{x})^2$	$(y_i - \bar{y})$	$(y_i - \bar{y})^2$	$(x_i - \bar{x})(y_i - \bar{y})$
4.26	10.41	18.15	108.40	44.35	-0.67	0.44	0.09	0.01	-0.06
4.26	10.49	18.15	110.02	44.68	-0.67	0.44	0.17	0.03	-0.11
4.26	10.38	18.15	107.72	44.21	-0.67	0.44	0.06	0.00	-0.04
4.26	10.78	18.15	116.16	45.91	-0.67	0.44	0.46	0.21	-0.31
3.33	10.56	11.09	111.56	35.17	-1.60	2.55	0.24	0.06	-0.39
3.33	10.25	11.09	105.13	34.14	-1.60	2.55	-0.06	0.00	0.10
3.33	10.20	11.09	104.05	33.97	-1.60	2.55	-0.12	0.01	0.19
3.33	10.41	11.09	108.37	34.67	-1.60	2.55	0.09	0.01	-0.15
4.44	10.43	19.71	108.84	46.32	-0.49	0.24	0.11	0.01	-0.06
4.44	10.30	19.71	106.16	45.75	-0.49	0.24	-0.01	0.00	0.01
4.44	10.25	19.71	104.99	45.49	-0.49	0.24	-0.07	0.01	0.03
4.44	10.37	19.71	107.50	46.03	-0.49	0.24	0.05	0.00	-0.02
6.00	10.28	36.00	105.75	61.70	1.07	1.15	-0.03	0.00	-0.04
6.00	10.05	36.00	100.92	60.27	1.07	1.15	-0.27	0.07	-0.29
6.00	9.84	36.00	96.84	59.05	1.07	1.15	-0.48	0.23	-0.51
6.00	10.24	36.00	104.90	61.45	1.07	1.15	-0.08	0.01	-0.08

Table E1(continued): Calculation of input parameters for regression and correlation coefficients for samples with aggregate C1

	$x\ (Cu)$	$y\ (OPI)$	x^2	y^2	xy	$(x_i - \bar{x})$	$(x_i - \bar{x})^2$	$(y_i - \bar{y})$	$(y_i - \bar{y})^2$	$(x_i - \bar{x})(y_i - \bar{y})$
	3.78	10.39	14.29	108.05	39.29	-1.15	1.31	0.08	0.01	-0.09
	3.78	10.46	14.29	109.34	39.53	-1.15	1.31	0.14	0.02	-0.16
	3.78	10.51	14.29	110.49	39.73	-1.15	1.31	0.19	0.04	-0.22
	3.78	10.31	14.29	106.23	38.96	-1.15	1.31	-0.01	0.00	0.01
	6.81	10.34	46.38	106.94	70.42	1.88	3.55	0.02	0.00	0.04
	6.81	9.78	46.38	95.61	66.59	1.88	3.55	-0.54	0.29	-1.02
	6.81	10.46	46.38	109.45	71.25	1.88	3.55	0.14	0.02	0.27
	6.81	10.07	46.38	101.33	68.55	1.88	3.55	-0.25	0.06	-0.47
	5.55	10.15	30.80	103.04	56.34	0.62	0.39	-0.17	0.03	-0.10
	5.55	10.31	30.80	106.34	57.23	0.62	0.39	-0.01	0.00	0.00
	5.55	10.58	30.80	111.98	58.73	0.62	0.39	0.26	0.07	0.16
	5.55	10.20	30.80	104.04	56.61	0.62	0.39	-0.12	0.01	-0.07
	5.24	10.37	27.46	107.57	54.35	0.31	0.10	0.05	0.00	0.02
	5.24	10.32	27.46	106.57	54.09	0.31	0.10	0.01	0.00	0.00
	5.24	10.14	27.46	102.72	53.11	0.31	0.10	-0.18	0.03	-0.06
	5.24	10.53	27.46	110.79	55.15	0.31	0.10	0.21	0.04	0.07
Σ	**157.64**	**330.16**	**815.50**	**3407.79**	**1623.11**	**0.00**	**38.92**	**0.00**	**1.30**	**-3.35**

Correlation

$$r = \frac{\sum\left((x_i - \bar{x})(y_i - \bar{y})\right)}{\sqrt{\sum(x_i - \bar{x})^2 \sum(y_i - \bar{y})^2}} \quad \textbf{(A-1)}$$

Regression

Linear regression was done using the method of least squares. This is represented as follows:

$$\frac{\sum\big((x_i - \bar{x})(y_i - \bar{y})\big)}{\sum(x_i - \bar{x})^2} \quad \textbf{(A-2)}$$

$\bar{x} = 4.93$

$\bar{y} = 10.32$

$\sum\big((x_i - \bar{x})(y_i - \bar{y})\big) = -3.35$

$\sum(x_i - \bar{x})^2 = 38.92$

$\sum(y_i - \bar{y})^2 = 1.30$

$r = -0.4715$

$$\frac{\sum\big((x_i - \bar{x})(y_i - \bar{y})\big)}{\sum(x_i - \bar{x})^2} = \frac{-3.35}{38.92}$$

$$= -0.086$$

T-tests for comparison of samples with different coarse aggregates

The following example looks at the calculations involved in the t-test conducted to compare the OPI results to of the sample groups using fine aggregate F1 with the two different coarse aggregates. These results can be viewed in Table 4-5.

Table E2: OPI Results for samples C1F1 and C2F1

Specimen No.	C1	C2
1	10.41	10.28
2	10.49	10.42
3	10.38	10.62
4	10.78	10.52
Mean	10.51	10.46

Variance

$$s^2 = \frac{\sum_1^n (x_i - \bar{x})^2}{n-1}$$

$s_1 = 0.0329$

$s_2 = 0.0208$

Check for equal variance:

H_0: $s_1^2 = s_2^2$
H_1: $s_1^2 \neq s_2^2$
$\alpha = 0.05$ (5 %)

$$F = \frac{s_1^2}{s_2^2}$$

$$= 1.59$$

$$F_{3,3}^{0.05} = 9.28$$

The observed F-value of 1.59 < 9.28. We therefore cannot reject the null hypothsis and conclude that the variances are the same.

The pooled variance is calculated as follows:

$$s^2 = \frac{(n_1 - 1)s_1^2 + (n_2 - 1)s_2^2}{n_1 + n_2 - 2}$$

$$= 0.0269$$

T-test

H_0: $\mu_1 = \mu_2$
H_1: $\mu_1 \neq \mu_2$
$\alpha = 0.05$ (5 %)

$$t = \frac{\bar{x}_1 - \bar{x}_2 - (\mu_1 - \mu_2)}{\sqrt{\frac{s^2}{n_1} + \frac{s^2}{n_2}}}$$

$$= -0.455$$

Since this is a two sided test, for a 5 % significance level, we look for the t-value $t_6^{0.025}$.

$$t_6^{0.025} = \pm 2.447$$

The observed t-value of -0.455 > -2.447. We therefore cannot reject the null hypothesis and conclude that the observed mean OPIs of the two samples are the same. In other words, the difference between the mean OPIs observed for samples C1F1 and C2F1 is not significant at the 5 % level.